

DISSERTATION

MU-OPIOID SYSTEM IN THE MAMMALIAN RETINA

Submitted by

Shannon K. Gallagher

Department of Biomedical Sciences

In partial fulfillment of the requirements

For the Degree of Doctor of Philosophy

Colorado State University

Fort Collins, Colorado

Fall 2013

Doctoral Committee:

Advisor: Jozsef Vigh

Tod R. Clapp

Juliet R. Gionfriddo

Shane T. Hentges

Kathryn M. Partin

ABSTRACT

MU-OPIOID SYSTEM IN THE MAMMALIAN RETINA

Until recently, the most solid evidence suggesting a role for endogenous opioids in mammalian visual processing has been the existence of μ -opioid receptors (MORs) in the retina. Nonetheless, in most reports the location of these receptors has been limited to retinal regions rather than specific cell-types. Reports on expression of endogenous opioids in the adult mammalian retina were missing, and even in juveniles have been sparse. Additionally, our knowledge of the possible physiological functions of opioid signaling in the retina is based on only a handful of studies using exogenous opioids. For example, the recent resurgence in retinal opioid research has focused on the somewhat controversial role of δ -opioid receptors in neuroprotection. The purpose of this work was to identify if the endogenous opioid peptide preferred by MORs, β -endorphin, is present in the mammalian retina, and to determine its possible influence on the light-evoked signaling of retinal neurons that express MORs. We have identified through use of transgenic mice, in situ hybridization and immunohistochemistry (IHC) that the cholinergic “Starburst” amacrine cells express β -endorphin. Using IHC we’ve shown that multiple neuronal cell types in the mouse retina possess MORs, including dopaminergic amacrine cells and intrinsically photosensitive retinal ganglion cells (ipRGCs). ipRGCs play a central role in mammalian non-image forming vision. Neuromodulatory processes that are capable of altering ipRGCs activity are likely to have profound consequences on light-mediated behavior and/or disease. Using IHC, we found that M1-M3 types of ipRGCs are MOR+ in both mouse and rat. Using electrophysiological techniques we found that DAMGO, a MOR selective agonist, dramatically reduces both duration and rate of light-evoked firing from rat and mouse

ipRGCs. Our study is the first to demonstrate opioid modulation of light-evoked activity of neurons in mammalian retina. These findings demonstrate a new role for endogenous opioids in the mammalian retina and provide a novel site of action—MORs on ipRGCs—through which exogenous, systemically applied, opioids could exert an effect on light-mediated behaviors.

ACKNOWLEDGMENTS

I am thankful for the many opportunities I have had here at Colorado State University. Mark Frasier, Tod Clapp and Erin Bisenius have been wonderful in advising and guiding my path in graduate school. Jozsef Vigh took a chance on me, as I did on him, and I'm thankful for the opportunities he provided me in his lab. I truly appreciate everyone I've worked with in Vigh Lab, and would like to thank Dezaray Varland and Ryan Tooker for their help, support and friendship. My family has always been supportive of my adventures, and graduate school was no exception. Without their love and encouragement I know I would not have made it through this. My amazing partner, Angela, is my inspiration. She challenges me daily and makes me want to be better. I am so very thankful for everything she has done and continues to do for me.

TABLE OF CONTENTS

ABSTRACT.....	ii
ACKNOWLEDGEMENTS.....	iv
LIST OF FIGURES.....	vii
Chapter 1: Introduction.....	1
1.1. Endogenous opioids.....	2
1.2. Opioids receptors.....	2
1.3. Retina.....	3
1.4. Opioids in the mammalian retina.....	11
1.5. Hypothesis and aims of this study.....	12
Chapter 2: β -endorphin expression in the mouse retina.....	13
2.1. Summary.....	13
2.2. Introduction.....	14
2.3. Materials and methods.....	17
2.4. Results.....	26
2.5. Discussion.....	42
Chapter 3: μ -opioid receptor expression in the mammalian retina.....	49
3.1. Summary.....	49
3.2. Introduction.....	50
3.3. Materials and methods.....	51
3.4. Results.....	55
3.5. Discussion.....	61
3.6. Related findings.....	63

Chapter 4: Conclusion.....	71
4.1. Opioid modulation of ipRGCs light responses	72
4.2. Dark-light switch	75
4.3. Exogenous opioids.....	77
References.....	80
Appendices.....	101
Appendix I	102
Appendix II.....	114

LIST OF FIGURES

1.1. Diagram of retinal anatomy and circuitry	4
1.2. Morphology of M1-M5 ipRGCs types	9
1.3. Diagram of major central projections of M1 ipRGCs	10
2.1. DsRed fluorophore expression in the retina of POMC transgenic mice.....	27
2.2. POMC-DsRed+ soma distribution.....	29
2.3. Calcium-binding proteins in POMC-DsRed+ cells in confocal images of vertical cryostat sections	31
2.4. Inhibitory amacrine cell marker detection in POMC-DsRed cells in confocal images of vertical cryostat sections.....	33
2.5. POMC-DsRed transgene colocalizes with the cholinergic amacrine cell marker ChAT	35
2.6. POMC-DsRed+ neurons in the arcuate nucleus and the pituitary show β -endorphin immunoreactivity.....	37
2.7. In the retina of POMC-DsRed transgenic mice, a subset of DsRed+ amacrine cells colocalizes β -endorphin.....	39
2.8. In situ hybridization reveals POMC mRNA in the GCL and INL of wild-type mouse retinas.....	40
2.9. ChAT+ amacrine cells express β -endorphin in the wild-type mouse retina.....	41
2.10. β -endorphin antibody labeling is specific to POMC neurons in both retina and hypothalamus.....	43
3.1. Immunohistochemical localization of MORs in mouse retinal and hippocampal tissues	55
3.2. Some ganglion cells and GABAergic amacrine cells are MOR+.....	56
3.3. Dopaminergic amacrines in the INL are MOR+.....	57

3.4. Localization of DOR immunolabeling in mouse retinal and rat dorsal root ganglion tissues	59
3.5. Multiple inner retinal cell-types including dopaminergic amacrine cells are DOR+	60
3.6. Localization of MOR immunolabeling in mouse retina	64
3.7. Some Brn3b+ retinal ganglion cells are MOR+	66
3.8. In the rat intrinsically photosensitive retinal ganglion cells (ipRGCs) are MOR+	67
3.9. In the mouse intrinsically photosensitive retinal ganglion cells (ipRGCs) are MOR+	69
3.10. Brn3b+ intrinsically photosensitive retinal ganglion cells (ipRGCs) are MOR+	70
4.1. Multielectrode array recording of intrinsically photosensitive retinal ganglion cells light response	73
4.2. Graph representing a single MEA experiment showing the total light response of ipRGCs under different concentrations of DAMGO	74

1. Introduction

For over a thousand years, extracts from the opium poppy have been used to relieve pain and induce feelings of euphoria (Corbett et al., 2006). Although opioids have been extensively used and studied, their production and function throughout the body are still not fully understood. Recent discoveries highlight diverse and complex endogenous and exogenous opioid functions throughout the body effecting not only pain modulation and emotional response, but also having profound effects on development, immune function, feeding behavior, respiratory and cardiovascular regulation, and tissue-protection (for review: Sauriyal et al., 2011 and Feng et al., 2012). Adding to this complexity, the physiological changes associated with opioid withdrawal following chronic therapeutic use or abuse (Morgan & Christie, 2011). With the understanding that endogenous opioids play key roles in many regulatory processes and exogenous opioids have multiple adverse and off-target effects, there is a need for further identification and characterization of specific opioid systems and a necessity for site directed opioid modulation and treatment. Recent advances in biomedical research, especially in using transgenic mouse models, have facilitated such scientific pursuits. The current work sought to identify and characterize the opioid system in the mammalian retina with emphasis on the mu-opioid system.

This section reviews: (1) endogenous opioids; (2) opioid receptors; (3) the fundamental structure of the mammalian retina, pointing out specific aspects relevant for this study; and (4) opioids in the mammalian retina.

1.1. Endogenous opioids

The endogenous opioids are derived from three independent genes encoding three prohormone peptides with a shared N-terminal tetrapeptide sequence Tyr-Gly-Gly-Phe (Reviewed in Sauriyal et al., 2011). The propeptide proenkephalin contains two pentapeptide

proteins, leu-enkephalin and met-enkephalin, as well as the heptapeptide met-enkephalin-7 and the octapeptide met-enkephalin-8 (reviewed in Khalap et al., 2005). Prodynorphin yields dynorphin A and B, and α - and β -neoendorphin (reviewed in Schwarzer, 2009). The propeptide proopiomelanocortin (POMC) is unique as it gives rise to non-opioid peptides, including adrenocorticotrophic hormone (ACTH), α -, β - and γ -melanocyte stimulating hormone (α -MSH, β -MSH and γ -MSH, respectively) and the corticotropin-like intermediate lobe peptide (CLIP) (Millington, 2007). Importantly, POMC also yields the opioid peptide β -endorphin (Akil et al., 1981). Each of the three opioid peptide families preferentially binds to a specific opioid receptor.

1.2. Opioids receptors

Three types of opioid receptors have been identified and are referred to as μ -, δ - and κ -opioid receptors (MOR, DOR and KOR, respectively). These receptors are distributed throughout the central and peripheral nervous system, as well as in paracrine and endocrine tissues, accounting in part for the diverse and complex opioid effects (Reviewed in Williams et al., 2001). Although there is no absolute peptide/receptor pair specificity, β -endorphin has the highest affinity for the MOR, the enkephalins bind preferentially to the DOR, and the dynorphin family to the KOR (Kieffer, 1995). These opioid receptors belong to the family of G-protein-coupled receptors and have 50-70% gene homology across the three types (Reviewed in Sauriyal et al., 2011).

Signal transduction

The opioid receptor signaling pathway has been well characterized and is initiated by the binding of a ligand to the receptor. This ligand/receptor interaction causes an intracellular conformational change that facilitates coupling of G-proteins, primarily $G_{i/o}$, to the opioid

receptor (Williams et al., 2001). Once coupled to the receptor, the trimeric G-protein complex dissociates and the G_{α} - and $G_{\beta\gamma}$ -subunits proceed to inhibit adenylyl cyclases and/or directly modulate ion channels (reviewed in Busch-Dienstfertig & Stein, 2010).

Once dissociated from the complex, the G_{α} -subunits inhibit adenylyl cyclases causing a decrease in cyclic adenosine 3',5'-monophosphate (cAMP). As a second messenger, cAMP can regulate many effectors leading to modulation of ion channels, Ca^{2+} signaling, regulation of gene transcription and cellular metabolism (Sassone-Corsi, 2013). The decrease of cAMP through opioid receptor activation has been shown to function in the modulation of hyperpolarization-activated inwardly-rectifying current (I_h) (Ingram & Williams, 1994; Svoboda & Lupica, 1998) and inhibition of cAMP-dependant protein kinase-A (PKA) dependant pathways, including neurotransmitter release (Chieng & Williams, 1998; Shoji et al., 1999; Pierce et al., 2002). The G-protein $G_{\beta\gamma}$ -subunits have been shown to facilitate the inhibitory effect on voltage gated Ca^{2+} channels (Herlitze et al., 1996), and activation of potassium conductances including the G-protein-activated inwardly rectifying K^+ (GIRK) channels (Jan & Jan, 1997). Together, the sum of the modulatory effects as a result of opioid receptor activation is primarily and overwhelming inhibitory.

1.3. Retina

Vision is a complex sensory process that permits the detection of size, color, distance, motion, and orientation within the observed environment—a process that begins in the retina (Gaillard & Sauve, 2007). The retina is a highly organized laminar tissue largely made up of five main classes of neurons: classical-photoreceptors (rods and cones), horizontal cells, bipolar cells, amacrine cells, and ganglion cells (Fig. 1.1; Sung & Chuang, 2010; Wässle, 2004).

The retina also contains glial cells and the retinal pigmented epithelial (RPE) cells. The RPE functions as a photon sink absorbing stray photons and plays an important role in the recovery of bleached photopigments. Müller cells are “housekeeping” glia that remove waste and are vital for retinal health (Lamba et al., 2008).

Outer retina

The outer retina consists of the outer nuclear layer (ONL)—also known as the photoreceptor layer as this is where the somas of rods and cones are located—and the outer plexiform layer (OPL) (Fig. 1.1 Rod photoreceptors are responsible for scotopic, or dark / low light vision, whereas cone vision predominates under photopic, or well-lit conditions. Although the importance of the outer retina cannot be overstated in regards to normal visual function, the specifics of this study will focus on the inner retina.

Inner retina

The inner retina includes the inner nuclear layer (INL), the inner plexiform layer (IPL) and the ganglion cell layer (GCL) (Fig. 1.1). The INL is the most heterogeneous nuclear layer in the retina containing horizontal, bipolar, amacrine, Müller and displaced retinal ganglion cell somas,

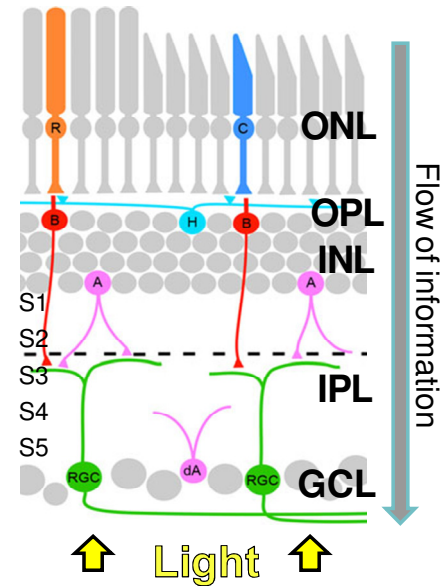


Figure 1.1. Diagram of retinal anatomy and circuitry. Light passes through the retina and reaches the classical photoreceptors, rods (R) and cones (C), in the outer nuclear layer (ONL). Rods and cones synapse within the outer plexiform layer (OPL) with bipolar cells (B) whose cell bodies are found in the inner nuclear layer (INL). Bipolar cells synapse with retinal ganglion cells (RGC) within the inner plexiform layer (IPL). Modulation of this signal occurs in the outer and inner retina by inhibitory interneurons (horizontal cells (H) and amacrine cells (A/dA)). The retinal ganglion cells (RGCs), most often found in the ganglion cell layer (GCL), send the signal along their axons (forming the optic nerve) to diverse brain regions for further processing. S1-S5: sublaminae 1-5. Modified with permission from Fox & Guido, 2011 (see Appendix I).

with amacrine cells making up almost 40% of all the INL cell bodies (Jeon et al., 1998). Within the IPL, processes from the inner retina's two nuclear layers converge to form synapses within distinct laminae. The IPL has been classically divided into ON and OFF sublaminae corresponding with the location of bipolar cell axonal synapses (Fig. 1 dashed line; also, see "bipolar cell" below). It has been further subdivided into five layers of equal thickness and designated sublamina 1-5 (Fig. 1.1; Marc, 1986; Kolb, 1997). The inner most retinal layer, the GCL, is comprised of retinal ganglion cells (RGCs) and displaced amacrine cells (Jeon et al., 1998; Kong et al., 2005).

Bipolar cells

Bipolar cells (BCs) are second-order retinal neurons which gather synaptic input from photoreceptors in the OPL and pass it on to ganglion cells in the IPL. As with all cells in the retina, BCs have been classified initially based on their morphology and subsequently based on their physiology. The mammalian retina contain at least 10 morphologically distinct types of BCs (Wässle, 2004), subdivided into two main functional BC types (ON-type and OFF-type). This designation is based on the polarity of their response to light; illumination of the receptive-field center results in depolarization of ON-type BCs and hyperpolarization of OFF BCs (Werblin & Dowling, 1969).

Amacrine cells

Amacrine cells (ACs) are the most diverse class of cells in the mammalian retina with ~30 identified morphologically distinct types (Masland, 2012). Because of soma size, location and dendritic stratification within the sublaminae of the IPL, distinct roles for AC types have been inferred—with physiological characterizations confirming such functional differences (Masland,

2001). These interneurons are generally considered inhibitory and are subdivided into glycinergic or γ -aminobutyric acidergic (GABAergic) ACs (Vaney, 1989; Marc et al., 1998). All glycinergic AC somas are found in the INL while GABAergic AC somas are evenly divided between the INL and GCL (orthotopic and displaced (dACs) ACs, respectively). GABAergic ACs have been shown to coexpress many neuroactive substances, including peptides (Haverkamp & Wässle, 2000). As a group, ACs play a vital role in modulating bipolar cell output as well as other AC and ganglion cell activity (Dowling & Boycott, 1966; Masland, 2001). Two well characterized AC types important to this study are the cholinergic and dopaminergic ACs.

Cholinergic “Starburst” amacrine cells

Cholinergic ACs, also called “starburst” ACs (SACs) for their characteristic dendritic arborization, are the principle cholinergic neurons of the retina and one of the most numerous AC types (Masland, 2005). In addition to releasing acetylcholine (ACh) SACs also release GABA and may express non-classical neurotransmitters including adenosine (O’Malley & Masland, 1989; Haverkamp and Wässle, 2000; Masland, 2005). SACs have two populations that loosely mirror each other, one in the INL and one displaced in the GCL, which form a semi-regular mosaic across the entire retina (Whitney et al., 2008). Both populations send dendrites into the IPL forming narrowly stratified bands (Famiglietti, 1983). SACs in the INL project to the border of sublaminae 1 and 2 and contribute to OFF-pathways, whereas the displaced SACs in the GCL project to the border of sublaminae 3 and 4 and contribute to ON-pathways (for example, see Fig.2.5; Tauchi & Masland, 1984; Haverkamp & Wässle, 2000).

SACs have been shown to perform at least two distinct functions: during development they facilitate retinal waves that are essential for activity-dependent neural development, and in the

mature retina they provide key inhibition of directionally selective RGCs essential for motion detection (Masland, 2005). Retinal waves are bursts of excitatory activity that, during development, are propagated through RGCs across the retina (Ford & Feller, 2012) and critical in strengthening and fine tuning synaptic development (Zheng et al., 2005). In the mature retina, the most studied function of SACs is their contribution to coding for direction of moving objects in the visual field (reviewed in Taylor & Smith, 2012). SACs can code for direction of movement of a stimulus in their dendrites (Euler et al., 2002) and provide input to directionally selective retinal ganglion cells (dsRGCs), which fire action potentials in response to movement of an object in the preferred direction. The role of SACs in the neural computation of dsRGC signals is fundamental as selective elimination of SACs completely abolishes directional selective coding of dsRGC (Yoshida et al., 2001).

Dopaminergic amacrine cells

In the mammalian retina, dopaminergic amacrine cells (DACs) are found in the INL with their processes forming an overlapping meshwork within sublamina 1 of the IPL (Fig. 1.1; for example, see Fig.3.3). Along with being the only source of retinal dopamine, DACs are GABAergic and work through classic synapses to modulate inner retinal activity (Wulle & Wagner, 1990; Contini & Raviola, 2003). However, as almost all identified retinal cell types express dopamine receptors, DACs influence the vast majority of cells through paracrine secretion of dopamine (Witkovsky, 2004). Although the complexity of dopamine's role in the retina is not fully understood, dopamine is known to tune the retinal circuitry from scotopic rod driven vision to photopic cone mediated vision as night transitions to day (Witkovsky, 2004; Newkirk et al., 2013). Therefore, DAC signaling underlies one of the most important adaptation processes in the retinal.

Retinal ganglion cells

Retinal ganglion cells (RGCs) are the output elements of the retina, their axons form the optic nerve, by which visual information is conveyed to the brain. Most of the RGCs are located in the GCL, although about half of the cells in the mouse GCL are displaced amacrine cells (Jeon et al., 1998, Kong et al., 2005). Additionally, there are some displaced RGCs found in the INL though these accounts for only a small percentage of total RGCs (Bauh & Dann, 1988; Doi et al., 1995). Since Cajal's historical study of retinal cell morphology (1892), morphological classification of ganglion cells in multiple species have been attempted (for example: Polyak, 1941; Boycott and Wassle, 1974), including the mouse retina (Doi et al., 1995; Sun et al., 2002; Badea & Nathans, 2004; Kong et al., 2005; Coombs et al., 2006; Völgyi et al., 2009). These studies, however, brought somewhat varying results. Recently, groups have used molecular markers to try and characterize RGCs, and use of transgenic animals have aided in identifying specific RGC types and their functions. Of interest to this study, are the recently identified intrinsically photosensitive RGC.

Intrinsically photosensitive retinal ganglion cells

The mammalian retina possesses three types of photoreceptors. The classical rods and cones as discussed above, and a third newly identified type, termed the intrinsically photosensitive retinal ganglion cells (ipRGCs) (Berson et al., 2002). ipRGCs, using the photopigment melanopsin, can capture light information independent of rods or cones (Hattar et al., 2002; Panda et al., 2002). These RGCs, which account for ~2-3% of all RGCs, provide light cues for the synchronization of circadian rhythms and play important roles in other non-image forming visual processes including the pupillary light reflex (reviewed in Sand et al., 2012). Recent

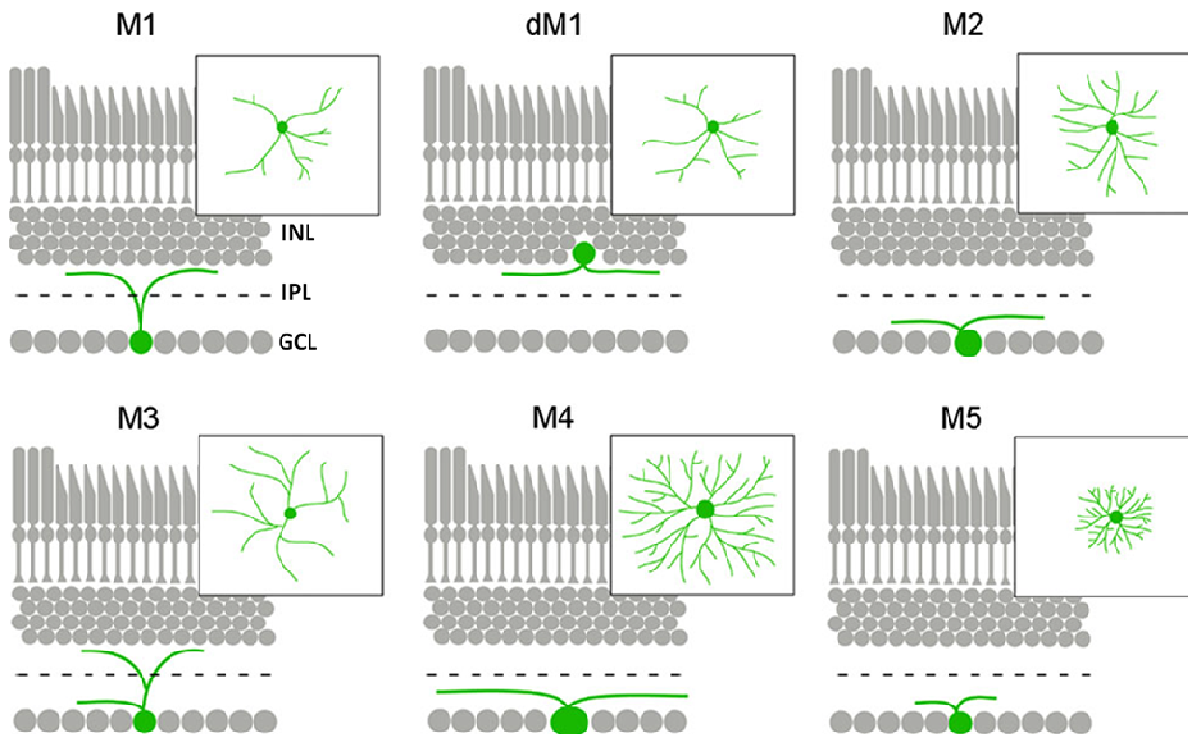


Figure 1.2. Morphology of M1-M5 ipRGCs types. Differences in soma size and dendritic arborizations are noted between cell types. dM1: displaced M1 ipRGC. Modified with permission from Fox & Guido, 2011 (see Appendix I).

discoveries expand on the evolving role of ipRGCs, identifying tight interconnections within retinal circuitry and targets within discrete brain regions responsible for both image and non-image forming visual pathways (Baver et al., 2008; Ecker et al., 2010). Early studies of ipRGCs focused on one morphologically distinct cell type now called “M1” (Berson et al., 2002; Hattar et al., 2002). As the role for ipRGCs expanded, so did the number of identified cell types which now includes M1-M5 (Fig. 1.2; Sand et al., 2012). M1-M3 ipRGC types mediate mainly non-image forming visual systems and are specifically relevant to the current study.

The M1 cell type account for almost half of all ipRGCs (Fox & Guido, 2011). This cell type was first identified because of its high levels of melanopsin and subsequent robust intrinsic light response (Berson et al., 2002; Hattar et al., 2002). M1 type ipRGCs have only been shown to mediate non-image forming visual processes (Fox & Guido, 2011). M1 cells have ~13 μ m

diameter somas with sparsely branching dendrites stratifying in sublamina 1 of the IPL forming a photoreceptive net across the retina (Fig.2; Berson et al., 2010; Fox & Guido, 2011). These cells are the only confirmed ipRGC type that have representative displaced somas, though the existence of displaced M2s has been suggested

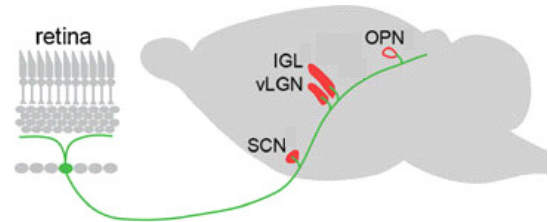


Figure 1.3. Diagram of major central projections of M1 ipRGCs. Suprachiasmatic nucleus (SCN), ventral lateral geniculate nucleus (vLGN), intergeniculate leaflet (IGL), olivary pretectal nucleus (OPN). Modified with permission from Fox & Guido, 2011 (see Appendix I).

(Fig. 1.2; Karnas et al., 2013). The M1 cells have been further characterized by their expression pattern of the POU domain regulatory transcription factor Brn3b (Jain et al., 2012). M1 cells that are Brn3b positive project to the shell of the olivary pretectal nucleus (OPN) and are responsible for the ipRGC component of the pupillary light reflex, whereas Brn3b negative M1 cells project to the suprachiasmatic nucleus (SCN) of the hypothalamus and mediate photoentrainment of the circadian rhythm (Fig. 1.3; Chen et al., 2011). These cells have also been shown to target the intergeniculate leaflet (IGL) and ventral lateral geniculate nucleus (vLGN), both relevant to photoentrainment (Harrington, 1997), the ventrolateral preoptic area (VLPO) which plays a role in sleep regulation, and the superior colliculus (SC) responsible for visual targeting (Fig. 1.3; Hattar et al., 2006).

Less is understood about the other ipRGC cell types. Some studies actually group ipRGCs as either M1 or non-M1 cells further blurring the differences between M2-M5 (for example: Jain et al., 2012). Still, some key attributes can be ascribed to M2 and M3 subtypes.

The M2 cells are almost as numerous as M1s but have significantly lower levels of melanopsin resulting in a weaker light response (Schmidt & Kofuji, 2009). These ipRGCs have a slightly larger soma (~15µm diameter) and their dendrites stratify in sublamina 5 of the IPL (Fig.

1.2; Berson et al., 2010). M2 ipRGCs have been shown to send some projections to the SCN alongside M1 cells but appear to play a minimal role in photoentrainment of the circadian rhythm (Chen et al., 2011). They also project to the core of the OPN and the SC (Ecker et al., 2010).

M3 type ipRGCs are few in number and their retinal distribution is sparse. These cells are the only bistratified ipRGCs that have been identified, with their dendritic arbors stratifying in both sublaminae 1 and 5 (Fig. 1.2; Fox & Guido, 2011). M3 ipRGCs have similarities with M2 cells including soma size (~17 μ m), melanopsin expression and light responsiveness (Schmidt & Kofuji, 2011). Additionally, although M3 cells project into the OFF sublamina, it seems that they are driven synaptically, almost exclusively through ON-pathways (Schmidt & Kofuji, 2011).

1.4. Opioids in the mammalian retina

Until recently most research on retinal opioid peptides and their receptors has been done using fish and avian retinas (Djamgoz et al., 1981; Seltner et al., 1997; Fischer et al., 1998) and the majority of this work has focused on enkephalins (Slaughter et al., 1985; Su et al., 1986; Watt et al., 1988). In mammals, some early work using stereospecific binding of opioid analogs and autoradiographic labeling of tritiated-opioids suggested the presence of opioid receptors in the retina (Medzihradsky, 1976; Wamsley et al., 1981; Borbe et al., 1982). Over the past few years, however, there has been increased interest in retinal opioid systems. Recent work, although contradictory, has pointed to the possible neuroprotective role of opioids in the mammalian retina with focus being on the DOR system (Ma et al., 2005; Riazi-Esfahani et al., 2008; Peng et al., 2009; Husain et al., 2012; Abdul et al., 2013). These studies have confirmed the presence of opioid receptors and the expression of enkephalins in the mouse and rat retinas (for example: Husain et al., 2009). However, no study has shown the expression of β -endorphin

(see chapter 2) in the mammalian retina and the localization of opioid receptors has at best been identified in specific regions rather than distinct cell types. With this knowledge, we sought to further identify and characterize the opioid system in the mammalian retina, with emphasis on the mu-opioid system.

1.5. Hypothesis and aims of this study

Our overall hypothesis is that the opioid system, specifically the μ -opioid receptor (MOR) and its endogenous opioid peptide, β -endorphin, is present in the mammalian retina and it plays a role in the regulation of light-driven retinal functions. The specific aims of this work are threefold: (1) Identification of β -endorphin expression in the mouse retina; (2) Identification of μ -opioid receptor possessing cell types in mouse retina; and (3) evaluation of a possible physiological effect of μ -opioid receptor activation in the mammalian retina. The next two chapters will address aims 1 & 2 directly, and preliminary results for aim 3 will be discussed in the concluding chapter.

2. β -endorphin expression in the mouse retina

The first aim of this work was the identification of β -endorphin expression in the mouse retina. Standard immunohistochemical and histological techniques were utilized in the characterization of β -endorphin immunopositive cells in transgenic and wild-type mouse retinas. This chapter includes the complete published manuscript for this aim, *β -endorphin expression in the mouse retina* (Shannon K. Gallagher, Paul Witkovsky, Michel J. Roux, Malcolm J. Low, Veronica Otero-Corchon, Shane T. Hentges, Jozsef Vigh, *Journal of Comparative Neurology*, 2010). My contributions to this publication included performing and optimizing the vast majority of all immunohistochemistry (IHC) preparations using mouse retinal tissue, imaging and quantification of all retinal IHC preps and writing the much of the manuscript. Table and figure numbers have been modified to reflect that they are specific to this chapter, e.g. figure 1 is now figure 2.1. This article is reproduced with permission, and only minimal modifications were made to meet formatting requirements. No other modifications were made, as per the licensing agreement (copyright clearance found in Appendix I).

2.1. Summary

Evidence showing expression of endogenous opioids in the mammalian retina is sparse. In the present study we examined a transgenic mouse line expressing an obligate dimerized form of Discosoma Red Fluorescent Protein (DsRed) under the control of the pro-opiomelanocortin promoter and distal upstream regulatory elements to assess whether pro-opiomelanocortin peptide (POMC), and its opioid cleavage product, β -endorphin, are expressed in the mouse retina. Using double label immunohistochemistry, we found that DsRed fluorescence was restricted to a subset of GAD-67-positive cholinergic amacrine cells of both orthotopic and displaced subtypes. About 50% of cholinergic amacrine cells colocalized DsRed and a large

fraction of DsRed-expressing amacrine cells was positive for β -endorphin immunostaining, whereas β -endorphin immunoreactive neurons were absent in retinas of POMC null mice. Our findings contribute to a growing body of evidence demonstrating that opioid peptides are an integral component of vertebrate retinas, including those of mammals.

2.2. Introduction

In vertebrate retinas, neural processing of light signals is mediated primarily by the amino acid transmitters glutamate, GABA and glycine, with additional contributions from amines such as acetylcholine and amines such as dopamine and 5-hydroxytryptamine (reviewed in Ehinger, 1982). This short list, however, does not include a number of additional chemical messengers that influence retinal signal processing, for the retina also contains about 50 identified neuroactive peptides (reviewed in Brecha, 2003). In this study we focus on the retinal distribution of an opioid peptide, β -endorphin and its precursor protein pro-opiomelanocortin (POMC).

The great diversity of the retinal peptide population has made it difficult to formulate a general framework for the roles peptides play in retinal operation, but some generalizations can be made about peptide organization and function. Many of the identified retinal peptides have been shown to coexist with an amino acid or amine co-transmitter (Casini and Brecha, 1992; Cuenca and Kolb, 1998; Vaney et al., 1989; Hannibal et al., 2000), consistent with observations in other parts of the central nervous system (CNS) reporting co-release of classical neurotransmitters and peptides from the same neuron (Hökfelt et al., 2000). Moreover, almost all the retinal peptides are found in inner retinal neurons, particularly in subtypes of amacrine cell (Brecha, 2003).

Endogenous opioid peptides possess a shared N-terminal tetrapeptide sequence Tyr-Gly-Gly-Phe and are divided into three families, originating from three large precursor proteins. Proenkephalin gives rise to two pentapeptide proteins, leu-enkephalin and met-enkephalin, the heptapeptide met-enkephalin-7 and the octapeptide met-enkephalin-8. Prodynorphin is cleaved to generate dynorphin A/B and α -neoendorphin (reviewed in Khalap et al., 2005). The alternative cleavage products of proopiomelanocortin include the opioid β -endorphin, the melanocortins adrenocorticotrophic hormone (ACTH), α -, β - and γ -melanocyte stimulating hormone (α -MSH, β -MSH and γ -MSH, respectively) and the corticotropin-like intermediate lobe peptide (CLIP) (Millington, 2007). Each opioid peptide family preferentially binds to specific peptide receptors, known as mu-, delta- and kappa opioid receptors (μ -OR, δ -OR and κ -OR, respectively). Although there is no absolute peptide/receptor pair specificity, β -endorphin binds preferentially to the μ -OR, the enkephalins show highest affinity for the δ -OR, and the dynorphin family for the κ -OR (Kieffer, 1995).

Most research on retinal opioid peptides has been done on fish and avian retinas (Djamgoz et al., 1981; Seltner et al., 1997; Fischer et al., 1998) and the majority of this work has focused on enkephalins, which are found in amacrine cells that colocalize GABA or glycine (Watt et al., 1988) and also the peptides somatostatin and neurotensin (Yang et al., 1997). With regard to mammalian retinas, Altschuler et al., (1982) provided immunocytochemical evidence for the presence of enkephalin in inner retinal neurons of the guinea pig retina, but functional studies of enkephalin actions in mammalian retinas are lacking.

Only sparse data exist for the presence or function of endorphin-like peptides and their receptors in mammalian retinas. Medzihradsky (1976) found that rat retinal homogenates showed stereospecific binding of etorphine, a synthetic, non-selective analog of morphine.

Binding studies with the non-selective opioid receptor ligand [³H]diprenorphine showed saturable specific binding in the rabbit retina (Slaughter et al., 1985). However, further analysis of binding site subtypes was precluded by the low density of binding sites. Wamsley et al., (1981), using [³H]dihydromorphine, found autoradiographic labeling over the inner plexiform and ganglion cell layers (IPL and GCL, respectively) in rat and monkey retinas. Since dihydromorphine shows a ten times higher affinity for μ -OR compared to δ -ORs, high affinity binding of dihydromorphine suggests the presence of μ -ORs in these retinas. Similarly, [³H]naloxone binding indicated that μ -ORs are present in bovine retinal homogenates: specific [³H]naloxone binding was most completely inhibited by the μ -OR specific compound, levorphanol (IC₅₀=1 nM)(Borbe et al., 1982).

Given the weak data base for opioid peptides and receptors in mammalian retinas, we decided to take advantage of a transgenic mouse model in which Discosoma red fluorescent protein (DsRed) is expressed under the transcriptional control of the mouse POMC gene promoter and neuronal regulatory elements (Hentges et al., 2009). In this transgenic mouse we found that POMC-DsRed expression was confined to cholinergic amacrine cells. Additionally, we demonstrated by immunocytochemistry that the opioid POMC cleavage product β -endorphin was located within cholinergic amacrine cells, whereas immunoreactivity for the alternative melanocortin cleavage products, ACTH and α -MSH, was not detected in inner retina. We provide quantitative data on the fractions of the cholinergic amacrine cell population which express β -endorphin. In a brief report, Brecha et al., (1995), utilizing an antibody against the μ -OR, found immunoreactivity in ganglion cell bodies and dendrites of the rat retina. Our data, in conjunction with the report of Brecha et al., (1995) suggest a close spatial apposition of β -

endorphin release and binding sites in inner retina, thus providing an initial anatomical framework for further study of opioid peptide function in mammalian retinas.

2.3. Materials and methods

Animals

Wild type C57BL/6J mice were obtained from Jackson Laboratories, Bar Harbor ME. The POMC-DsRed transgenic mouse line (Hentges et al., 2009), was used to assess POMC promoter-driven expression of the red fluorescent protein DsRed. Tissue from POMC knockout mice (Smart et al., 2006) was used as a negative control for specificity of the β -endorphin antiserum. Mice were kept on a 12-hour light:12-hour dark cycle with lights on at 6:00 AM, fed standard chow and water *ad libitum*. Adult male and female mice were used for experimentation. Animals were handled in compliance with the Colorado State University Institutional Animal Care and Use Committee and all procedures met United States Public Health Service Guidelines.

Production of transgenic mice

Mice expressing the tdimer2(12) engineered form of DsRed (Campbell, et al., 2002) under the control of pro-opiomelanocortin gene (*Pomc*) regulatory elements were produced by standard techniques and validated as described elsewhere (Hentges et al., 2009). In brief, the transgene contained 11.8 kb of mouse *Pomc* genomic sequences extending from nucleotide positions -13.3 kb to +3.2 kb, numbered relative to the transcriptional start site, that includes two distal neuronal regulatory enhancers (deSouza, et al., 2005), the proximal promoter, exon 1 and intron 1. The 5' flanking sequences were modified by an internal deletion of 4.7 kb ranging from positions -6.8 kb to -2.1 kb that were shown previously to be unnecessary for neuronal expression of transgenes (deSouza, et al., 2005). Tdimer2(12) coding sequences followed by SV40T antigen transcriptional stop and polyadenylation signals were ligated to the *Pomc*

sequences at a *SmaI* restriction site engineered into the 5' UTR of exon 2 at nucleotide position +3.2 kb. The transgene DNA was purified from its pBlueScript (Stratgene) plasmid vector backbone after restriction endonuclease digestion at unique polylinker sites on both sides of the cloned insert and used for nuclear microinjection into fertilized one-cell mouse embryos. In some experiments, POMC-DsRed transgenic mice were further crossed with a glutamic acid decarboxylase (GAD)-67 enhanced green fluorescent protein (EGFP) transgenic mouse line (Tamamaki et al., 2003). The GAD67-EGFP transgene faithfully labels gamma amino butyric acid (GABA)ergic neurons. In these mice, EGFP colocalizes with GAD67, GABA and neuropeptides that are expressed in CNS GABAergic neurons (neuron-nuclear specific protein, calretinin, parvalbumin and somatostatin; Tamamaki et al., 2003). Furthermore, in the retinas of the GAD67-EGFP strain, most (99%) of the EGFP+ cells co-localize GABA (May et al., 2008). Genotyping of the compound transgenic mice with double-labeled POMC- and GAD67-expressing cells (Hentges et al., 2009) was performed using polymerase chain reaction (PCR) and primer sets specific for the EGFP and DsRed transgenes. Generation and breeding of neuronal-specific POMC-KO mice were described in detail elsewhere (Smart et al., 2006). In brief, transgenic mice were generated with a modified genomic construct predicted to express POMC in pituitary cells, but not in neurons. A 9.7-kb *EcoRI-EcoRI* mouse genomic DNA fragment containing the 3 *Pomc* exons and proximal promoter elements was subcloned into pBluescript SK (Stratagene) and used to construct the pituitary-specific POMC rescue transgene pHalEx2* (*Tg*), which contains a unique oligonucleotide sequence inserted into the 5' UTR of exon 2 to provide a probe for specific detection of mRNA transcribed from the transgene, but not from endogenous *Pomc* alleles. The novel strain of transgenic mice was generated by nuclear microinjection of linearized pHalEx2* Tg DNA into B6D2 F2 hybrid 1-cell embryos. The

pHalEx2* Tg allele was backcrossed from a single identified founder to inbred C57BL/6J mice (Jackson Laboratory) for 2 consecutive generations and subsequently crossed onto the *Pomc*^{-/-} genetic background by an additional 2 generations of double-heterozygous matings. Genotyping was performed by PCR.

Immunohistochemistry

Mice were killed between 10:00 and 14:00 hours by exposure to CO₂ followed by cervical dislocation, or were deeply anesthetized with isoflurane and decapitated before both eyes were enucleated. A small incision was made at the ora serrata, and the whole eye was fixed at room temperature in freshly prepared 4% paraformaldehyde in 0.1M phosphate buffered saline (PBS; pH 7.35) for 15 min. The cornea and lens were removed and the eyecups left in the same fixative solution for an additional 5 min.

Both whole-mounted retinas and cryostat sectioned retinas were used for immunohistochemistry. For whole-mounts, isolated retinas were washed 3 x 15 min in 0.1 M PBS at room temperature, then incubated in blocking solution (0.3% Triton X-100 v/v, 0.1% sodium azide w/v and 1% bovine serum albumin w/v in PBS) for 1-2 hours at room temperature or overnight at 4°C. Retinas were incubated overnight in primary antibodies diluted in blocking solution (Table 2.1) at room temperature on a shaker table. Retinas were then washed (3 x 15 min) in PBS and incubated, either at room temperature for 2 hours or overnight at 4°C, in the appropriate secondary antibodies. After a final 3 x 15 min wash in PBS, retinas were mounted on glass slides in Vectashield (Vector Laboratories, Burlingame, CA).

For cryostat sections, fixed eye cups were cryoprotected in 30% sucrose overnight, embedded in OCT (Ted Pella Inc.) and cut into 20µm thick vertical sections. Sections were mounted on glass slides and stored frozen until immunostained using the above protocol. For

immunostaining of peptides, either a fluorescent secondary or 3,3'-Diaminobenzidine (DAB) amplification was employed. For DAB amplification, sections were washed in PBS, then incubated in 1% hydrogen peroxide in PBS for 30-60 minutes. Slides were then washed in PBS, incubated in ABC complex (Vectastain ABC kit, Vector Laboratories) for 2 hours at room temperature, and subsequently in DAB solution (Peroxidase substrate kit DAB, Vector Laboratories) until optimal staining was obtained (5-10 minutes). Slides were washed in Tris-buffered saline (TBS; pH 7.4) and mounted in TBS or Vectashield.

Antibody Specificity

ACTH. Highly purified, iodination-grade ACTH from rat pituitary glands was used as the immunogen for the production of an anti-ACTH antiserum in rabbit. Rat ACTH has 93% sequence homology with mouse (NCBI Blast). The purified antibody was provided by Dr. A. F. Parlow (parlow@humc.edu) of the National Hormone & Peptide Program (NHPP), who found that it did not cross react with any other pituitary hormones. In mouse CNS (Hentges et al., 2009) it was found that anti-ACTH immunoreactivity (ir) was abolished by preadsorption to ACTH 1-39 and was absent in POMC null mice.

α -MSH. The polyclonal α -MSH antiserum was raised in sheep against an immunogen consisting of α -MSH conjugated to bovine thyroglobulin. The specificity of the α -MSH antibody was demonstrated in rat hypothalamus by Elias et al., (1998) who showed that preadsorption of the antibody with its immunogen resulted in loss of specific staining.

Table 2.1. Primary Antibodies Applied in the Current Study.

Antibody	Antiserum	Immunogen	Source	Catalog # / Lot #	Dilution
Adrenocorticotrophic hormone (ACTH)	Rabbit Anti-ACTH	Rat pituitary ACTH	National Hormone & Peptide Program, Torrance, CA	AFP-156102789	1:10000
Alpha-Melanocyte Stimulating Hormone (α -MSH)	Rabbit Anti- α -MSH	α -MSH conjugated with bovine thymoglobulin	Millipore, Billerica, MA	AB5087 / LV1447004	1:10000
Beta Endorphin	Rabbit Anti- β -Endorphin	Synthetic, complete human β -endorphin	National Hormone & Peptide Program, Torrance, CA	AFP-791579Rb	1:5000-1:20000
Calbindin	Rabbit Anti-calbindin, Polyclonal	Recombinant calbindin	Millipore, Billerica, MA	AB1778 / LV1463639	1:2500
Calretinin	Rabbit Anti-calretinin, Polyclonal	Recombinant rat calretinin	Millipore, Billerica, MA	AB5054 / LV1532272	1:5000
Choline Acetyltransferase (ChAT)	Goat Anti-ChAT, Polyclonal	Human placental enzyme	Millipore, Billerica, MA	AB144P / LV1541569	1:200
Glutamate Decarboxylase -6 (GAD65)	Mouse Anti-GAD65	GAD enzyme, 64kDa subunit, rat brain	Developmental Studies Hybridoma Bank, University of Iowa, Iowa City, IA	GAD-6	1:1000
Glycine Transporter T1 (GLYT1)	Goat Anti-Gly-T1, Polyclonal	Synthetic peptide, rat GLYT1 C-terminus	Millipore, Billerica, MA	AB1770 / LV1392052	1:5000-1:10000

β -endorphin. The β -endorphin antiserum was produced in rabbit by Dr. A. F. Parlow using the synthetic peptide YGGFMTSEKSQTPLVTLFKNAIIKNAYKKGE, corresponding to complete human β -endorphin. Human β -endorphin has 94% sequence homology to mouse. The specificity of this antiserum was confirmed in the present study using POMC null mice, in which anti- β -endorphin immunoreactivity was absent in hypothalamus and retina, but present in those tissues of wild type mice.

Calbindin. The polyclonal anti-calbindin antibody was raised in rabbit against recombinant mouse calbindin-28k. Western blot analysis of human cerebellar homogenate with this antibody showed a single band of ~28 kDa in size (Matilla et al., 2001) similar to manufacturer's Western blot analysis of mouse brain lysate. In the developing mouse retina, de Melo and colleagues (2003) used this antibody to immunolabel specifically retinal horizontal cells, consistent with the observation that calbindin-28k is a horizontal cell specific marker in rod-dominant retinas

(Hamano et al., 1990). Haverkamp and Wässle (2000) used an antibody raised against recombinant rat calbindin-28k (Rabbit anti-calbindin, Swant, Bellinzona, Switzerland) to show that besides horizontal cells, some amacrine and ganglion cells, as well as three prominent layers in the IPL, showed calbindin immunoreactivity in the mouse retina. This immunohistochemical staining pattern has been observed in the inner retina in both mouse and rat studies using various other anti-calbindin antibodies (Moon et al., 2005 and Kielczewski et al., 2005, respectively) and it is in perfect agreement with our results (Figure 2.3).

Calretinin. Recombinant rat calretinin was used for the production of an anti-calretinin polyclonal antiserum in rabbit. The rat calretinin has 99% amino acid sequence homology to mouse calretinin (NCBI Blast). In immunoblots of rat tissues it recognizes both calcium-bound and calcium-unbound forms of calretinin (manufacturer's specifications). The molecular mass of calretinin is 29 kDa, and Choi et al., (2009) showed that, in Western blots of dog olfactory bulb tissue, this antibody recognized a corresponding single band. An immunohistochemical study by de Melo et al (2005) used this antibody as a marker for amacrine cells in the developing mouse retina. Gábiel and Witkovsky (1998) showed a similar labeling pattern in the adult rat retina, with calretinin+ amacrine cells located in both the INL and GCL, and three distinct bands in the IPL. This calretinin immunolabeling is in agreement with what Haverkamp and Wässle (2000) reported in the adult mouse retina, and with our results (Figure 2.3).

Choline Acetyltransferase (ChAT). The antigen-affinity purified polyclonal anti-ChAT antibody was generated in goat, using human placental ChAT enzyme. Human ChAT has 86% sequence homology to mouse ChAT (NCBI Blast). Its specificity was established in Western blots of rat brain and skeletal muscle, in which the antibody recognized a single band of 68-72

kD (Brunelli et al., 2005). In retina, this antibody selectively stains a subtype of amacrine cell that also internalize radioactive acetylcholine (Masland and Mills, 1979; Voigt, 1986).

Glutamic Acid Decarboxylase (GAD)65. Affinity purified GAD65 from adult rat brain was used to raise an anti-GAD6 monoclonal antibody in mouse. Rat GAD65 has 98% amino acid sequence homology to mouse GAD65 (NCBI Blast). In Western blot analysis of rat brain this antibody recognized a single band at 59 kD (Chang and Gottlieb, 1988). The corresponding band was absent in Western blots of mouse brain tissue taken from a GAD65 null mouse (Yamamoto et al., 2003).

Glycine Transporter 1 (GLYT-1). A polyclonal anti-GLYT-1 antiserum was raised in goat using a synthetic peptide (Table 2.1), corresponding to amino acids 614-633 at the carboxy-terminus of cloned rat GLYT-1. This peptide sequence is 95 % homologous to that of mouse. In our hands, preadsorption of the antibody with its immunogenic peptide completely abolished immunolabeling in the mouse retina.

For double immunolabeling experiments, preparations were tested with both sequential and concurrent immunohistochemical protocols, with no differences in staining patterns noted. Omission of the primary antibody/antibodies resulted in no immunoreactivity.

To verify that the DsRed transgene product was expressed in authentic POMC neurons and as a control for labeling in the retina, immunolabeling studies were performed in brain slices. Mice were deeply anesthetized and perfused transcardially with 4% paraformaldehyde in PBS. After perfusion, brains were post-fixed in 4% paraformaldehyde for 24 h at 4 °C before sectioning. Brain slices (50 µm thick) including the hypothalamic arcuate nucleus were prepared on a vibratome. Non-specific binding was reduced by incubating the sections in PBS containing 0.3% triton-x and 3% normal goat serum for 30 min at room temperature. Sections were

incubated in primary antibody overnight at 4°C. Antibody sources and concentrations are listed in Table 2.1. Sections were rinsed 3x15 min in PBS then exposed to a fluorescent secondary antibody for 2 hr at room temperature. The tissue was then rinsed and mounted on glass slides for imaging.

In situ hybridization

Eyes were fixed by immersion in PBS containing 4% paraformaldehyde for 1 hour at room temperature, then embedded in Shandon Cryomatrix (Anatomical Pathology International, Runcorn, UK) and frozen on dry ice. Cryosections (12 µm) were collected on RNase treated Super-Frost Plus Slides (Fisher Scientific, Illkirch, France). Slides were then washed for 5 minutes in PBS, acetylated and dehydrated in graded ethanol solutions (70, 90 and 100%). The antisense and sense probes were synthesized and digoxigenin-labeled from the template T9962 obtained from Genepaint (<http://www.genepaint.org>), using SP6 and T7 polymerase, respectively (Promega, Madison, WI, USA), and Dig-UTP (Roche Diagnostics, Basel, Switzerland). The antisense probe targets position 3-967 from the POMC sequence, with the addition of a 105-base long poly A.

After a first step of proteinase K digestion (0.01 µg/ml in 50mM Tris, 5mM EDTA, 0.05% Tween-20, pH 8.0) in PBS, sections were prehybridized for 30 minutes in Hyb-mix solution (Ambion, Austin, TX, USA), hybridized for 5 hours 30 min at 64°C in Hyb-mix containing 300ng/ml riboprobes, and labeled with an anti-digoxigenin antibody coupled to peroxidase (Roche Diagnostics, Basel, Switzerland).

Confocal laser microscopy

Fluorescent images were taken with a Zeiss LSM 510 confocal microscope (Carl Zeiss, Oberkochen, Germany) or with a Nikon PM 800 confocal microscope equipped with a digital

camera controlled by the Spot software program (Diagnostic Instruments, Sterling Heights, MI). On both microscopes, to avoid crosstalk between laser channels, digital images were acquired separately from each laser channel and then merged. Digital files were further processed with deconvolution software (AutoQuant Imaging, Watervliet, NY). For whole-mounted retinas, confocal Z-stack images (200 μm x 200 μm , in a 5x5 matrix) were taken at 40x from the vitreal surface to the OPL in 3-4 μm steps. For vertically cryosectioned retinas, single images or Z-stack images were taken at 40x or 63x in 2-3 μm increments. For all acquisitions, sequential scans at the different wavelengths were performed. Brightness and contrast of images were adjusted in Photoshop CS3 (Adobe 10.1). All such adjustments were made uniformly to the entire digital image.

Quantification and data analysis

Images were compiled and analyzed using Zeiss LSM Images Examiner software (Carl Zeiss, Oberkochen, Germany). Cell counts for each whole-mounted retina were obtained through compilation of Z-stack 40x images from both inner nuclear layer (INL) and ganglion cell layer (GCL) over 1 mm^2 areas in both central and peripheral retinal areas. Cell counts for cryostat sectioned retinas or whole-mounts were performed manually. Statistical analysis was done using paired-Student's t-test (Microsoft Excel, 2003); P-values ≤ 0.05 were considered significant. All graphs were generated with Sigma Plot (Sigma plot 2001, Systat Software Inc.). Cumulative quantitative data are presented as averages \pm SEM.

We performed a nearest-neighbor analysis (Wässle and Riemann, 1978) of DsRed+ cells on a representative retina obtained from a POMC-DsRed transgenic mouse as follows: Confocal images of five, 200 μm x 200 μm areas (quadrates) were randomly selected from both the peripheral and the central retina. Nearest-neighbor distances were measured with 0.1 μm

resolution manually for all DsRed+ cells from center to center of the somas in these quadrates by using Zeiss LSM Images Examiner software (Carl Zeiss, Oberkochen, Germany) in both the INL and GCL. The measurements in the five quadrates at similar eccentricity (i.e. central (C) or peripheral (P)) and within same cellular layers were plotted on histograms using 5 μm binning of the distances. Accordingly, 4 separate histograms (C-INL, C-GCL, P-INL and P-GCL) were generated. Numbers of measurements / bin were normalized to the total number of measurements (n) within the area. The normalized histograms were fitted by a normal Gaussian function:

$$p(r) = k \exp[-1/2((r-\mu)/\sigma)^2]$$

where μ is the mean, σ is the standard deviation of the measurements and k is a normalizing factor (Wässle and Riemann, 1978). The correlation between the histograms and the Gaussian fit (R^2 : coefficient of determination) was calculated by Sigmaplot.

2.4. Results

Distribution of POMC-DsRed+ cells in the retina

A transgenic mouse line was used to assess POMC promoter-driven red fluorophore (DsRed) expression in the retina (Hentges et al., 2009). In a low magnification image of a whole-mounted POMC-DsRed mouse retina (Fig. 2.1A) numerous DsRed-expressing (DsRed+) somas were seen throughout the tissue. Vertical sections (Fig. 2.1B) revealed DsRed+ somas located either at the border of INL and IPL, or within the GCL. Two distinct DsRed+ bands were seen in the middle third portion of the IPL (Fig. 2.1B). No DsRed fluorescence was detected in the outer retina. All DsRed+ somas had a similar round shape and size (diameter $8.5 \pm 1.0 \mu\text{m}$; n=104

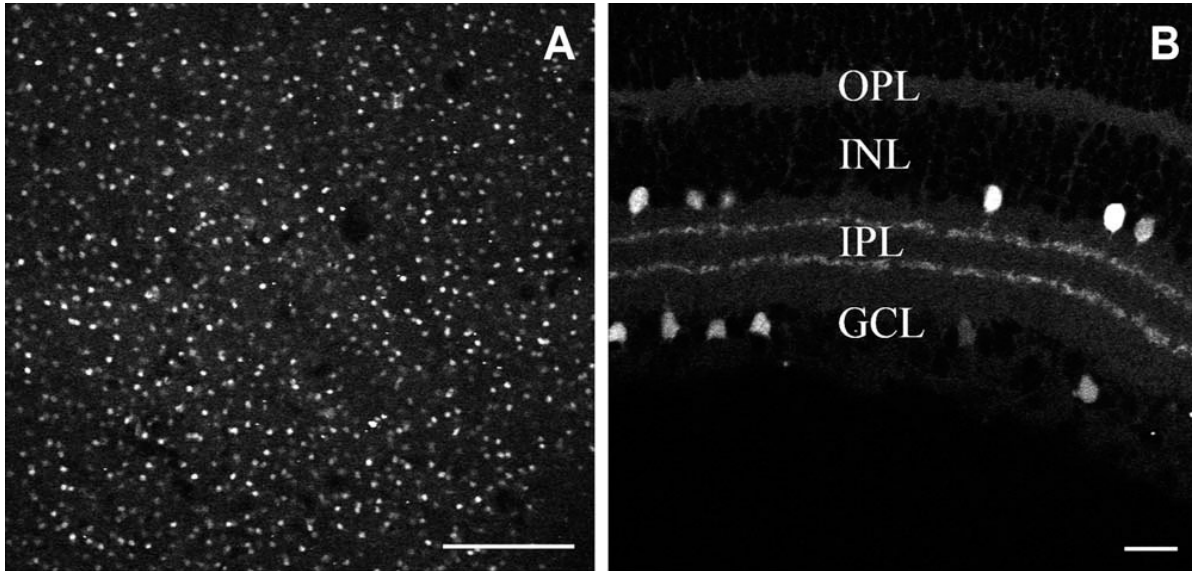


Figure 2.1. DsRed fluorophore expression in the retina of POMC transgenic mice in confocal images of whole-mounted (A) and vertically cryosectioned retinas (B). **A:** Low-power image of a POMC-DsRed retinal whole-mount focused on the INL, showing fluorescent cell bodies of similar shape, size and distribution; scale bar: 200 μ m. **B:** Vertical cryostat section through the POMC-DsRed retina showing bright fluorescent cell bodies of similar shape and size distributed in both the INL and the GCL, with their processes forming two distinct bands within the IPL; scale bar: 20 μ m.

taken from 12 retinas). At low magnification, DsRed fluorescence intensity in labeled somas appeared to be even across cells, indicating a similar expression level of the fluorophore, although no quantification was attempted on this point. The apparent differences in the brightness of DsRed fluorescence among immunostained somas (Fig. 2.1A) resulted from slight differences in the plane of optical sectioning through the imaged cells.

To obtain the retinal density of DsRed+ somas/mm², cell counts were carried out on whole-mounted retinas (n=9 from different animals from 4 different litters), in 5 by 5 adjacent quadrates, 200 μ m x 200 μ m each, at both the center (near the optic nerve) and at the retinal periphery, focusing at both the INL/IPL border and the GCL. Data obtained from a single representative retina are illustrated in Figure 2.2A. Note the variability in the number of DsRed+ cells across quadrates: in the plotted example, cell counts in the INL varied between 29 and 66 in central

retina, and between 28 and 63 in peripheral retina (averaging 47 ± 1.9 and 42 ± 1.7 , respectively). Similarly, in the GCL, cell counts ranged from 17-37/quadrant in central retina and 21-39 in peripheral retina (averaging 27 ± 1.0 and 28 ± 1.6 , respectively). In addition, we found variation in the average DsRed+ cell numbers/quadrant across animals: in the INL, ranging from 28 to 56 in central INL and 30-59 in peripheral INL (giving an overall average of 46 ± 0.8 and 42 ± 0.9 , respectively). In the GCL the comparable variation across animals ranged from 23 to 48 in central retina and 17-43 in peripheral retina (averaging 32 ± 0.7 and 30 ± 0.7 , respectively). Mean cell density/ mm^2 values were obtained by summing cell numbers in 25 quadrants, for both the INL and the GCL in their respective locations and averaging those values across animals (n=9). The analysis of cell density data are summarized in Figure 2.2B. We found that the density of ($1182\pm 64/\text{mm}^2$ vs. $803\pm 86/\text{mm}^2$, $p<0.00001$) and periphery ($1039\pm 87/\text{mm}^2$ vs. $756\pm 77/\text{mm}^2$, $p<0.000009$, paired Student's t-test). Within their respective cellular layers, a slightly higher density of DsRed+ somas was found at the central INL and GCL than in the periphery, but the differences were statistically significant only in the INL (INL, $p<0.02$; GCL: $p<0.09$, paired Student's t-test).

Nearest-neighbor analysis (Wässle and Riemann, 1978) was performed to quantify the tiling regularity of the DsRed+ somas in the retina (for details see Methods). Histograms generated from the nearest-neighbor distance data at each area (INL and GCL at both the center and periphery) were fit well by Gaussian functions (R^2 ranged from 0.89 to 0.98; Fig. 2.2), indicating that distances followed a normal distribution. The average distance between the nearest DsRed+ cells in the INL was $21.0\pm 7.0 \mu\text{m}$ (n=290) at the center and $24.2\pm 7.5 \mu\text{m}$ (n= 207) at the periphery. The comparable average distances in the GCL were $21.6\pm 11.0 \mu\text{m}$ at the center and $24.9\pm 7.5 \mu\text{m}$ at the periphery (n=195 and n=182, respectively). The regularity of DsRed+ soma

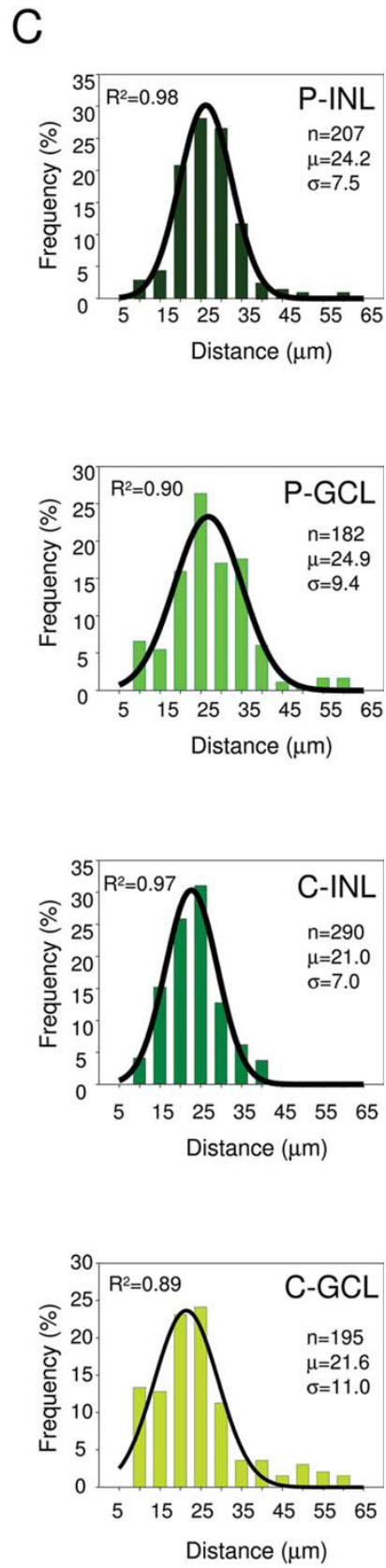
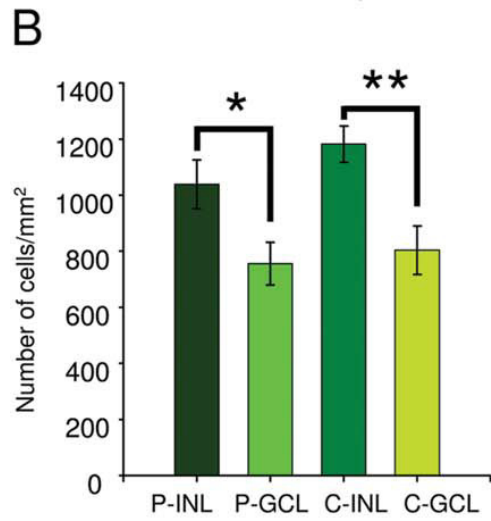
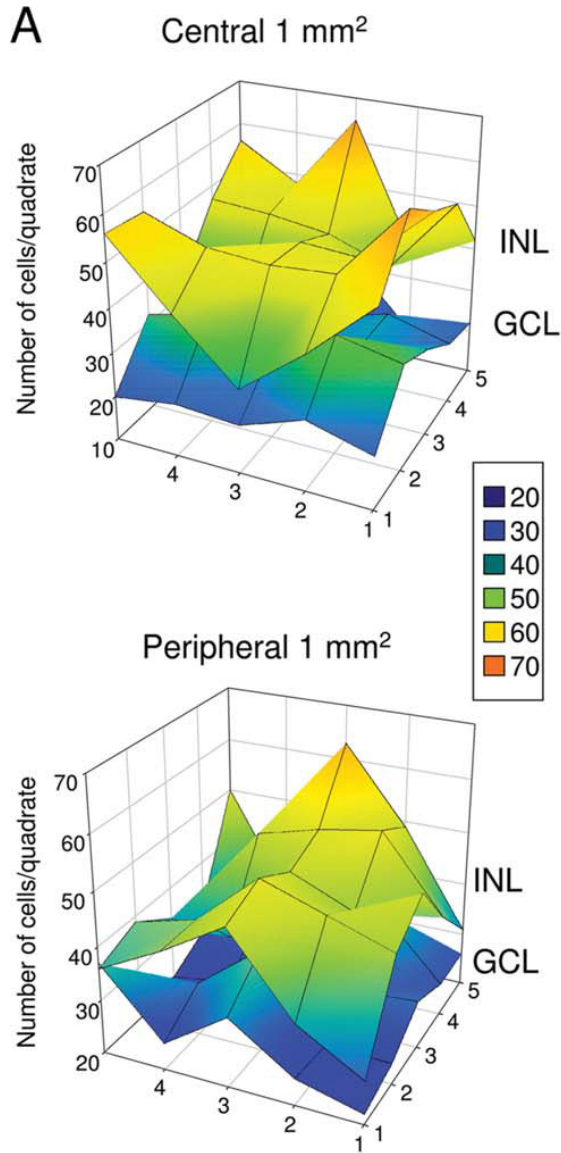


Figure 2.2. A: POMC-DsRed+ soma distribution in a single representative retina. Cell body counts were performed in the inner nuclear and ganglion cell layers (INL and GCL, respectively) over a 1 mm² area compiled from 5x5, adjacent, 200 μm x 200 μm confocal Z-stack images at both the center (C) and at the periphery (P) of the retina. The 3D surface plot shows that despite small differences in the soma counts/quadrant, POMC-DsRed somas were rather evenly distributed in each nuclear layer. However, there are more DsRed+ somas in every INL quadrant than in the corresponding GCL area. The number of total DsRed+ cells/mm² plotted in this example: C-INL:1198; C-GCL:677; P-INL:1068; P-GCL:715. Inset shows how the number of cells counted in the 200 μm x 200 μm quadrants corresponds to colors used for the surface plot. **B:** Cumulative data (n=9) showing POMC-DsRed soma distribution, comparing cell counts within nuclear layers in the periphery (P) and center (C) and between inner nuclear and ganglion cell layers of the mouse retina (i.e. P-INL, P-GCL, C-INL and C-GCL, respectively); error bars represent SEM; *: p<0.00001; **:p<0.000009, paired Student's t-test. **C:** Histograms of the nearest-neighbor distances at (P) and (C) in both inner nuclear and ganglion cell layers of the mouse retina (i.e. P-INL, P-GCL, C-INL and C-GCL, respectively). Bin size: 5 μm. Absolute numbers of observations/ bin were normalized to the total number of measurements (n). Normalized histograms were fitted with Gaussian distribution functions (solid lines). R²: coefficient of determination; μ: average of nearest-neighbor distances; σ: standard deviation.

distribution given by the mean distance (μ) divided by the standard deviation (σ) (Wässle and Riemann, 1978) revealed higher regularity in the INL (R=3.0 at the center and R=3.2 at the periphery) than in the GCL (R=1.9 at the center and R=2.6 at the periphery).

To assess the position of the DsRed+ bands in the IPL, vertical sections of DsRed+ mouse retinas were immunostained for two calcium binding proteins, calretinin and calbindin. Calretinin and calbindin are expressed in a congruent trilaminar pattern in the IPL of the mouse retina (Haverkamp and Wässle, 2000). We found that the inner DsRed+ band overlapped with the inner calretinin (Fig. 2.3A-C) and calbindin (Fig. 2.3D-F) strata between sublaminae 3 and 4, whereas the outer DsRed+ band in the IPL co-localized with the outermost strata of both calretinin and calbindin. Accordingly, the outer DsRed+ band is situated between sublaminae 1 and 2 (Ghosh et al., 2004).

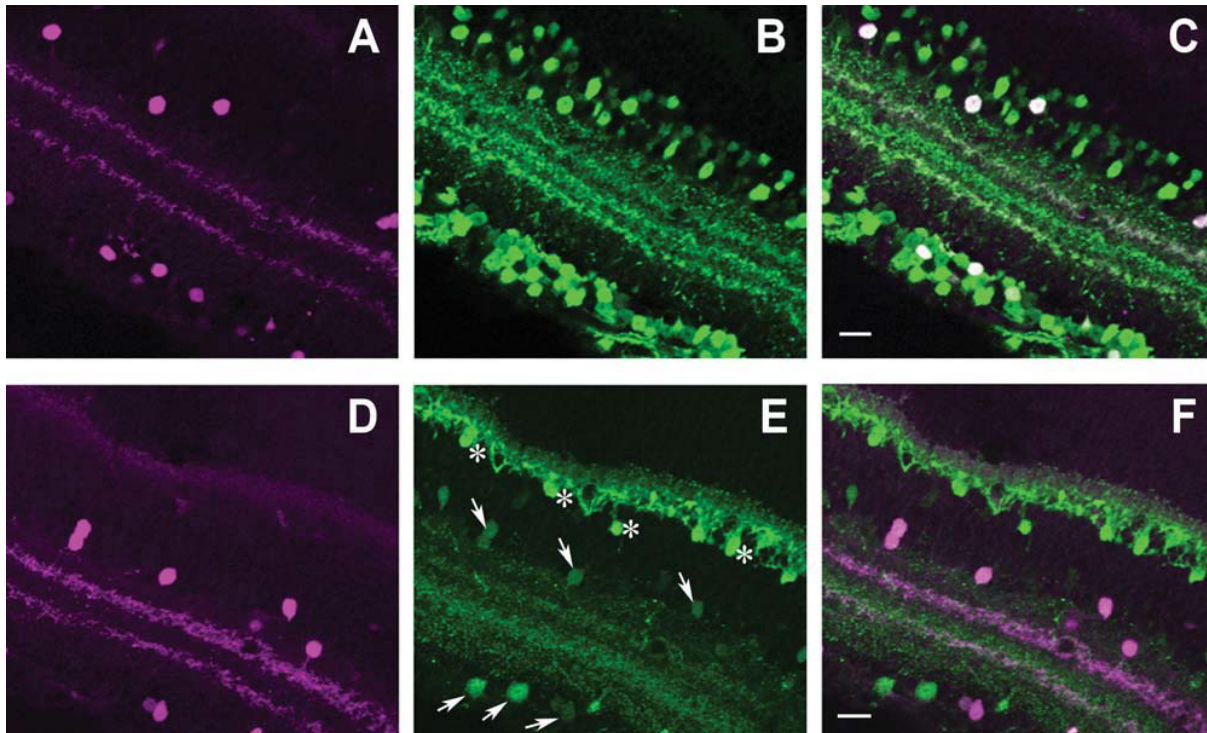


Figure 2.3. Calcium-binding proteins in POMC-DsRed+ cells in confocal images of vertical cryostat sections. **A, D:** POMC-DsRed (magenta) retina showing soma distribution in both the INL and GCL with two bands in the IPL. **B:** Confocal image illustrating the same region as in **A**, showing numerous calretinin+ (green) somas in the INL and GCL and three distinct bands within the IPL. **C:** A merged image of **A** and **B** showing colocalization of POMC-DsRed+ and calretinin+ somas, as well as colocalization of POMC-DsRed+ bands with the inner and outer calretinin+ IPL bands. **E:** Confocal image of the same region as in **D**, showing calbindin+ (green) somas in two distinct regions of the INL with somas also in the GCL and in three distinct bands in the IPL. The calbindin+ (putative horizontal cell) somas (asterisks) at the outer border of the INL and their projections seen in the OPL were more brightly stained than were somas and processes located in the inner retina (arrows). **F:** A merged image of **D** and **E** showing colocalization of POMC-DsRed+ somas and bands with calbindin+ somas and inner and outer IPL bands. Note, all POMC-DsRed+ somas and bands colocalize with calretinin and calbindin. Scale bar: 20µm.

The morphology of POMC-DsRed+ cells with somas in the INL suggested DsRed was expressed by amacrine cells. However, in the mouse retina, about half of the cells in the GCL are ganglion cells, and the other half are displaced amacrine cells (Jeon et al., 1998; Kong et al., 2005), therefore the DsRed+ somas located in the GCL could be either amacrine or ganglion cells, or both. To examine further the identity of DsRed+ retinal neurons in both INL and GCL,

we looked for colocalization of the DsRed signal with well characterized neurochemical markers for amacrine cells.

POMC-DsRed+ cells in the retina are a subset of GABAergic amacrine cells

The mammalian retina has about 30 morphological subtypes of amacrine cell (MacNeil and Masland, 1998); half of them are glycinergic, the other half are GABAergic (Vaney, 1989).

GABA and glycine have not been detected in the same amacrine cells in mammals (Marc et al., 1998; Haverkamp and Wässle, 2000).

In immunohistochemical studies, the glycine transporter 1 (GLYT-1) is preferred to glycine as a marker for glycinergic amacrine cells over glycine, since some cone bipolar cells also contain glycine, whereas only glycinergic amacrine cells express GLYT-1 (Vaney et al., 1998; Pow, 1998, Zafra et al., 1995; Haverkamp and Wässle, 2000).

GLYT-1 immunolabeling was performed on vertical cryostat sections of POMC-DsRed mouse retinas. As shown in Figure 2.4A-C, DsRed+ cells did not colocalize with GLYT-1 indicating that DsRed+ cells in the mouse retina were not glycinergic amacrine cells.

In GABAergic neurons, including GABAergic amacrine cells, GABA is synthesized mainly via decarboxylation of glutamic acid by two isoforms of glutamic acid decarboxylases (GADs), distinguished according to their molecular masses, 65 and 67 kDa (GAD65 and GAD67, respectively). GABAergic amacrine cells in the mammalian retina can express either or both GAD isoforms (Vardi and Auerbach, 1995; Costa and Hokoc, 2003). We found that GAD65 immunostaining was confined to neuronal somas that lacked DsRed fluorescence (Fig. 2.4D-F).

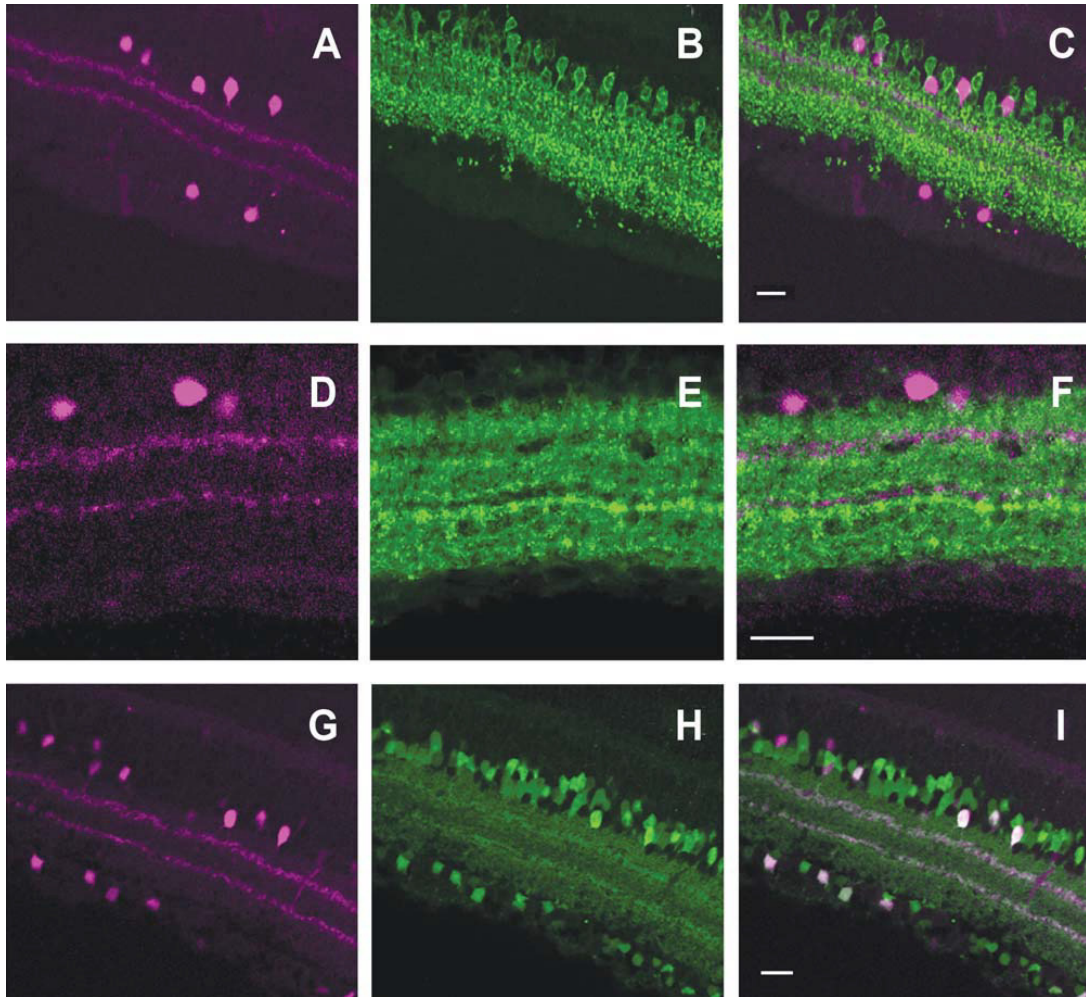


Figure 2.4. Inhibitory amacrine cell marker detection in POMC-DsRed cells in confocal images of vertical cryostat sections. **A, D:** POMC-DsRed (magenta) retina showing soma distribution in both the INL and GCL with two bands in the IPL. **B:** Image representative of the same region as **A**, showing GLYT-1 immunolabeling (green) for numerous cell bodies in the INL with projections throughout the IPL. Note the absence of GLYT-1-ir somas in the GCL. **C:** A merged image of **A** and **B**, showing no colocalization of POMC-DsRed+ cell bodies with GLYT-1 immunolabeling. Additionally, although GLYT-1+ projections are broadly distributed within the IPL, they do not colocalize with the two DsRed+ bands. **E:** Image displaying the same region as in **D**, showing faint GAD65+ somas (green) in the INL and GCL with widespread projections throughout most of the IPL. Note the two distinct bands characterized by an absence of GAD65+ projections in the IPL. **F:** A merged image of **D** and **E** showing no colocalization of GAD65-ir cell bodies or their projections with the two POMC-DsRed+ bands, which distribute within horizontal spaces in the IPL devoid of GAD65-ir. **G:** DsRed+ somas (magenta) and projections of a POMC-DsRed / GAD67-EGFP double transgenic mouse. **H:** Image illustrating the same region as in **G**, showing GAD67-EGFP+ somas in both the INL and the GCL and two bands within the IPL from their projections. **I:** A merged image of **G** and **H** showing strong colocalization of POMC-DsRed+ cell bodies in both the INL and GCL with GAD67-EGFP+ somas. Furthermore, colocalization of these markers in two IPL bands is also seen. Scale bars: 20 μ m.

Furthermore, GAD65 immunolabeling was clearly absent from the DsRed+ IPL strata, whereas other layers of the IPL were strongly labeled, indicating that GAD65 is transported to amacrine cell processes.

To assess the expression of GAD67 in POMC-DsRed+ amacrine cells, we crossed the POMC-DsRed line with a GAD67-EGFP knock-in mouse line that marks GAD67 positive GABAergic neurons in the nervous system (Tamamaki et al., 2003) including the retina (May et al., 2008). In retinas of progeny carrying both GAD67-EGFP and POMC-DsRed constructs, cell counts were performed in whole-mounted retinas (n=2) in 1 mm² areas divided into 200 μm x 200 μm quadrates, at the center and periphery in both INL and GCL. A total of 10029 DsRed+ cells was counted (Table 2.2), of which 9982 (99.5%) colocalized EGFP, i.e., virtually every POMC-DsRed+ cell was EGFP+. Examination of retinal cross sections, moreover, revealed that the two DsRed+ bands in the IPL colocalized EGFP+ in GAD67-EGFP mice (Fig. 2.4G-H).

Table 2.2. DsRed+ soma counts in 2 retinas of progeny carrying both GAD67-EGFP and POMC-DsRed constructs.

	DsRed only (/mm ²)	DsRed + / GAD67+ (/mm ²)	DsRed + / GAD67+ (%)
Retina1_Periphery_INL	2	1253	99.8
Retina2_Periphery_INL	15	1455	98.9
Retina1_Periphery_GCL	0	1091	100
Retina2_Periphery_GCL	15	1041	98.5
Retina1_Center_INL	4	1392	99.7
Retina2_Center_INL	1	1406	99.9
Retina1_Center_GCL	7	1214	99.4
Retina2_Center_GCL	3	1130	99.7

Retinal POMC-DsRed+ neurons are a subset of cholinergic amacrine cells

Cholinergic amacrine cells form two functional subpopulations in the mammalian retina: OFF types with somas located at the INL/IPL border whose processes arborize in a thin layer

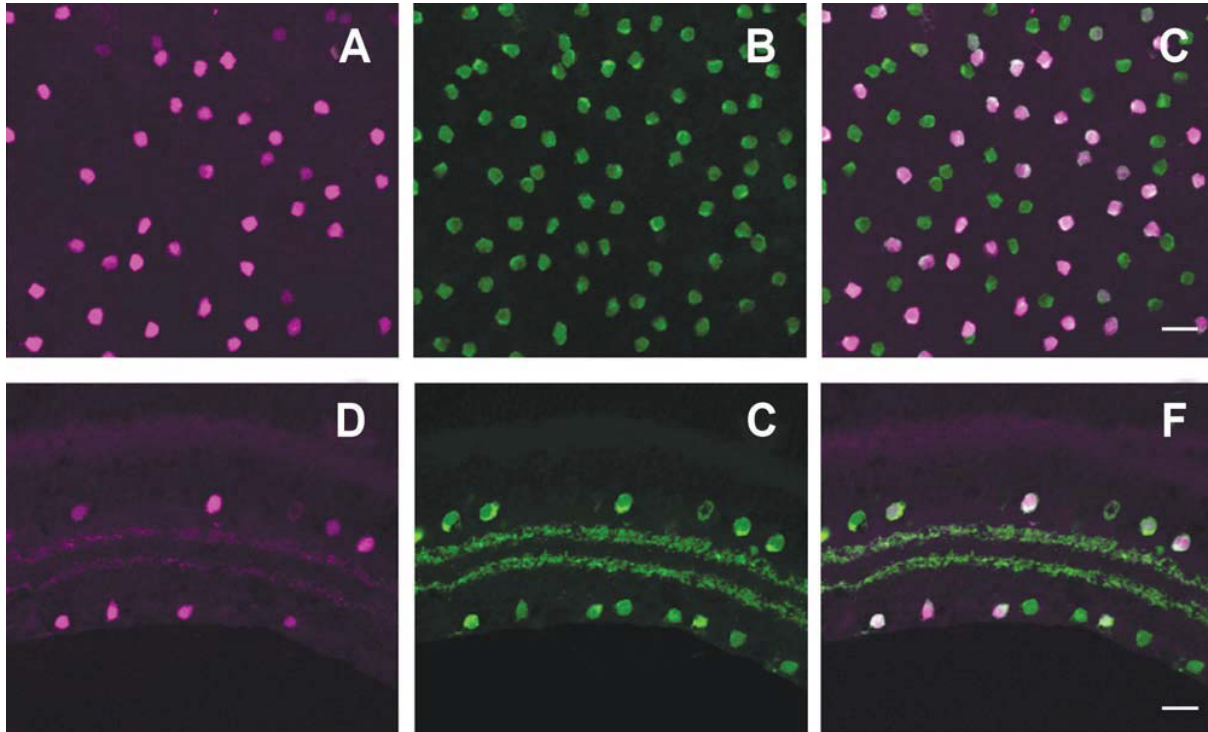


Figure 2.5. POMC-DsRed transgene colocalizes with the cholinergic amacrine cell marker ChAT in confocal images of retinal whole-mounts (**A-C**) and vertical cryostat section (**D-E**). **A:** High-power image of a whole-mounted POMC-DsRed (magenta) retina focused on the INL. **B:** Image illustrating the same region as **A**, showing numerous ChAT+ soma. **C:** A merged image of **A** and **B**, showing strong colocalization of POMC-DsRed+ cell bodies with ChAT (green). Note that not all ChAT+ somas are POMC-DsRed+. **D:** Vertical cryostat section through POMC DsRed (magenta) retina showing the distribution of labeled somas in both the INL and GCL and two bands of labeled processes in the IPL. **E:** Image of the same region as **D**, showing ChAT-ir cell bodies (green) evenly distributed within the INL and GCL and two distinct ChAT-ir bands in the IPL. **F:** A merged image of **D** and **E** demonstrating strong colocalization of POMC-DsRed+ somas and ChAT+ somas within the INL and GCL with further colocalization within two distinct bands of labeled processes in the IPL. Scale bars: 20µm.

between sublaminae 1 and 2 of the IPL, and ON types with somas displaced to the GCL and whose processes arborize between IPL sublaminae 3 and 4 (Haverkamp and Wässle, 2000). The overall distribution of cholinergic amacrine cell somas and their processes was therefore very similar to that of POMC-DsRed+ amacrine cells. Furthermore, cholinergic amacrine cells colocalize calbindin and calretinin (Ghosh et al., 2004) as we found for POMC-DsRed+ retinal neurons. Therefore, we tested directly whether POMC-DsRed, and the cholinergic amacrine cell marker,

choline-acetyltransferase (ChAT)-ir colocalized. We observed that POMC DsRed+ somas colocalized ChAT in both GCL and INL (Fig. 2.5A-C). Consistent with the somatic colocalization, we found strong colabeling of both POMC-DsRed+ strata with ChAT in the IPL (Fig. 2.5D-F). Counts were performed on 5 whole-mounted retinas from 5 different POMC DsRed+ mice (see Methods). The data summarized in Table 2.3 revealed that essentially all POMC-DsRed+ cells were cholinergic in the POMC-DsRed retinas (16439 out of 16457 counted in total), but only approximately 50% of all ChAT+ cells expressed DsRed signal.

Table 2.3. Summary of DsRed+ soma counts in 5 retinas from 5 animals carrying POMC-DsRed constructs, immunolabeled for ChAT

	DsRed+ total (/mm ²)	DsRed+ / ChAT+ (/mm ²)	ChAT+ only (/mm ²)	ChAT+ total (/mm ²)	DsRed+ / ChAT+ (%)	ChAT+ / DsRed+ (%)
Periphery_INL	918 ± 73	917 ± 73	887 ± 97	1804 ± 89	51 ± 4	100 ± 0.04
Periphery_GCL	640 ± 68	640 ± 68	835 ± 106	1475 ± 85	46 ± 5	100
Center_INL	1097 ± 77	1077 ± 77	977 ± 21	2050 ± 72	53 ± 2	100 ± 0.1
Center_GCL	655 ± 53	654 ± 53	931 ± 45	1586 ± 49	44 ± 3	100 ± 0.04

POMC gene products expressed in DsRed+ hypothalamic neurons and in the pituitary.

Although transgenic mice may reliably express a detectable level of fluorophore under neuronal promoter control, this result has to be further evaluated because of the complex regulation of such transgene expression. Multiple reports show great variation in promoter-driven fluorescent marker expression across brain areas (von Engelhardt et al., 2007; Caputi et al., 2009). In extreme cases, not only are the expression levels different, but the fluorophore can be expressed in cell populations in which the promoter does not normally drive expression in wild type mice (ectopic expression). As a case in point, a ChAT-EGFP transgenic mouse line expresses EGFP in retinal amacrine cells having a different morphology than the cholinergic cells that would be expected to be labeled by the transgene (Haverkamp et al., 2009), although a

good correspondence between EGFP and ChAT expression was found elsewhere in the brain of the same transgenic animals (von Engelhardt et al., 2007). Furthermore, the transgene containing the same *Pomc* regulatory elements as those used in the present report and an EGFP fluorophore reporter resulted in nearly perfect eutopic expression of EGFP in POMC neurons of the hypothalamus, but also ectopic expression in immature granule cell neurons of the dentate gyrus in the hippocampus (Overstreet et al., 2004).

Thus, neuronal expression of the DsRed fluorophore, although under the control of the POMC promoter, does not automatically indicate the expression of the large precursor polyprotein POMC or any of its specific cleavage products (ACTH, β -endorphin, or α -MSH). To determine whether POMC gene products were expressed in the mouse retina, we performed immunohistochemical studies to examine possible colabeling of POMC-DsRed+ amacrine cells with antibodies directed against ACTH, β -endorphin, or α -MSH. As a positive control, identical immunostaining was carried out first on pituitaries and brain sections containing the arcuate nucleus of the hypothalamus from POMC-DsRed mice, since the expression of POMC products has been well documented in these regions (Bicknell, 2008).

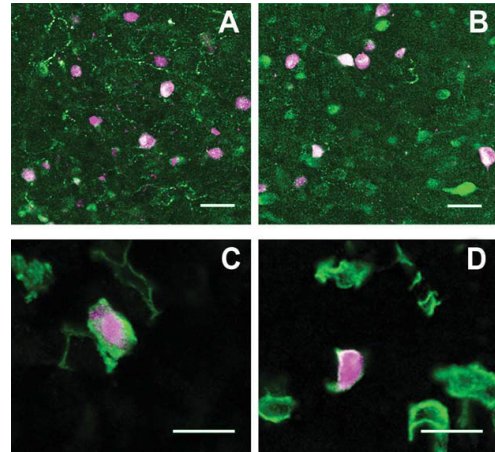


Figure 2.6. POMC-DsRed+ neurons in the arcuate nucleus and the pituitary show β -endorphin immunoreactivity. **A:** β -endorphin immunoreactivity (green) was limited to neuronal fibers and showed only weak immunoreactivity in cell bodies of DsRed+ hypothalamic neurons (magenta). **B:** Inhibiting axonal transport by colchicine increased β -endorphin immunoreactivity in the soma of DsRed+ POMC neurons. In the pituitary, DsRed+ cell (magenta) are immunolabeled for β -endorphin (**C**) and ACTH (**D**) (both green) without colchicine treatment. Scale bars: 20 μ m.

POMC DsRed neurons showed specific ir for ACTH with nearly 100% overlap between DsRed and ACTH-ir in the hypothalamus, independent of the sex of mice used for the studies (Hentges et al., 2009). β -endorphin and α -MSH antibodies also revealed immunoreactive products in DsRed+ hypothalamic neurons, but, for both antibodies, immunostaining was more prominent in fibers than in cell bodies (Fig. 2.6A). Inhibiting axonal transport by intraventricular (i.c.v.) injection of colchicine (Sigma; 10 μ g in 1 μ l) 18 hrs before tissue collection, greatly increased β -endorphin staining intensity in the somas of DsRed+ POMC neurons, confirming that the POMC-DsRed transgene labeled authentic POMC neurons (Fig. 2.6B). In the pituitary, both the β -endorphin and the ACTH antibodies labeled somas, some of which were DsRed+ (Fig. 2.6C, D, respectively). Importantly, all of the DsRed+ anterior lobe cells were corticotrophs because they were colabeled with one or the other POMC peptide antiserum.

DsRed+ retinal amacrine cells express β -endorphin.

Whole-mounted DsRed-expressing retinas were treated with antibodies against ACTH, β -endorphin, or α -MSH as described above for the hypothalamic studies. Unlike the hypothalamus and pituitary, in retinal whole-mounts only the β -endorphin antibody labeled POMC-DsRed+ amacrine cells. Cell counts were performed in two retinas over 1 mm², at the center in one of them and at the periphery in the other. The data are presented in Table 2.4. Most, but not all β -

Table 2.4. Summary of DsRed+ soma counts in 2 retinas from 2 animals carrying POMC-DsRed construct, immunolabeled for β -endorphin.

	DsRed+ total (/mm ²)	DsRed+ / β end+ (/mm ²)	β end+ only (/mm ²)	β end+ total (/mm ²)	β end+ / DsRed+ (%)	DsRed+ / β end+ (%)
Retina1_Periphery_INL	1279	79	14	93	6.1	84.9
Retina1_Periphery_GCL	937	35	16	51	3.7	68.6
Retina2_Center_INL	1221	33	12	55	2.9	73.3
Retina2_Center_GCL	596	1	1	2	0.1	50

endorphin+ somas colocalized DsRed, whereas the percentage of POMC-DsRed expressing cells that colocalized β -endorphin varied between 0.1 and 6.1 %, depending on retinal area: the highest degree of colocalization was observed in the INL at the periphery and the least was in the GCL at the center (Fig. 2.7A-C). Colchicine treatment either i.c.v. or directly into the posterior chamber of the eye (10 μ g in 1 μ l) 18 hr before tissue collection did not increase the number of β -endorphin+ somas in whole-mounted POMC-DsRed retinas (n=4, not illustrated).

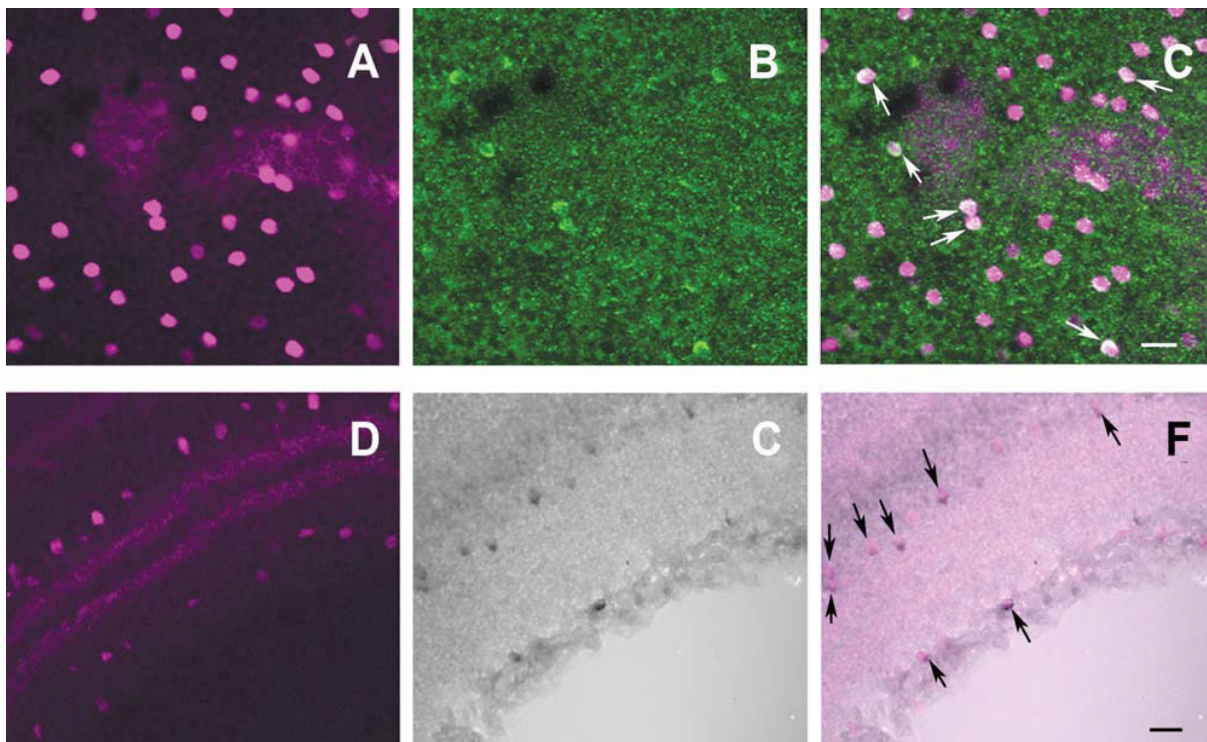


Figure 2.7. In the retina of POMC-DsRed transgenic mice, a subset of DsRed+ amacrine cells colocalizes β -endorphin. **A:** High-power image of a whole-mounted POMC-DsRed (magenta) retina focused on the INL. **B:** Image displaying the same region as **A**, showing distinct β -endorphin+ cell bodies (green) of similar size and shape. **C:** A merged image of **A** and **B**, showing colocalization of β -endorphin and DsRed expression in somas (white arrows). **D:** Vertical cryostat section through POMC-DsRed (magenta) retina showing the distribution of labeled somas in both the INL and GCL with two bands in the IPL. **E:** DAB amplification of cryostat sectioned retinas for visualization of β -endorphin, illustrating the same region as **D**. Note β -endorphin-ir within somas in both the INL and GCL. **F:** A merged image of **D** and **E**, showing perfect colocalization of β -endorphin+ cell bodies with POMC-DsRed signal (black arrows). Note that not all DsRed+ cells show β -endorphin-ir. Scale bars: 20 μ m.

Immunostaining for β -endorphin also was performed on vertical cryostat sections of POMC-DsRed retinas using DAB amplification. As can be seen in Figure 2.7D-F, β -endorphin+ somas were located within the INL and GCL. Furthermore, most β -endorphin+ cells colocalized with POMC-DsRed+ cells within these cellular layers. Importantly, β -endorphin staining with DAB intensification in vertical retinal sections revealed more β -endorphin+ cells, and a higher colocalization percentage between POMC-DsRed and β -endorphin: approximately 44% of DsRed+ somas were labeled for β -endorphin compared to the whole-mount data obtained with β -endorphin immunolabeling (6% at most). It is noteworthy that even with the DAB we did not detect β -endorphin-ir in all DsRed+ cells. DAB amplification did not reveal ACTH or α -MSH immunopositive retinal cells under similar conditions (not illustrated).

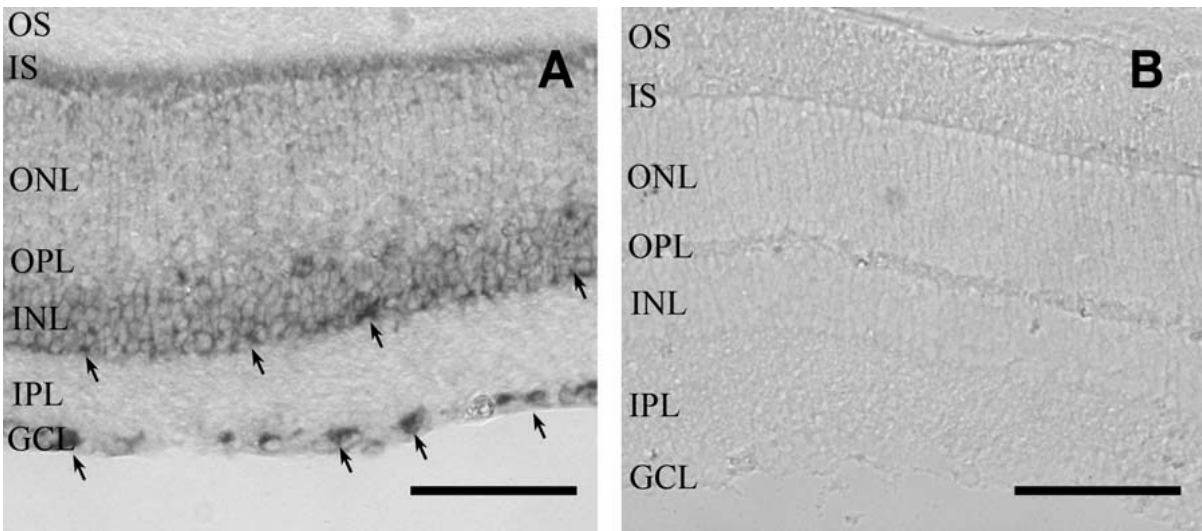


Figure 2.8. In situ hybridization reveals POMC mRNA in the GCL and INL of wild-type mouse retinas (A). Note the dark reaction product obtained with the antisense probe, indicative of POMC mRNA expression in somas located in the GCL and in INL (arrows). (B): The sense probe failed to label any structure in the retina. OS: photoreceptor outer segment layer; IS: photoreceptor inner segment layer; ONL: outer nuclear layer; OPL: outer plexiform layer; INL: inner nuclear layer; IPL: inner plexiform layer; GCL: ganglion cell layer. Scale bars: 80 μ m.

POMC mRNA expression in wild-type mouse retina

To investigate whether *Pomc* promoter-driven DsRed expression in cholinergic amacrine cells was a byproduct of transgenic manipulation, we investigated POMC mRNA expression in wild type mouse retina with *in situ* hybridization. POMC mRNA was reliably detectable in somas located at the inner border of the INL as well as in somas located in the GCL. A faint signal was occasionally visible in the outer part of INL, towards the OPL (Fig. 2.8A). We did not find POMC mRNA signal in the IPL. The control sense probe did not give any signal (Fig. 2.8B).

These results demonstrate that *Pomc* is expressed in the mouse retina. Moreover, the POMC mRNA signal location strongly supports the supposition that a fraction of cholinergic amacrine cell somas express POMC mRNA in the wild type mouse, indicating that the red signal in the cholinergic amacrine cell of the POMC-DsRed mice was not ectopic. However, further studies are needed to completely rule out the possibility that some level of expression is ectopic.

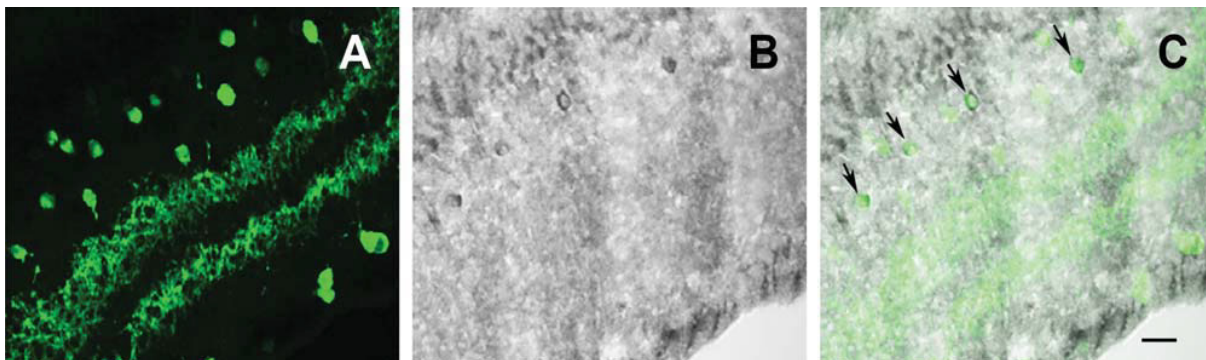


Figure 2.9. ChAT+ amacrine cells express β -endorphin in the wild-type mouse retina. **A:** A slightly tangential section of wild-type mouse retina showing ChAT+ (green) soma distribution in the INL and GCL together with two bands of immunolabeled processes in the IPL. **B:** DAB amplification of cryostat sectioned retinas for visualization of β -endorphin, illustrating the same region as **A**. **C:** A merged image of **A** and **B**, showing uniform colocalization of β -endorphin+ cell bodies with ChAT+ cells, black arrows. Note that not all ChAT+ cells are β -endorphin+. Scale bar: 20 μ m.

Cholinergic amacrine cells express β -endorphin in wild-type, but not in the POMC knock out mouse retina

To assess whether cholinergic amacrine cells indeed express β -endorphin we performed double immunostaining for β -endorphin and ChAT on vertical cryostat sections of wild-type mouse retinas. As can be seen in Figure 2.9A-C, DAB-intensified β -endorphin staining occurs in wild-type retinas. Out of 132 β -endorphin cells 108 (82%) were also ChAT+. On the other hand, in the same retinal sections a total of 1274 ChAT+ amacrine cells was counted, therefore approximately 9 % of ChAT+ cells co-expressed β -endorphin in the wild-type mouse retina. In contrast, in the retinas of POMC-KO mice, no β -endorphin colabeling of ChAT+ retinal neurons in vertical cryostat sections was observed (compare Fig. 2.10 A-C to D-F, wild-type vs. POMC-KO, respectively). The number of β -endorphin+ fibers and somas is relatively high in the hypothalamus of both POMC-DsRed transgenic (Fig. 2.6B-C) and wild-type mice (Fig. 2.10G). No neuronal staining was observed for β -endorphin in the arcuate nucleus of POMC-KO mice (Fig. 2.10H), consistent with a lack of β -endorphin labeling in the retina of POMC-KO mice (Fig. 2.10E-F). These findings confirm the specificity of the β -endorphin antibody used in the present studies.

2.5. Discussion

The present data demonstrate that expression of the POMC-DsRed transgene is almost exclusively confined to a well defined class of retinal cells, the GAD67-positive, cholinergic amacrine cells. Furthermore, a sizeable fraction of the POMC-DsRed amacrine cells is immunoreactive for the opioid product, β -endorphin, but not for ACTH or α -MSH. Wild-type mouse retina also expresses POMC mRNA as demonstrated by *in situ* hybridization. The

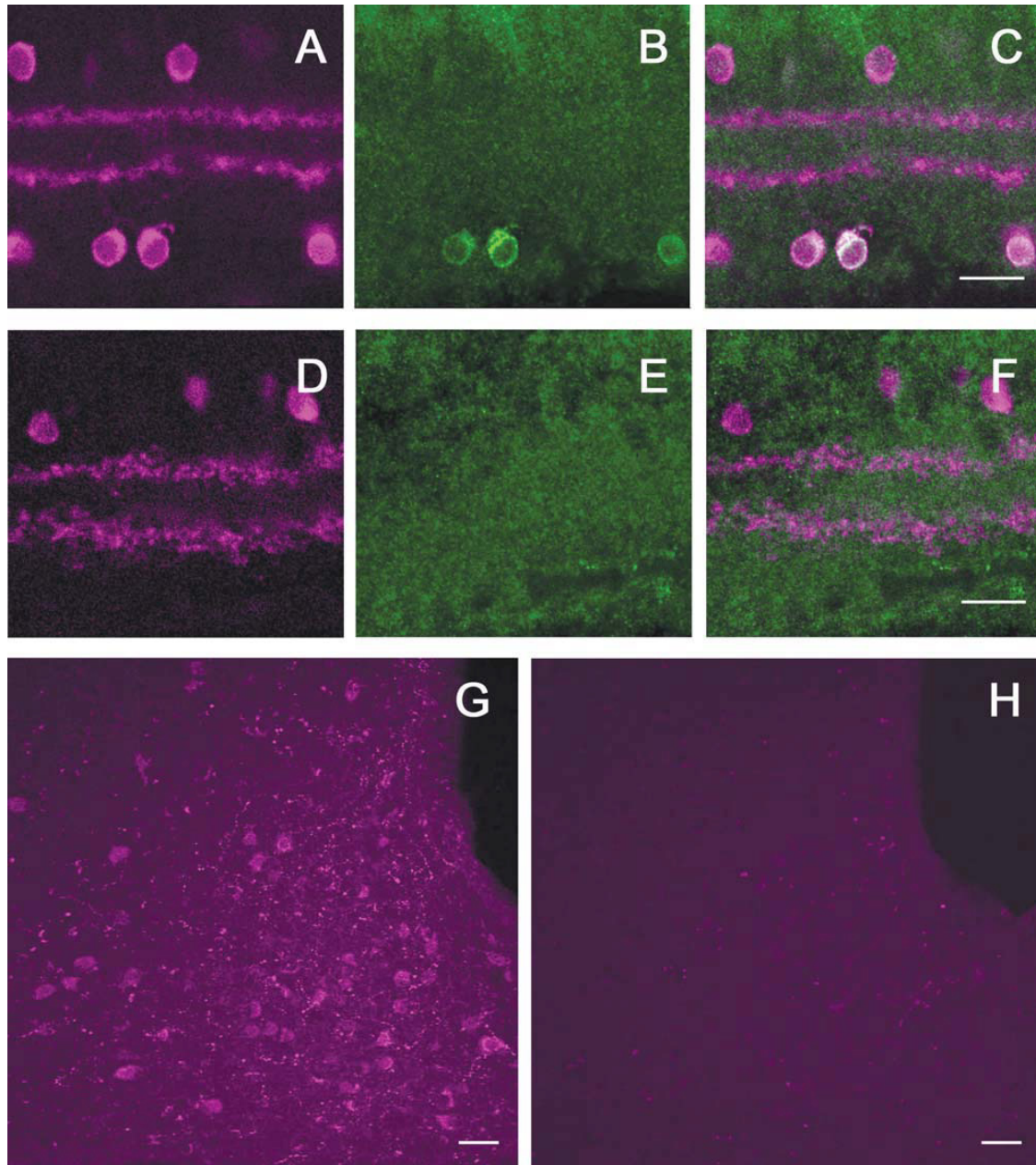


Figure 2.10. β -endorphin antibody labeling is specific to POMC neurons in both retina and hypothalamus. **A:** POMC-DsRed (magenta) retina showing DsRed+ soma distribution in both the INL and GCL with two DsRed bands in the IPL. **B:** Same region as in **A**, showing β -endorphin+ somas within GCL. **C:** A merged image of **A** and **B**, showing colocalization of POMC-DsRed+ cell bodies with β -endorphin+ somas. **D:** Vertical cryostat section through POMC-KO retina immunolabeled for ChAT (magenta), showing ChAT+ cell bodies, with two bands in the IPL. **E:** Image illustrating the same area as **D**, stained with anti-bodies against β -endorphin (green), showing no specific labeling of somas or projections. **F:** A merged image of **D** and **E**, showing only ChAT+ cell bodies and projections. **G:** β -endorphin immunolabeling (magenta) in the arcuate nucleus of hypothalamus in wild type mouse. **H:** β -endorphin immunolabeling (magenta) in the arcuate nucleus of the hypothalamus in POMC KO (*Pomc^{-/-Tg}*) mouse. Scale bars: 20 μ m.

location of POMC mRNA expressing somas was similar to that of cholinergic amacrine cells, validating the immunohistochemical data. Finally, double-label immunohistochemistry revealed that β -endorphin is present in cholinergic amacrine cells in wild-type mouse retinas. A small fraction of neurons expressing β -endorphin-immunoreactivity was not cholinergic, but we have no further information about these cells beyond their location in inner retina.

Together, the data demonstrate that β -endorphin is expressed in a subset of ChAT+ amacrine cells in the mouse retina. Whether β -endorphin expression marks a functionally distinct subclass of cholinergic amacrine cells across the retina has to be further investigated. The absence of ACTH and α -MSH immunoreactivity in retinal neurons could be secondary to selective processing of POMC at the carboxyl end within these cells. Alternatively, the non-opioid POMC peptides may somehow be selectively degraded or released so they do not achieve detectable levels in the neuronal soma.

Reliability of transgenic mouse lines

Transgenic mouse lines with reporter genes expressed in retinal cells have become an increasingly important tool for extending our knowledge of retinal structure and function. The basic approach is straightforward: couple a fluorophore, such as EGFP, or DsRed in the present case, to a cell-type specific promoter sequence to achieve reliable, high levels of marker expression in the targeted neuron population. Numerous examples show, however, that the expression pattern of the marker may not match completely the distribution of the targeted cells. Sometimes the transgenic fluorescent signal: (1) cannot be detected in the entire neuron populations as expected based on the natural expression pattern of the promoter (Oliva et al., 2000); (2) extends beyond the targeted population (Raymond et al., 2008) or (3) localizes to a set of cells completely distinct from the intended targets (Sarthý et al., 2007). These scenarios may

even combine when a given transgenic marker expression is compared across different areas of the central nervous system. One example is the ChAT-EGFP mouse line (von Engelhardt et al., 2007) in which transgenic EGFP expression and immunohistochemical ChAT signal showed perfect correspondence in cranial nerve nuclei or in spinal cord motoneurons, but only 35% of ChAT+ striatal, and 42% ChAT+ cortical neurons expressed EGFP. Furthermore, in the retina of this ChAT-EGFP mouse line, although EGFP was expressed by a single amacrine cell population, it was distinct from the population found to be ChAT+ by immunostaining (Haverkamp et al., 2009).

These concerns notwithstanding, retinal transgene expression usually remains constant for a given mouse line. Therefore studying and characterizing labeled neurons constitutes a viable tool that can be used to extend our knowledge of retinal circuitry and function (Raymond et al., 2008; Haverkamp et al., 2009). In the POMC-DsRed mouse line DsRed signal was consistently expressed in about 50% of ChAT+ amacrine cells across animals and we found a good correspondence between expression of the transgenic signal (DsRed) and an endogenous product (β -endorphin) in the retina. Thus the transgenic approach helped us to identify neurons expressing POMC and in turn, its cleavage product, even though the transgenic POMC-DsRed signal expression exceeded the number of amacrine cells stained for β -endorphin.

The cell counts of DsRed+ neurons underlying the nearest-neighbor analysis established that POMC-expressing amacrine cells are found evenly dispersed in both central and peripheral retina in both orthotopic and displaced layers. However, the regularity of DsRed+ neuron distribution (R) among the population of cholinergic amacrine cells was higher in the INL than in the GCL (~3 vs. ~2, respectively). Spatial pattern analysis performed on the entire population of cholinergic amacrine cells in the mouse retina (Whitney et al., 2008) revealed a similar difference between the

regularity indexes calculated from nearest-neighbor distances in the INL and GCL although at higher overall regularity (4-5 vs. 3, respectively). Based on their detailed analysis Whitney and colleagues (2008) concluded that even the less regularly packed GCL mosaic of cholinergic cells is non-random, representing a degraded version of a more regular, self-spacing mosaic. Based on our nearest-neighbor analysis, POMC-DsRed+ neurons also form a (degraded) regular mosaic as a regularly distributed subpopulation of cholinergic amacrine cells. However, this tentative conclusion needs further testing, since the nearest- neighbor analysis alone is not always enough to discriminate regular spatial mosaics from random distributions (Whitney et al., 2008; Eglén et al., 2003)

The discrepancy in the relative numbers of DsRed+ and β -endorphin+ cells may indicate an asynchronous rhythm in β -endorphin synthesis across the total population of cells. In that regard, in the frog retina, β -endorphin expression follows a seasonal rhythm (Jackson et al., 1980). In mammalian retinas, moreover, many genes have been shown to wax and wane on a diurnal or circadian cycle (Storch et al., 2007). Whether β -endorphin production in the mammalian retina is rhythmic remains to be tested.

Opioids may influence retinal function via opioid receptors in the mammalian retina

Opioid binding sites were shown first in rat (Howells et al., 1980), and subsequently in rabbit retina homogenates (Slaughter et al., 1985). In monkey and rat retinas, opioid binding sites are distributed over the IPL and GCL (Wamsley et al., 1981). This is consistent with μ -OR immunoreactivity in the IPL of rat retina, which is associated with bistratified ganglion cells, whose processes ramify in sublaminae 2/3 and 4 (Brecha et al., 1995). A recent report also demonstrated κ and δ -OR immunofluorescence in the IPL and GCL in rat retina (Husain et al., 2009).

Very little is known about the physiological effects of opioids in the retina. Early studies indicate that enkephalins are released from amacrine cells upon depolarization in a calcium-dependent manner (Su et al., 1983) and inhibit GABA release in the chicken retina (Watt et al., 1984), suggesting that GABAergic amacrine cells possess opioid receptors. Similarly, in goldfish retina exogenous enkephalin enhanced ON ganglion cells spiking plausibly via a disinhibition exerted on GABAergic amacrine cells (Djamgoz et al., 1981). These findings are in accord with the nature of signal transduction pathways linked to the G-protein-coupled μ , κ , or δ opioid receptors (ORs): all three classes have been shown to inhibit adenylate cyclase and voltage-gated calcium channels, or increase inwardly rectifying potassium currents, depending on the studied cell type (see Kieffer, 1995 for review). Although the actual opioid-evoked effects on (GABAergic) amacrine cells are not known, any of the possible opioid actions listed above ultimately leads to inhibition of neuronal activity. Supporting this notion, an ERG study performed in frog and turtle, showed that enkephalin agonists produced inhibitory effects (Vitanova et al., 1990).

On the contrary, in isolated rabbit retinas light-evoked acetylcholine release was enhanced by the μ -OR selective agonist [D-Ala², MePhe⁴, Gly-ol⁵]-enkephalin (DAMGO), independent of GABA- or glycine-mediated inhibition (Neal et al., 1994). The same study showed that kainate-induced acetylcholine release is also enhanced by DAMGO. Taken together, a direct, excitatory opioid effect on cholinergic amacrine cells via μ -OR was proposed (Neal et al., 1994). Nevertheless, to explain the DAMGO effect the putative opioid receptors in the rabbit retina should be located presynaptically on cholinergic amacrine cell processes known to arborize around these strata instead of bistratified ganglion cell dendrites as originally reported in the rat (Brecha et al., 1995). Further study is required to determine whether μ -OR agonist DAMGO

indeed influences cholinergic amacrine cells directly to enhance acetylcholine release (Neal et al., 1994).

Starburst amacrine cells receive excitatory inputs from bipolar cells, and provide directionally coded inputs to directionally selective ganglion cells (Zhou and Lee, 2008). Whether or not opioids influence the retinal computation for motion detection has not yet been investigated. Opioid receptors have also been implicated in ischemia-induced retinal degeneration. However, at this point the role of opioid signaling in this regard is somewhat controversial: in one report intraperitoneal application of the non-specific opioid receptor antagonist, naloxone, prevented ischemic retinal degeneration (Lam et al., 1994) whereas in the other, the general opioid receptor agonist, morphine, was found to be beneficial for the survival of ischemia-challenged inner retinal neurons (Husain et al., 2009). Hypoxic preconditioning also led to up-regulation of δ -OR in rat retinas (Peng et al., 2009).

In summary we have shown that a large fraction of cholinergic amacrine cells, which have a fundamental role in processing information about motion within the mammalian retina (Zhou and Lee, 2008), express β -endorphin. The relevant receptor for β -endorphin, the μ -OR, is reported to be located on ganglion cell dendrites within the IPL (Brecha et al., 1995) which places them in close spatial apposition to the sites of β -endorphin release. Although functional data are lacking, these anatomical findings suggest a role for β -endorphin in ganglion cell signal processing, analogous to what has been reported for other retinal peptides (Zalutsky and Miller, 1990a,b).

3. μ -opioid receptor immunolabeling in the mammalian retina

The second aim of this work was the identification of cell types possessing μ -opioid receptor in mouse retina. Standard immunohistochemical techniques and known molecular markers for retinal cell-types were used. This chapter includes a complete published manuscript, *Dopaminergic amacrine cells express opioid receptors in the mouse retina* (Shannon K. Gallagher, Julia N. Anglen, Justin M. Mower, Jozsef Vigh, *Visual Neuroscience*, 2012), as well as unpublished data relevant to this aim. My contributions to this publication included experimental design, performing and optimizing all immunohistochemistry (IHC) preparations, imaging of all IHC preps, quantification, analysis and interpretation of all data, along with writing and editing of the manuscript. The manuscript will discuss δ -opioid receptors as well, but that information is secondary to the scope of this work. This article is reproduced with permission, and only minimal modifications were made to meet formatting requirements. No other modifications were made, as per the licensing agreement (copyright clearance found in Appendix I).

3.1. Summary

The presence of opioid receptors has been confirmed by a variety of techniques in vertebrate retinas including those of mammals; however, in most reports the location of these receptors has been limited to retinal regions rather than specific cell-types. Concurrently, our knowledge of the physiological functions of opioid signaling in the retina is based on only a handful of studies. To date, the best documented opioid effect is the modulation of retinal dopamine release, which has been shown in a variety of vertebrate species. Nonetheless, it is not known if opioids can affect dopaminergic amacrine cells (DACs) directly, via opioid receptors expressed by DACs. This study, using immunohistochemical methods, sought to determine whether (1) μ - and δ -opioid

receptors (MORs and DORs, respectively) are present in the mouse retina, and if present, (2) are they expressed by DACs. We found that MOR and DOR immunolabeling was associated with multiple cell-types in the inner retina, suggesting that opioids might influence visual information processing at multiple sites within the mammalian retinal circuitry. Specifically, colabeling studies with the DAC molecular marker anti-tyrosine hydroxylase antibody showed that both MOR and DOR immunolabeling localize to DACs. These findings predict that opioids can affect DACs in the mouse retina directly, via MOR and DOR signaling, and might modulate dopamine release as reported in other mammalian and non-mammalian retinas.

3.2. Introduction

Endogenous opioids play an important role in processing sensory information such as pain (Akil et al., 1984; Pan et al., 2008), but only sporadic data suggest that endogenous opioids are present in the mammalian retina: enkephalin was detected in inner retinal neurons of guinea pigs (Altschuler et al., 1982) and in rat retinal extract (Peng et al., 2009), and we recently demonstrated the expression of β -endorphin in cholinergic amacrine cells in mouse (Gallagher et al., 2010). The three classes of opioid receptors do not show exclusive endogenous substrate specificity, however, β -endorphin binds preferentially to μ -opioid receptors (MORs), enkephalins to δ -opioid receptors (DORs) and dynorphins to κ -opioid receptors (KORs) (Kieffer, 1995). Out of these three receptor classes, binding studies with [3 H]dihydromorphine indicated autoradiographic labeling in the inner plexiform and ganglion cell layers (IPL and GCL, respectively), suggesting the presence of MORs and/or DORs in rat and monkey retinas (Wamsley et al., 1981). In rat retina, Peng et al., (2009) showed the presence of both MORs and

DORs through RT-PCR and Western blot analysis, and MORs were also detected by immunohistochemistry on processes of bistratified ganglion cells (Brecha et al., 1995).

In the mammalian retina opioids regulate cell proliferation during development (Isayama & Zagon, 1991), influence cell survival following hypoxic or ischemic challenge (Husain et al., 2009; Peng et al., 2009; Riazi-Esfahani et al., 2009) and regulate dopamine release via DOR and MOR activation (Dubocovich & Weiner, 1983). As dopamine—released from dopaminergic amacrine cells (DACs)—exerts action in a paracrine fashion on most retinal cell-types to promote adaptation to bright light conditions (Witkovsky, 2004), opioid regulation of dopamine release could have profound physiological consequences in the retinal circuitry.

The aim of this study was to investigate the presence and the location of opioid receptors in the mouse retina with immunohistochemical methods. Here we show that MOR and DOR immunolabeling is associated with ganglion- and GABAergic amacrine cells, including DACs. We propose that in the mouse retina β -endorphin, released from cholinergic amacrine cells (Gallagher et al., 2010), acts on MORs (and perhaps DORs) relatively close to its release site in the inner retina, and might affect visual processing by amacrine, and ganglion cells, much like substance P (Brecha et al., 1989; Zalutsky & Miller, 1990). Specifically, the results of this study predict that in the mouse retina endogenous opioids can exert their effect via direct action on MORs and DORs expressed by DACs and might modulate dopamine release.

3.3. Materials and methods

Animals

Adult male and female wild-type C57 and C57BL/6J mice, GAD67-EGFP transgenic mice (Tamamaki et al., 2003) and Sprague-Dawley dams were used for experimentation. Animals

were handled in compliance with the Colorado State University Institutional Animal Care and Use Committee and all procedures met United States Public Health Service Guidelines. All efforts were made to minimize the number of animals used and any possible discomfort. Mice were obtained from Jackson Laboratories, Bar Harbor, ME, and rats from Harlan Laboratories, Indianapolis, IN. Animals were kept on a 12 hr light:12 hr dark cycle with lights on at 6:00 AM, fed standard chow and water *ad libitum*.

Immunohistochemistry

Immunohistochemical procedures on retina-, brain-, and dorsal root ganglia (DRG)-sections were conducted as previously described for retinal sections (Gallagher et al., 2010), except an antigen retrieval step (15 min in boiling 10 mM sodium citrate) followed by 0.5% sodium borohydride treatment for 45 min was included. Brain slices were prepared from anesthetized (i.p. 0.1 – 0.15 ml of 50 mg/ml Beuthanasia-D (Schering-Plough Animal Health)) mice transcardially perfused with 0.1 M phosphate buffer (PB) and 4% paraformaldehyde (PFA) in PB. After perfusion brain was removed, post-fixed for 1-2 hrs, cryoprotected and sectioned (50 μ m). Rats were anesthetized with isoflurane and euthanized via decapitation. DRGs were removed, fixed in 4% PFA, cryoprotected and sectioned (20 μ m).

Antibodies

Antibody raised against Brn-3a. This goat anti-Brn-3a antibody (C-20) was generated against a synthetic peptide corresponding to the N-terminus region of human Brn-3a (Santa Cruz Biotechnology: sc-31984). Western blot analysis of rat retina lysate yielded a 48 KD band (Nadal-Nicolás et al., 2009). In the mouse retina, this antibody has been used to exclusively label retinal ganglion cells (Galindo-Romero et al., 2011).

Antibodies raised against δ -opioid receptors (DORs). The first rabbit anti-DOR antibody was generated against a synthetic peptide corresponding to amino acids 2-18 (ELVPSARAELQSSPLVN) of the N-terminus of mouse DOR (Alomone Labs: AOR-014 / AN-01). Western blot analysis of rat cortex lysate showed bands representing receptor monomers (37-43 kD) and dimers / oligomers (>75 kD) which were absent in experiments preincubated with control peptide (manufacturer's specifications). This antibody was used in mouse DRG, showing immunolabeling of both large and small neurons which was abolished via preadsorption with control peptide and absent in DOR knock-out mice (Wang et al., 2010).

The second polyclonal rabbit anti-DOR antibody (Millipore: AB1560 / LV1480422) used in this study was raised against the N-terminus of mouse DOR (LVPSARAELQSSPLV). Western blot analysis of adult rat brain homogenate identified bands representing receptor monomers, dimers, and possible oligomers, which were blocked with preadsorption in control peptide (Persson et al., 2005). In rat, this antibody has been shown to label DOR+ and large, medium, and small neurons in DRG (Kabli & Cahill, 2007). In our hands, this anti-DOR antibody showed similar and appropriate labeling in cryostat sectioned rat DRG (data not shown).

Antibodies raised against μ -opioid receptors (MORs). The first rabbit anti-MOR antibody used in this study was generated against a peptide corresponding to amino acids 22-38 (CSPAPGSWLNLSHVDGN) of the extracellular N-terminus of rat MOR (100% homology with that of mouse) (Alomone Labs: AOR-011 / AN-01). Western blot analysis of rat hippocampus lysate showed a band of 55-60 kD (manufacturer's specifications).

The second rabbit anti-MOR antibody (Epitomics: 3675-1 / H101201) was raised against a synthetic peptide corresponding to amino acids 386-398 (LENLEAETAPLP) of the intracellular C-terminus of mouse MOR. Western blot analysis of mouse brain homogenates resulted in a

broad band labeling of ~70-80 kDa in wild-type but not in knockout mouse preparations (Lupp et al., 2011). In our hands, this antibody showed similar immunolabeling in mouse hippocampus (data not shown) as seen in rat (Lupp et al., 2011).

Antibody raised against Tyrosine Hydroxylase (TH). The mouse anti-TH monoclonal antibody (Millipore: MAB318 / LV1556893) was generated against TH purified from PC12 cells, and its characterization in mouse retina has been previously described (Gallagher et al., 2010).

Data from images

Confocal laser microscopy. Fluorescent images were taken with a Zeiss LSM 510 confocal microscope (Carl Zeiss, Oberkochen, Germany). For all acquisitions, sequential scans at the different wavelengths were performed. Z-stack images through the full thickness of immunolabeled tissues were taken at 40x, 2-5 μm increments. Brightness and contrast of images were adjusted uniformly in Photoshop CS3 (Adobe 10.1). Images were compiled and analyzed using Zeiss LSM Image Examiner software (Carl Zeiss, Oberkochen, Germany).

Quantification and data analysis. Compiled single-plane (“Z-stack”) images were used for subjective, visual assessment of immunolabeling colocalization. Quantitative analysis of opioid receptor colocalization with TH immunolabeling was performed on single-plane confocal images through the center of TH+ cell bodies or processes (see dashed lines in Fig. 3.2C) using Image J software (NIH, Bethesda, MD, USA). The JACoP plug-in was used to calculate the Pearson’s coefficient \pm SEM (Bolte & Cardelières, 2006) using the Costes’ approach. Pearson’s coefficient (PC) provides an analysis of pixel intensity and location in a dual-channel image with values ranging from -1 to 1 (-1: negative correlation; 0: no correlation; 1: complete correlation) (Gonzalez & Wintz, 1987). The Costes’ approach sets an automatic threshold level for both channels to eliminate inconsistent or irreproducible results. Furthermore, it provides a statistical

probability for disrupting the level colocalization (PC) found on a given two channel image by randomizing the pixels independently 1000 times. In practice, $P > 95\%$ indicates that a colocalization pattern is non-random (Costes et al., 2004; Bolte & Cardelières, 2006).

3.4. Results

μ -opioid receptors in the mouse retina

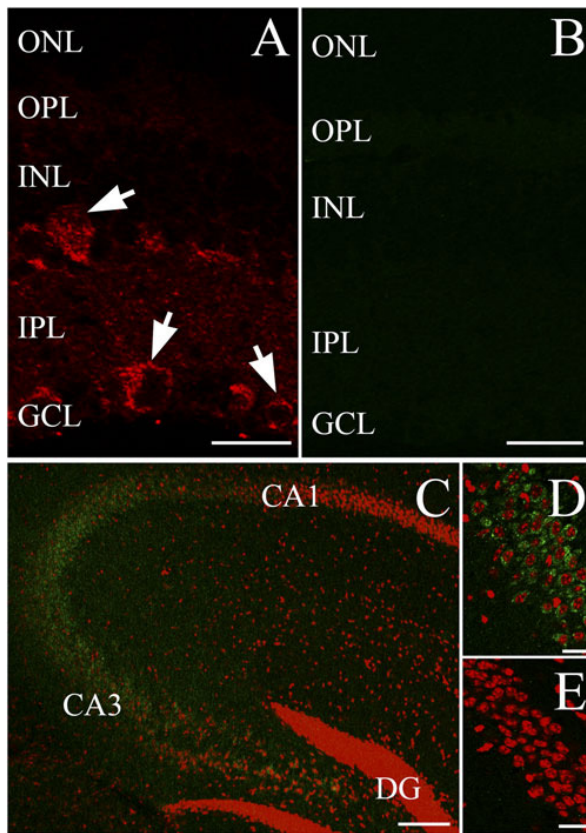


Figure 3.1. Immunohistochemical localization of MORs in mouse retinal and hippocampal tissues. **A:** 40x confocal single-plane image of vertical cryosectioned mouse retina showing immunolabeling with anti-MOR antibody directed against the N-terminus of MOR (Alomone). MOR+ puncta are observed in the inner retina with discernible cells labeled in the INL and GCL (arrows). **B:** 40x image similar to **A** showing control peptide preadsorption for MOR antibody. **C:** 10x confocal image of mouse brain slice focusing on the hippocampus. MOR antibody showing appropriate immunolabeling (green), colabeled with the nuclear marker ToPro3 (red). **D:** 40x focused confocal image of the CA3 region of mouse hippocampus immunolabeled for MORs (green), colabeled with ToPro3 (red). **E:** 40x image similar **D** showing preadsorption of MOR antibody with control peptide, colabeled with ToPro3 (red). ONL: outer nuclear layer; OPL: outer plexiform layer; INL: inner nuclear layer; IPL: inner plexiform layer; GCL: ganglion cell layer; DG: dentate gyrus. Scale bars: **A, B, D, and E:** 20 μ m, **C:** 100 μ m.

To assess the immunohistochemical labeling of μ -opioid receptors (MORs) in the mouse retina, an antibody recognizing the N-terminus of MOR (Alomone) was tested on vertical cryostat sections. This antibody at 1:500 dilution produced punctate labeling in the inner retina which was associated with somatic profiles in both the inner nuclear layer (INL) and ganglion cell layer (GCL), but no immunolabeling was noted in the outer retina (arrows, Fig. 3.1A). MOR immunolabeling was completely abolished by preincubation of the antibody with its

control peptide (1:10, antibody: control peptide—per manufacture’s guidelines) (Fig. 3.1B).

Control experiments were performed on mouse brain coronal sections. MOR immunolabeling of hippocampal neurons corresponded nicely with previous reports in mouse (Kwon et al., 2008) (Fig. 3.1C,D). Similar to the retina, preadsorption of the MOR antibody with its immunogenic peptide blocked the immunolabeling of hippocampal neurons (Fig. 3.1E).

The GCL is comprised of ganglion cells (GCs) and displaced amacrine cells (Jeon et al., 1998; Kong et al., 2005), whereas the INL is the most heterogeneous nuclear layer in the mouse retina containing horizontal, bipolar, amacrine and Müller cell somas, with amacrine making up a large fraction (~39%)

of all the INL somata (Jeon et al., 1998). Due to the diverse size, morphology and location of the MOR+ somas (Fig. 3.1A), it was likely that there are multiple types of MOR bearing cells in the inner retina. In a GAD67-EGFP knock-in mouse line, the presence of EGFP reliably marks GAD67 positive GABAergic neurons in the central nervous system (Tamamaki et al., 2003) including various GABAergic amacrine cells the retina (May et al., 2008). We found that MOR immunolabeling occasionally colocalized with the GAD67-EGFP signal in both the INL and GCL (Fig. 3.2A, asterisk and arrow, respectively). The presence of MOR+/ GAD67-EGFP- cells in the GCL (Fig. 3.2A, arrowheads) indicated that

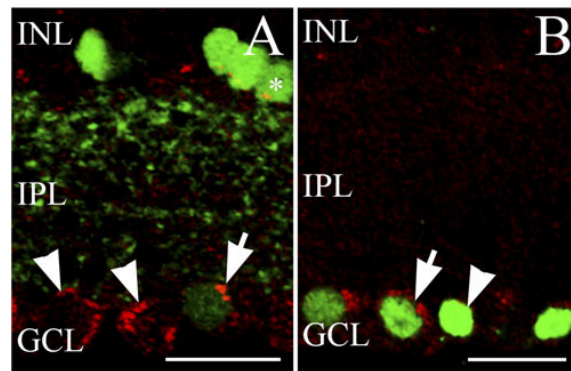


Figure 3.2. Some ganglion cells and GABAergic amacrine cells are MOR+. **A:** 40x single-plane merged image of vertically sectioned GAD67-EGFP mouse retina immunolabeled for MOR (red; Alomone). GAD67-EGFP somas are seen in the INL (bright green) and GCL (dim green) with processes in the IPL. Punctate MOR+ labeling of a displaced GABAergic amacrine cell is shown in the GCL (arrow). Some putative MOR+ somas in the GCL are GAD67-EGFP negative (arrowheads). In the INL some GAD67-EGFP cells colabel MOR+ puncta that could indicate colocalization (asterisks). **B:** 40x merged confocal image of cryosectioned wild-type mouse retina co-immunolabeled for MOR (red) and Brn-3a (green). Some Brn-3a+ retinal ganglion cells (arrow), but not all (arrowhead), are MOR+. INL: inner nuclear layer; IPL: inner plexiform layer; GCL: ganglion cell layer. Scale bars: 20µm.

displaced amacrine cells lacking GAD67-EGFP and/or GCs express MORs as well. To further test this notion, colabeling studies were performed using a known GC marker, Brn-3a (1:200 dilution), which label many but not all GCs in the mouse retina (Xiang et al., 1995). We found several Brn-3a labeled cell bodies in the GCL colocalize with MOR immunolabeling (Fig. 3.2B, arrow), but not all Brn-3a cells were colabeled with MOR (Fig. 3.2B, arrowhead).

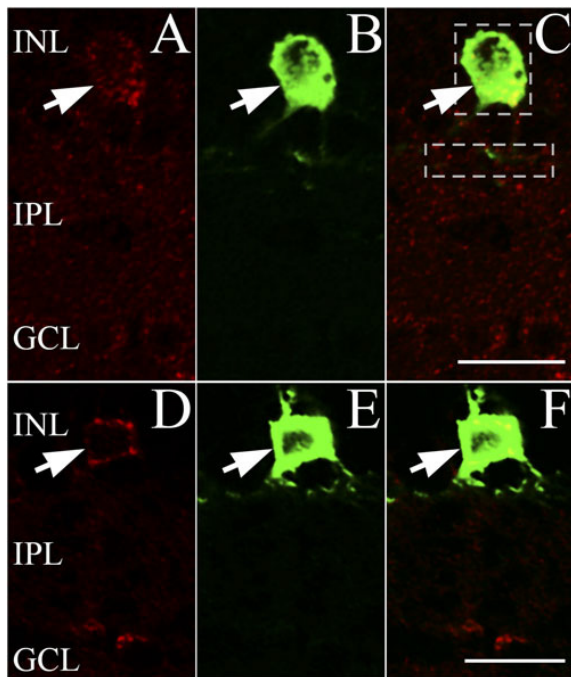


Figure 3.3. Dopaminergic amacrine cells in the INL are MOR+. **A:** 40x single-plane image of vertically sectioned mouse retina showing MOR+ (red) puncta in the INL (arrow) using the N-terminus directed MOR antibody (Alomone). **B:** Image displaying the same retinal region as **A**, immunolabeled for TH (green) showing a single TH+ cell (arrow) in the INL with TH+ projections in the IPL at the border with the INL. **C:** A merged image of **A** and **B**, displaying colocalization of the MOR+ and TH+ cell (arrow). **D:** 40x confocal image, vertical section of mouse retina showing immunolabeled somata (red) in the INL (arrow) with the anti-MOR antibody directed against the C-terminus of the receptor (Epitomics). **E:** Image illustrating the same region as in **D**, showing a TH+ (green) soma in the INL (arrow). **F:** A merged image of **D** and **E**, indicating colocalization of MOR and TH immunolabeling. INL: inner nuclear layer; IPL: inner plexiform layer; GCL: ganglion cell layer. Dashed lines (**C**) demarcate example focused images used for colocalization analysis (see Methods). Scale bars: 20µm.

To evaluate whether DACs are also MOR+, a colabeling study was performed with the DAC marker anti-tyrosine hydroxylase (TH) antibody (Witkovsky et al., 2005). A representative image (Fig. 3.3A-C) shows colocalization of MOR and TH immunolabeling in the INL (arrow). Visual evaluation of 124 TH+ DAC somas in retinal sections from nine different mice showed that 117 (> 94%) were also MOR+.

A more objective test to assess whether MOR and TH immunolabeling precisely overlap is to calculate Pearson's coefficient (PC) using Costes' approach (see Methods). Analysis of five MOR / TH immunolabeled somata (see Fig. 3.3C dashed line for example of focused somatic

colocalization analysis) from three animals gave an average PC of 0.603 ± 0.015 ; $P = 100\%$. This PC indicates colocalization between TH and MOR and the P-value proves that it is non-random. Similar analysis of three TH+ DAC somas that were deemed as MOR- by visual assessment was also performed. The results of this analysis ($PC=0.4 \pm 0.094$; $P = 100\%$) suggest that our (subjective) visual assessment was too conservative and underestimated the colocalization percentage; based on these results in the mouse retina essentially every (TH+) DAC soma was labeled with the MOR antibody directed against the N-terminus.

Processes from DACs form a distinct horizontal band at the border of the INL and IPL (Witkovsky et al., 2005). Both visual assessment and quantitative analysis of colocalization were performed on five images focused on TH+ processes (see Fig. 3.3C IPL dashed line for example) yielding little to no colocalization with MOR immunolabeling ($PC=0.062 \pm 0.006$).

Studies with a second anti-MOR antibody directed against the C-terminus of MOR (1:10 dilution) showed similar immunolabeling in the inner retina as was seen with the N-terminus-directed MOR antibody (compare Fig. 3.3D with 3.1A and 3.3A). Additionally, this second MOR antibody provided consensus colabeling with TH (arrow, Fig. 3.3D-F). We found $> 93\%$ of TH+ somas were MOR+ by visual assessment (28/30, four mice), whereas no colocalization was noted in the IPL. Detailed statistical evaluation of colocalization was performed on five images focused on TH+ cell bodies from three animals resulted in a PC of 0.754 ± 0.025 , with a P-value of 100%, indicating a non-random colocalization between TH and MOR immunolabeling provided by the C-terminus antibody.

δ -opioid receptors in the mouse retina

The physiological data in rabbit retina showed that DADLE reduces dopamine release (Dubocovich & Weiner, 1983). DADLE, a synthetic enkephalin, is considered to be a δ -opioid

receptor (DOR)-selective agonist (Kosterlitz et al., 1980). Therefore, cryostat sectioned mouse retinal tissue was labeled with an antibody directed against the N-terminus of DOR (Alomone). This antibody (1:500 dilution) provided punctate immunolabeling in the inner retina, with the strongest signal seen in the INL (arrows, Fig. 3.4A). Preadsorption of the antibody with its control peptide (1:10, antibody: control peptide—per manufacture’s guidelines) completely blocked labeling (Fig. 3.4B). Immunohistochemical studies of DOR distribution have been performed extensively in the rat dorsal root ganglia (DRG). In our hands this anti-DOR antibody also labeled neurons within the rat DRG (Fig. 3.4C) consistent with published data (Kabli & Cahill, 2007), which

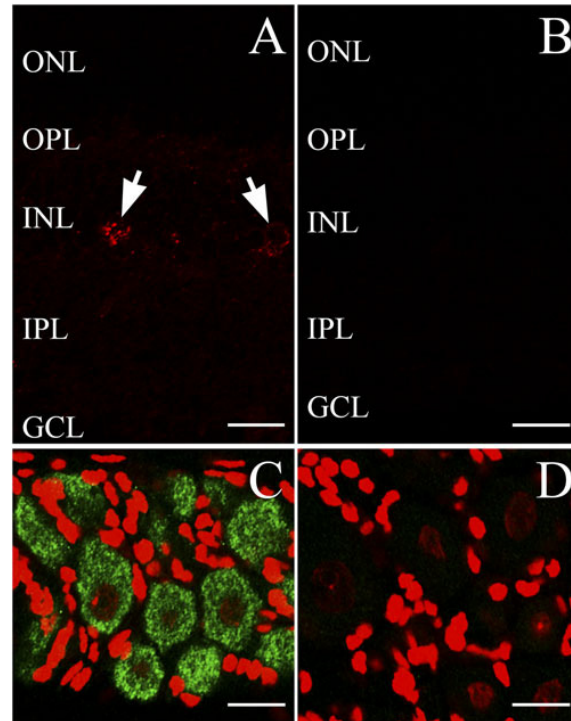


Figure 3.4. Localization of DOR immunolabeling in mouse retinal and rat dorsal root ganglion tissues. **A:** 40x confocal image of cryosectioned mouse retina immunolabeled with an anti-DOR antibody (Alomone). Note the puncta in the inner retina with putative somatic labeling in the INL (arrows). **B:** 40x image similar to **A** showing control peptide preadsorption for DOR (Alomone) antibody. **C:** 40x confocal image of rat DRG with DOR+ somas (green). Colabeled with the nuclear marker ToPro3 (red). **D:** 40x image similar to **C** showing preadsorption of DOR antibody with control peptide, colabeled with ToPro3 (red). ONL: outer nuclear layer; OPL: outer plexiform layer; INL: inner nuclear layer; IPL: inner plexiform layer; GCL: ganglion cell layer. Scale bars: 20µm.

was completely abolished by preadsorption with its control peptide (Fig. 3.4D). Taken together, the DOR immunolabeling provided by the anti-DOR antibody from Alomone appeared to be specific both in the DRG and in the retina.

Colabeling studies with anti-TH antibody indicated that one of the DOR+ retinal cell types is the DAC (Fig. 3.5A-C, arrow). Out of 36 TH+ DAC somata analyzed from retinal sections of three mice, 35 (> 97%) were judged to be DOR+ by visual assessment.

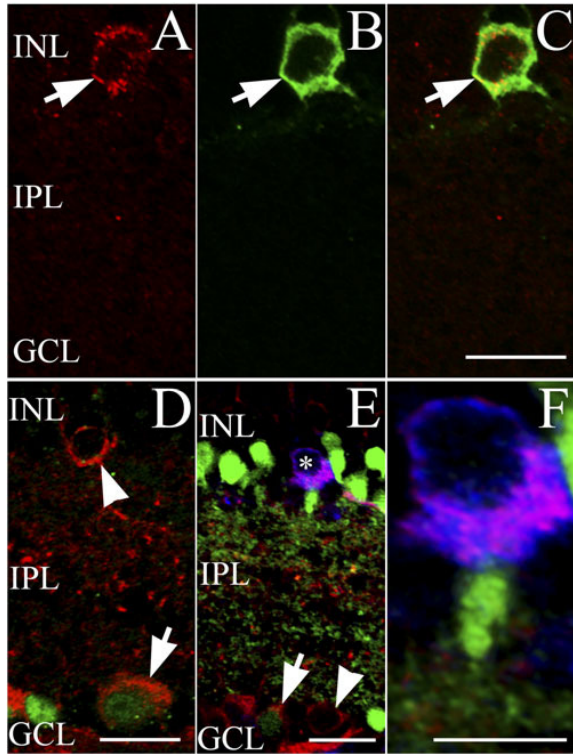


Figure 3.5. Multiple inner retinal cell-types including dopaminergic amacrine cells are DOR+. **A:** 40x single-plane confocal image, vertical section of mouse retina showing DOR+ (red; Alomone) somata (arrow). **B:** Image displaying the same region as **A**, immunolabeled for TH (green). **C:** A merged image of **A** and **B**, showing a DOR+ and TH+ amacrine cell in the INL (arrow). **D:** 40x single-plane merged confocal image of vertically sectioned wild-type mouse retina co-immunolabeled for DOR (red; Millipore) and Brn-3a (green). Some Brn-3a+ retinal ganglion cells are MOR+ (arrow). Arrowhead indicating a putative DOR+ soma in the INL. **E:** A 40x single-plane merged confocal image of cryosectioned GAD67-EGFP mouse retina co-immunolabeled for DOR (red; Millipore) and TH (blue). GAD67-EGFP somas are seen in the INL (bright green) and GCL (dim green) with processes in the IPL. A GABAergic (EGFP+) displaced amacrine cell in the GCL is DOR+ (arrow). Some putative DOR+ somas in the GCL are GAD67-EGFP negative (arrowhead). In the INL, a TH+ soma (blue) is DOR+ (asterisks). **F:** Focused view of dopaminergic amacrine cell from **E** showing that the TH+ soma is EGFP- and DOR+. INL: inner nuclear layer; IPL: inner plexiform layer; GCL: ganglion cell layer. Scale bars: **C**, **D**, and **F**: 20µm, **E**: 10µm.

Detailed colocalization analysis of five TH / DOR labeled cells from three animals resulted in a PC of 0.699 ± 0.052 and a P-value of 100%. These values indicate a strong and non-random somatic colocalization of DOR and TH immunolabeling in mouse retina.

Analysis of DOR and TH immunolabeling colocalization was also performed for TH+ processes. By visual assessment no colocalization was detected within the IPL. Computer based analysis of five images focused on TH+ processes in the IPL from three mice gave a PC of -0.058 ± 0.018 . Although negative, the near-zero PC implied non-colocalization of TH and DOR immunolabeling in the mouse IPL—suggesting that DOR labeling was limited to DAC somas. Similar results were obtained by using a second anti-DOR antibody from Millipore. This DOR antibody (1:500-1:600 dilution) labeled robustly within the inner retina, including somatic labeling within the INL (Fig. 3.5D, arrowhead) and Brn-3a+ GC somas in the GCL (Fig. 3.5D, arrow). Colabeling studies with DOR and TH antibodies in retinal sections made from GAD67-

EGFP mice showed corresponding colocalization of DOR and TH (Fig. 3.5E-F). Note, that the GAD67-EGFP signal does not colocalize with TH, consistent with the notion that DACs might use GAD65 to generate GABA (May et al., 2008; Witkovsky et al., 2008). Out of 62 TH+ cell bodies from six mice > 93% (58/62) were also deemed DOR+ by visual assessment. Detailed statistical evaluation of colocalization was performed on five images focused on TH+ cell bodies from five animals and resulted in a PC of 0.767 ± 0.032 and a P-value of 100%, confirming that the labeling pattern produced by second anti-DOR antibody also colocalized with that of anti-TH antibody, in a non-random manner. Although not investigated further in the current study, it is important to note the presence of DOR+, GAD67-EGFP+ displaced ACs (Fig. 3.5E, arrow) in the mouse retina.

3.5. Discussion

In the current study we demonstrate MOR immunolabeling in the mouse retina, for the first time showing strong somatic labeling in the INL and GCL (Fig. 3.1A). Although systematic classification of all MOR+ somas was not attempted in this study, the data indicate that in the mouse retina a subpopulation of Brn-3a+ GCs (Fig. 3.2B), GAD67+ GABAergic ACs (Fig. 3.2A), and dopaminergic amacrine cells (DACs) express MORs (Fig. 3.3). Similarly, DOR immunolabeling in the mouse retina implicated multiple DOR+ inner retinal cell-types (Fig. 3.4A), including Brn-3a+ GCs (Fig. 3.5D) and GAD67-expressing GABAergic amacrines (Fig. 3.5E). Importantly, our data confirm that DACs are DOR+ (Fig. 3.5A-C, E-F).

TH+ dopaminergic processes showed neither MOR nor DOR immunolabeling. This labeling pattern is not unprecedented: natriuretic peptide receptor labeling was also associated primarily with the somatic region of DACs (Abdelalim & Tooyama, 2010). Nonetheless, it is not

known whether the somatic punctate labeling is associated with functional neuropeptide receptors in the plasma membrane or with newly synthesized receptor protein in the cytoplasm.

The majority of opioid receptor activity is mediated through the Go/Gi -coupled superfamily of receptors, and the cellular effects include: (1) activation of inwardly rectifying potassium current; (2) inhibition of voltage-gated calcium current; and (3) inhibition of adenylate cyclase, depending on the actual cell-type (Kieffer, 1995). Consequently, opioid receptor activation is generally believed to be inhibitory at cellular level—often expressed as a reduction of transmitter release from neurons possessing opioid receptors, such as reduction of dopamine release in the striatum (Loh et al., 1976).

Morgan & Boelen (1996) proposed an intercellular feedback loop in the avian retina formed by the endogenous opioid system and DACs that mediates dark-light switch. Considering that besides birds (Su & Watt, 1987), retinal dopamine release is reduced by opioids in multiple species (turtle: Kolbinger & Weiler, 1993; rabbit: Dubocovich & Weiner, 1983), this model might be more generally applicable to vertebrate retinas. Here, MOR and DOR immunolabeling was found to be associated with (TH+) DACs in the mouse retina, which predicts that opioids modulate the function of DACs directly, via MORs and DORs located on DACs and might influence dopamine release as in other species.

Whether these opioid receptors are coexpressed in any other retinal cell-type besides DACs requires further study. However, in other parts of the mammalian nervous system, in cell-types that coexpress MOR and DOR, MOR/DOR heteromerization have been shown to modulate signaling (Gomes et al., 2004; Rozenfeld & Devi, 2011). Besides DACs, we found that MOR and DOR immunolabeling was associated with a heterogeneous cell population in the inner retina including GABAergic displaced amacrine and ganglion cells. These findings suggest that

opioids might affect retinal function at multiple sites of action, thus our work adds to a framework on which future histological and physiological characterizations can occur.

3.6. Related findings

Two additional IHC studies were performed to further identify MOR possessing cell-types in the mammalian retina. The first study used yet another anti-MOR antibody to evaluate MOR immunolabeling in the mouse retina. The second study focused on further characterizing MOR+ RGCs using both mouse and rat retinas.

Study 1

Confirmation and further characterization of the above findings were performed using similar methods. Additional primary antibodies were used in this study.

Antibody raised against Brn-3a. The mouse anti-Brn-3a (Millipore: MAB10585/NG166218, 1:50) antibody was generated against human retina Brn-3a amino acids 186-224 (LLGGSAPHMHSLGHLSPAAAAAMNMPSGLPHPGLV) identified from the human retina cDNA library (Nathans et al., 1986). Human POU-domain factor Brn-3a has 98% sequence homology to mouse Brn-3a (Xiang et al., 1995). Western blot analysis using this antibody against Brn-3a, -3b, or -3c containing fusion proteins revealed a single band associated with Brn-3a, with no reactivity to the other Brn-3 derived polypeptides (Xiang et al., 1995). This anti-Brn-3a antibody has been shown to label a large subset of mouse retinal ganglion cells (Xiang, et al., 1995), corresponding to *in situ* hybridization analysis in the developing mouse retina showing high levels of expression limited to the GCL (Gerrero et al., 1993). Additionally, a transgenic mouse line with targeted deletion of the Brn-3a gene was absent of any anti-Brn-3a immunoreactivity in the retina using this antibody for analysis (Xiang et al., 1996).

Antibody raised against μ -opioid receptors (MOR) (C-terminus). The antigen-affinity purified anti-MOR antibody was raised in rabbit against a synthetic peptide corresponding to amino acids 387-398 (LENLEAETAPLP) of the intracellular C-terminus of rat MOR (Sternini et al., 1996). Using human embryonic kidney 293 cell expression systems, this antibody showed immunolabeling of MOR cDNA transfected cells with no labeling of KOR or DOR transfected cells (Sternini et al., 1996). Preabsorption of this anti-MOR antibody with its immunogenic peptide eliminated MOR labeling in the mouse myenteric plexus (Sternini et al., 1996). Antibody specificity was further confirmed in mouse DRG showing appropriate immunolabeling in wild-type and a loss of immunolabeling in *mor* null mice (Scherrer et al., 2009).

Results

The anti-MOR antibody directed against the C-terminus sequence (generously provided by C.J. Evans, UCLA) was previously characterized in expression systems (Sternini et al., 1996) and in the mouse CNS (Scherrer et al., 2009). This antibody provided similar labeling of MORs in the inner retina (Fig. 3.6) as compared with the Alomone N-terminus specific anti-MOR antibody (Fig. 3.1A) and the other C-terminus anti-MOR antibody (Epitomics; Fig. 3.3D). MOR immunopositive somas were localized to the INL and GCL (Fig. 3.6).

Using this new anti-MOR antibody, MOR immunolabeling of TH+ DACs and Brn3a+ RGCs was confirmed (not shown). Quantification of Brn3a+ / MOR+ RGCs showed that approximately 42%

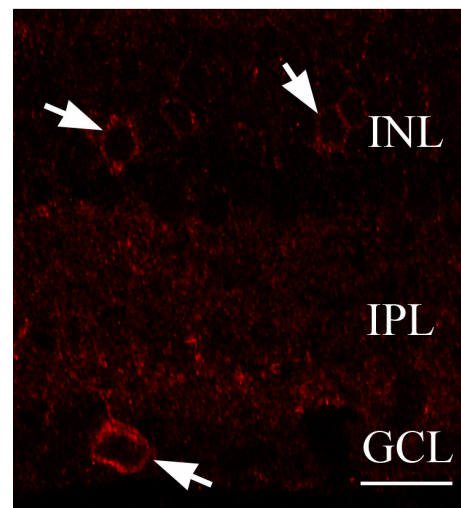


Figure 3.6. Localization of MOR immunolabeling in mouse retina. 40x confocal image of cryosectioned mouse retina immunolabeled with C-terminus specific anti-MOR antibody (C.J. Evans). Note the puncta in the inner retina with putative somatic labeling in the INL and GCL (arrows). Scale bar: 20 μ m.

(68/162, counted in two retinas, obtained from two different mice) of MOR+ somas appeared to colabel with Brn3a in the GCL. Only a subset of Brn3a+ RGCs was found to be MOR+ (68/516, ~13%) suggesting that few RGC types possess MORs.

Nonetheless, Brn3a+ cells do not account for all RGCs (Quina et al., 2005). A small subset (38/549 cells) of Brn3a- / MOR+ somas in the GCL appeared to also be RGCs. These cells had an average soma size of $13.9 \pm 1.5 \mu\text{m}$, which excludes them from being displaced amacrine cells (Müller et al., 2007). To further clarify these RGC findings, a second study was performed.

Study 2

Ganglion cells are the final output neurons of the retina and any modulation of their activity could have profound effects (see Chapter 1). Although there is no universally accepted classification of RGCs, it is clear that there are multiple identified types of RGCs projecting to diverse regions of the brain for image-forming and non-image forming visual processing (for example: Badea & Nathans, 2004; Ecker et al., 2010). The above findings suggest that multiple RGC types could possess MORs. To address this, an IHC study was performed using wild-type and transgenic mouse and wild-type rat retinas.

Materials and methods were used as described above. Additional animals and primary antibodies were used in this study.

Animals. Experiments were performed using adult male and female Sprague Dawley rats (Harlan Laboratories, Indianapolis, IN) and mice (generated by the GENSAT project, tissue generously provided by DM. Berson, Brown University). The melanopsin reporter mouse strain BAC *Opn4::EGFP* was used to identify M1-M3 ipRGC types, as previously characterized (Schmidt et al., 2008).

Antibody raised against Brn-3(b). The goat anti-Brn-3(b) antibody was generated against amino acids 397-410 (QRQKQKRMKYSAGI) corresponding to the C-terminus of human Brn3b (Xiang et al., 1993). The human POU-domain factor Brn-3b has 95% sequence homology to mouse Brn-3b (Xi et al., 1989). This anti-Brn-3(b) antibody has been shown to label a specific subset of mouse retinal ganglion cells with little to no overlap seen in colabeling studies using antibodies against either Brn3a or Brn3c (Jain et al., 2012). Furthermore, in our hands the anti-Brn3a antibody (Millipore) and this anti-Brn3(b) antibody showed no colabeling of RGCs in the mouse retina (not shown).

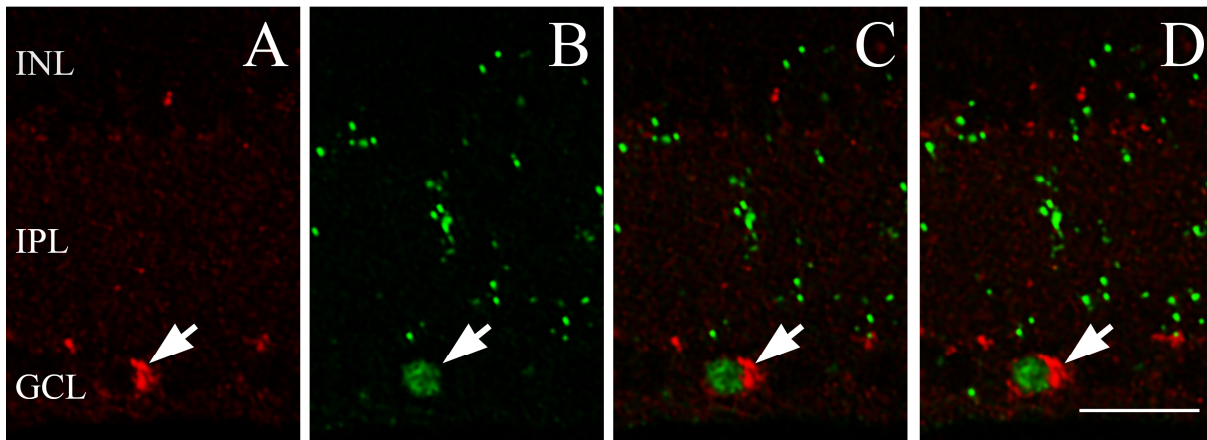


Figure 3.7. Some Brn3b+ retinal ganglion cells are MOR+. **A:** 40x single-plane confocal image of vertically sectioned mouse retina immunolabeled for MOR (red; Alomone). **B:** Image displaying the same retinal region as **A**, immunolabeled for Brn3b (green) showing a single Brn3b+ cell (arrow) in the GCL. This labeling appears to be restricted to the cells nucleus. Note: the punctate labeling in the IPL appears to be an artifact of this antibody; this image corresponds with previously published figures using this antibody (Jain et al, 2011). **C:** A merged image of **A** and **B**, displaying MOR+ somatic labeling around the Brn3b+ nucleus of the cell (arrow). **D:** A projected image compiled from 3 single-plane confocal images showing that the MOR+ labeling surrounds the Brn3b+ labeling (arrow). Scale bars: 20 μ m.

Antibodies raised against Melanopsin. Melanopsin is a photopigment that mediates the intrinsic light response of intrinsically photosensitive retinal ganglion cells (ipRGCs) in the mammalian retina, which are known to mediate a wide variety of light driven behaviors (Berson et al., 2002; reviewed in Sand et al., 2012). The first anti-melanopsin antibody is an affinity purified polyclonal antibody generated in goat against a peptide corresponding to the C-terminus

of rat melanopsin (Santa Cruz Biotechnology: sc-26962, 1:50). This antibody selectively labels a single band on Western blot analysis of (manufacturer's specifications). This antibody has been used in rat to selectively label M1-M3 types of ipRGCs (Graham et al., 2008; Van Hook et al., 2012).

The second anti-melanopsin affinity purified antibody was generated in rabbit against a thyroglobulins-conjugated synthetic peptide corresponding with the extracellular N-terminus of rat melanopsin (KMNSPSES RVPSSTLTQDPSF, lysine added for cross-linking purposes; generously provided by AT. Hartwick, OSU). In our hands this antibody faithfully colabels with the other anti-melanopsin antibody (Santa Cruz Biotechnology: sc-26962).

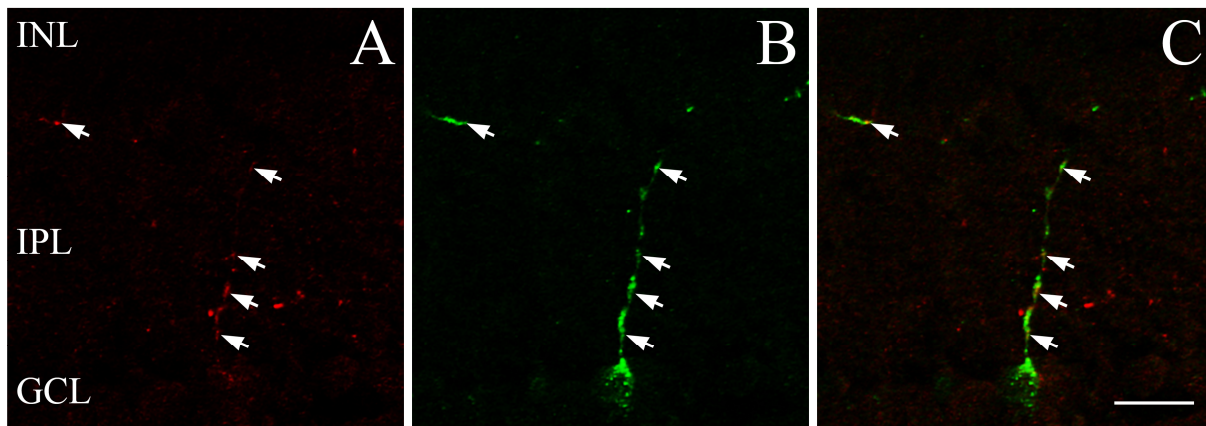


Figure 3.8. In the rat intrinsically photosensitive retinal ganglion cells (ipRGCs) are MOR+. **A:** 40x single-plane confocal image of cryosectioned rat retina immunolabeled for MOR (red; Alomone), showing punctate labeling within the IPL (arrows). **B:** Image displaying the same retinal region as **A**, immunolabeled for melanopsin (green) showing dendritic labeling traversing the IPL with a portion stratifying in sublamina 1 (arrows). **C:** A merged image of **A** and **B**, displaying colabeling of melanopsin and MOR in the IPL (arrows). Scale bars: 20 μ m.

Results

As discussed above, a subset of Brn3a+ RGCs possess MORs. Another member of the Brn3 family of transcription factors, Brn3b, has been shown to label a smaller proportion of RGCs in the mouse retina (Xiang et al., 1995). To assess whether the identified Brn3a- / MOR+ cells in the GCL are Brn3b+ RGCs, we performed a colabeling IHC experiment using MOR and Brn3b directed antibodies. As can be seen in figure 3.7(A-C), MOR+ puncta appear to colabel a Brn3b+

RGC. Although quantification of Brn3b+ / MOR+ RGCs was not undertaken, these results confirm that at least two distinct types of RGCs are MOR immunopositive, one using the transcription factor Brn3a and the other using Brn3b. These data, however, do not exclude the possibility of a third type of RGC that is neither Brn3a nor Brn3b immunopositive.

Interestingly, a number of recent studies seeking to identify and characterize the subtypes of intrinsically photosensitive retinal ganglion cells (ipRGCs) have shown that many of them are Brn3b immunopositive (Chen et al., 2011; Jain et al., 2012; Karnas et al., 2013). To evaluate if MORs are found on ipRGCs, we performed colabeling IHC studies with MOR and melanopsin directed antibodies. Because of antibody host cross-reactivity concerns and species limited immunolabeling, the initial IHC preparations were performed using retinal tissue from adult Sprague Dawley rats. It's noteworthy that a pilot IHC study for MOR immunolabeling in the rat retina showed inner retinal punctate labeling of the INL, IPL and GCL, and confirmed that rat TH+ DACs are also MOR+ (not shown). Interestingly, in the rat retina, MOR immunolabeling is strongest in the IPL although somatic labeling in the INL and GCL can be seen. Colabeling studies in adult rat retinas showed that melanopsin+ ipRGCs possess MORs on their dendrites (Fig. 3.8A-C). In fact, all melanopsin-positive ganglion cells (M1, displaced M1, M2/M3) had some MOR colabeling on their dendrites (19/19 cells from 2 animals).

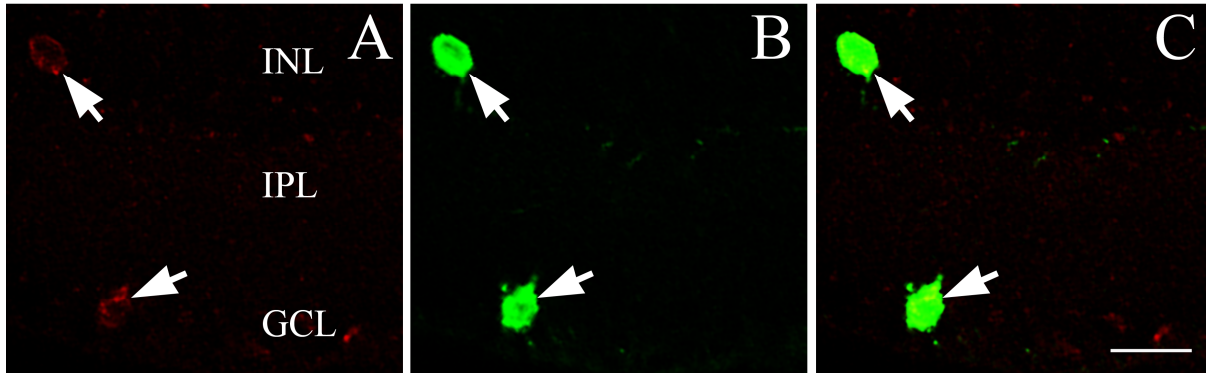


Figure 3.9. In the mouse intrinsically photosensitive retinal ganglion cells (ipRGCs) are MOR+. **A:** 40x single-plane image of vertically sectioned *Opn4*-EGFP mouse retina showing MOR+ (red) somatic labeling in the INL and GCL (arrows). **B:** Image displaying the same retinal region as **A**, showing EGFP+ ipRGCs (arrows). Note the displaced ipRGC in the INL. **C:** A merged image of **A** and **B**, displaying colabeling of MOR and EGFP in ipRGCs (arrow). Scale bars: 20 μ m.

To see if ipRGCs in the mouse retina also colabeled with MOR we took advantage of a transgenic mouse line that expressed the fluorescent protein EGFP in melanopsin expressing (*Opn4*) ipRGCs. As can be seen in figure 3.9(A-C) MOR immunolabeling does colocalize with EGFP+ ipRGCs. This MOR labeling pattern in the mouse retina is similar to what we have previously shown (Gallagher et al., 2012).

The transcription factor Brn3b is preferentially expressed in M2/M3 and in a subset of M1 ipRGC types (Jain et al., 2012; Karnas et al., 2013). It has been shown that Brn3b+ M1s are responsible for the ipRGC component of the pupillary light reflex, while the Brn3b- cell-type mediates photoentrainment of the circadian rhythm (see Chapter 1; Chen et al., 2011). To confirm our initial supposition that Brn3b+ / MOR+ cells represent, at least in part, ipRGCs, IHC was performed using retinas from the *Opn4*-EGFP mouse, immunolabeling for MOR and Brn3b. Our results, though not comprehensive, are in agreement with other studies showing Brn3b+ ipRGCs (Jain et al., 2012; Karnas et al., 2013). These cells are also MOR+ (Fig. 3.10A-D). Brn3b- / MOR+ ipRGCs (EGFP+) were also noted (not shown). These findings suggest that both sub-types of M1 as well as M2/M3 ipRGCs are MOR+ in the mouse retina.

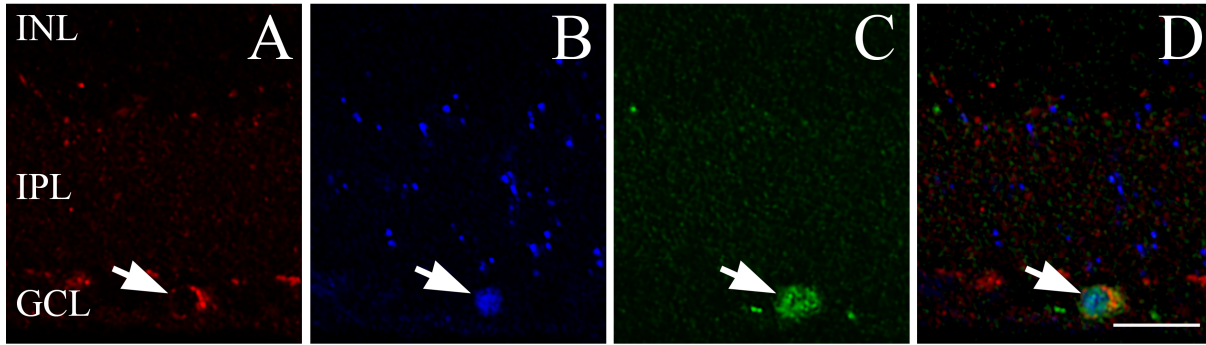


Figure 3.10. Brn3b+ intrinsically photosensitive retinal ganglion cells (ipRGCs) are MOR+. **A:** 40x single-plane image of vertically sectioned *Opn4*-EGFP mouse retina showing MOR+ (red) punctate labeling in the inner retina and somatic labeling in the GCL (arrow). **B:** Image displaying the same retinal region as **A**, showing a Brn3b+ (blue) soma in the GCL (arrow). Note: the punctate labeling similar to figure 3.7 and corresponding with previously published figures using this antibody (Jain et al, 2011). **C:** Same region as **A** and **B**, showing an EGFP+ ipRGC in the GCL (arrow). **D:** A merged image of **A**, **B** and **C**, displaying colabeling of MOR, Brn3b and EGFP in ipRGCs (arrow). Scale bars: 20µm.

Summary

The second aim of this work was to identify μ -opioid receptor immunopositive cell types in the mouse retina. MORs were identified on GABAergic amacrine cells, including DACs, and in multiple types of RGCs. In addition to the mouse data, we confirmed MOR immunolabeling of rat RGCs. In both animals we were able to show that M1-M3 ipRGC types are MOR+. Because ipRGCs have a direct role in light mediated reflexes and behaviors (see Chapter 1), the physiological relevance of MOR mediated modulation of ipRGCs could be profound.

4. Conclusion

There has been a recent resurgence in retinal opioid research, however much of it has focused on δ -opioid receptors possible neuroprotective role during hypoxic or ischemic insult (reviewed in Husain et al., 2012). Little has been shown relating to the μ -opioid system, although early receptor binding and autoradiography studies suggested its presence in the mammalian retina. Therefore, the purpose of this work was to identify and characterize the μ -opioid system in the mammalian retina. To that end, our overall hypothesis was that the opioid system, specifically the μ -opioid receptor (MOR) and its endogenous opioid peptide, β -endorphin, is present in the mammalian retina and it plays a role in the regulation of light-driven retinal functions. The specific aims of this work were threefold: (1) Identification of β -endorphin expression in the mouse retina; (2) Identification of μ -opioid receptor possessing cell types in mouse retina; and (3) evaluation of a possible physiological effect of μ -opioid receptor activation in the mammalian retina.

We have identified through use of transgenic mice, in situ hybridization and immunohistochemistry (IHC) that the cholinergic “Starburst” amacrine cells (SACs) express β -endorphin. Using IHC we’ve shown that multiple neuronal cell types in the mouse retina possess MORs, including dopaminergic amacrine cells (DACs) and ipRGCs. In this final chapter, preliminary results showing opioid modulation of ipRGCs light responses will be evaluate. Through the discussion of individual aspects of our findings, there will be an attempt to put this work into the context of overall retinal function. Additionally, the possible manipulation of this system by exogenous opioids will be discussed.

4.1. Opioid modulation of ipRGCs light responses

The discovery of melanopsin-containing intrinsically photosensitive retinal ganglion cells (ipRGCs) has fundamentally altered our understanding of how light regulates mammalian physiology and behavior. Recent discoveries have expanded on the evolving role of ipRGCs, with distinct subtypes being identified and diverse targets within brain regions responsible for image-forming and non-image-forming vision being found (Baver et al, 2008; Schmidt & Kofuji, 2009; Berson et al, 2010; Ecker et al, 2010; Estevez et al, 2012). Our finding that ipRGCs are MOR immunopositive suggests a possible role for opioid modulation of ipRGCs light response. Given that these cells can respond to light separate from synaptic inputs from the classic rod/cone pathways, ipRGCs seemed ideal for evaluating the effect of MOR activation on light induced spiking.

Although MOR immunolabeling of ipRGCs is a novel finding (see Chapter 3), it does not provide definitive proof of a direct physiological effect on ipRGCs function. To evaluate the effect of MOR activity on the light response of ipRGCs, we performed multielectrode array (MEA) recordings of ipRGCs light-induced spiking activity using P6-11 rat retinas (see Appendix II for materials and methods). Animals at this developmental stage have been shown to lack outer retinal inputs to RGCs (Sernagor et al., 2001), and ipRGCs have been shown to be light responsive after birth (Hannibal & Fahrenkrug., 2004). Thus, any light responsiveness from P6-11 retinas is mediated by the intrinsic response of ipRGCs (Sekaran et al., 2005; Tu et al., 2005; Perez-Leighton et al., 2011).

Flat-mount retinas secured in an MEA chamber were dark adapted for a minimum of one hour prior to exposure to a 20 second light stimulus every 20 minutes. To evaluate the effect of MOR activity on the light response of ipRGCs, DAMGO, a MOR selective agonist, was bath applied ~5 minutes prior to

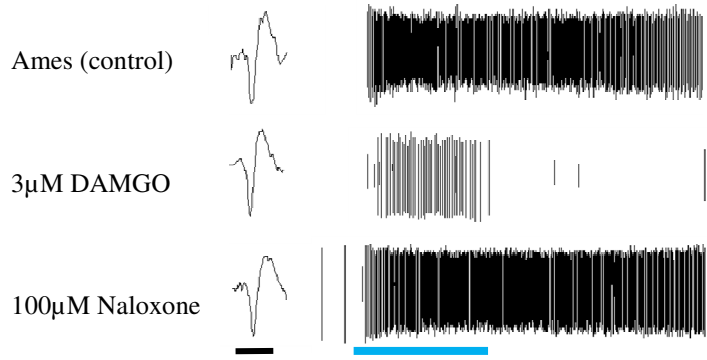


Figure 4.1. Light response of an ipRGC inhibited by MOR selective agonist DAMGO, single cell data. Light (470nm, 4×10^{15} photons $\text{cm}^{-2} \text{s}^{-1}$, blue bar) evoked ipRGC spikes recorded from a single MEA channel from a P11 rat retina. Each vertical line represents an extracellularly recorded action potential, shown on an extended time scale at the beginning of each condition. Scale bars: black=2ms, blue=20s.

light stimulus. As can be seen in figure 4.1, DAMGO (3 μM) greatly decreased the light response of a representative ipRGC as compared with the recording under control (Ames) conditions. This reduction was reversed by the non-selective opioid antagonist, naloxone, confirming an opioid-mediated modulation of ipRGCs light response (Fig. 4.1).

Preliminary MEA preparations showed that the MOR mediated effect on ipRGCs light response was found across all identifiable ipRGCs (147 cells). The intensity of light stimulus used (4×10^{15} photons $\times \text{cm}^{-2} \times \text{s}^{-1}$, 470 ± 5 nm) was strong enough to stimulate not only M1s, but also the relatively less sensitive M2/M3 ipRGCs (Perez-Leighton et al, 2011), suggesting that M1-M3 ipRGC types are modulated by MOR activation. This would be consistent with our immunohistochemical data. Because it appears all ipRGCs recorded during our MEA experiments were attenuated by DAMGO application, we sought to evaluate the total effect of DAMGO on ipRGCs light response at different concentrations.

DAMGO reduced the total light response of ipRGCs in a dose dependant manner (Fig. 4.2). Naloxone application reversed the attenuated ipRGCs, and in this experiment increased the light

response beyond control levels (Fig. 4.2). However, this naloxone mediated increase of ipRGCs light response was not consistent throughout our preliminary MEA experiments.

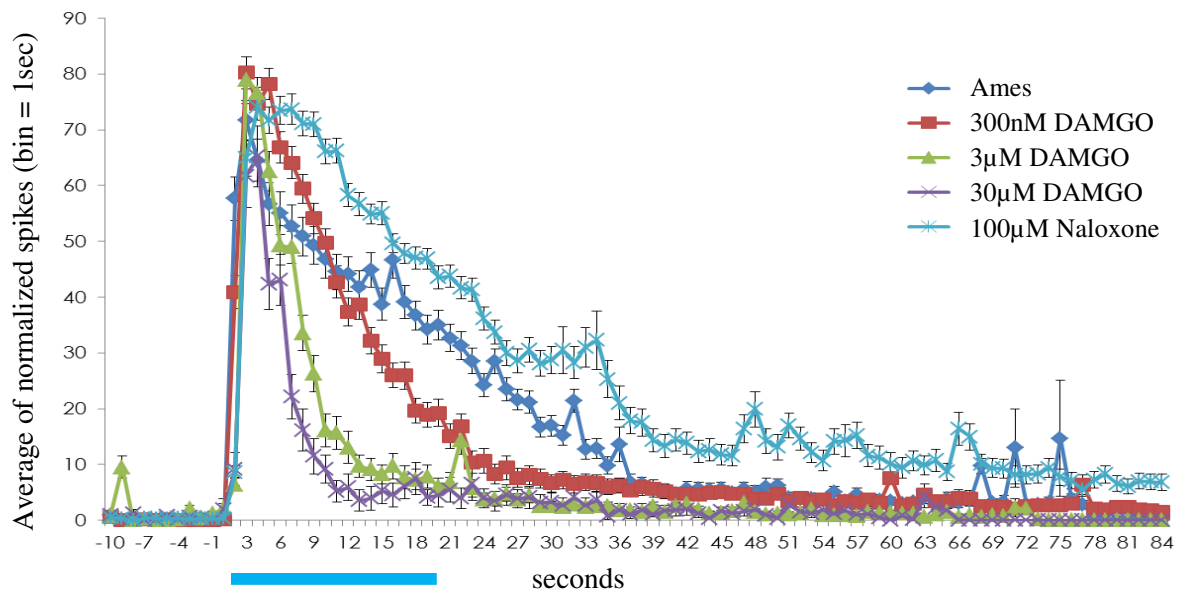


Figure 4.2. Graph representing a single MEA experiment showing the total light response of ipRGCs under different concentrations of DAMGO. Blue line = 20 second light stimulus.

Our finding in Chapter 3 that dopaminergic amacrine cells are immunopositive for both MORs and DORs made it important to evaluate whether DORs play a role in ipRGCs modulation. Using the DOR-EGFP mouse reporter line, others have shown that melanopsin+ ipRGCs are not EGFP+ (Roux MJ, et al. IOVS 2011;454:ARVO E-Abstract 4557). We performed an MEA experiment using a retina from a P11 rat, to evaluate if DOR activity affects ipRGCs light response. Neither the DOR selective agonist, DPDPE (100nM), nor the DOR selective antagonist, naltrindole (30nM) had an effect on ipRGCs light response (not shown). In this preparation, DAMGO (1µM) was still able to attenuate the ipRGCs light response.

Our preliminary MEA data demonstrated a MOR-mediated decrease in ipRGCs light-induced spiking activity. This attenuation of light response appeared to be dose dependant. Naloxone was able to recover the light response of ipRGCs back to control levels. Although naloxone is a non-selective opioid antagonist, our data showing that application of DOR

selective agonist or antagonist had no effect on ipRGCs light response suggested naloxone is antagonizing a MOR-mediated decrease in ipRGCs light response. In two experiments naloxone increased the light-induced spiking activity (see Fig. 4.2). This could imply endogenous opioids are present and modulating baseline ipRGCs light response. Future experiments need to clarify these data.

The role of endogenous opioids in retinal function is still unknown. Additional experiments are necessary to characterize the MOR-mediated modulation of ipRGCs. However, this preliminary study suggests an important role of the MOR system in non-image-forming vision. A manuscript on this aim is in preparation for publication, and will address further the MOR-mediated modulation of ipRGCs.

4.2. Dark-light switch

Dopaminergic amacrine cells

Our finding that DACs possess MORs supports data from multiple species claiming opioids modulate dopamine release (bird: Su & Watt, 1987; turtle: Kolbinger & Weiler, 1993; rabbit: Dubocovich & Weiner, 1983). In fact, it has been postulated that the opioid system in the avian retina works antagonistically with the retinal dopaminergic system to control, in part, the switch between light and dark adapted vision (Morgan & Boelen, 1996)—similar, or in addition to, the melatonin / dopamine reciprocal antagonism found in the mammalian retina (Wiechmann & Sherry, 2013). This model suggests a dark driven increase (or light driven decrease) of retinal opioid production and release. In support of this, a preliminary ELISA study on dark vs. light treated mouse retinas observed β -endorphin in the dark adapted animals while no detectable levels were found under light conditions (experiment kindly performed by ST. Hentges, Colorado State University). Further studies on dark vs. light adapted retinas will clarify this

finding. In situ hybridization for POMC could help evaluate expression levels under different light conditions as well.

As referenced above, melatonin has been shown to play a role in adaptation to dark conditions, in contrast to the light adaptive properties of dopamine in the retina (Huang et al., 2013). It has been shown in the rat pineal gland that opioids stimulate the release of melatonin (Esposti et al., 1988; Fraschini et al., 1989). Whereas, more recent work has demonstrated melatonin's analgesic actions are through its effects on increased release of β -endorphin (Shavali et al., 2005). Although their interaction is not well defined, it is clear that in the mammalian central nervous system there appear to be a reciprocal role for opioids and melatonin.

Melatonin synthesis in photoreceptors is under antagonistic control of dopamine (Tosini et al., 2012). Could activation of MORs in DACs lead to the upregulation and release of melatonin—facilitating the retina's adaptation to dark? Or perhaps the fact that MORs are found only in the inner retina implies some sort of segregation of dark adaptive processes (outer retina: melatonin / dopamine; inner retina: β -endorphin / dopamine)? However, melatonin receptors have been identified throughout the retina (Huang et al., 2013), which could point to the μ -opioid system being a redundant pathway for inner retinal dark adaptation, unless melatonin modulation targets retinal neurons different from those expressing opioid receptors. These and many other related questions remain to be answered. However, fitting our findings to the existing literature, we propose that the μ -opioid system in the mammalian retina serves in some capacity as a mechanism for dark adaptation—in opposition with dopamine, and in synergy with melatonin.

Intrinsically photosensitive retinal ganglion cells

We found MORs on M1-M3 ipRGC types in rat retinas and showed the modulatory effect of DAMGO on ipRGCs light responses. M1-M3 ipRGCs play critical roles in non-image-forming

visual processes (Hattar et al., 2006). Besides their role in the pupillary light reflex, the majority of M1-M3 ipRGCs functions are related to the circadian rhythm and sleep / wake cycle (Hattar et al., 2006)—two processes that require information about ambient levels of light (irradiance). Irradiance detection, though signaled through ipRGCs, includes input from rods and cones (Lall et al., 2010). Rods have been shown to play an important role in scotopic (dark/low light) and mesopic (mid-levels of light) contributions to ipRGCs irradiance signaling (Lall et al., 2010). This strengthening of the light signal is thought to facilitate detection over gradual changes in irradiance, such as dusk/dawn transitions (Lucas et al., 2012). This rod input, however, could provide aberrant light signals throughout scotopic conditions, leading to a disruption of photoentrainment of the circadian rhythm and sleep/wake cycle.

Given our preliminary finding that retinal β -endorphin level appears higher in the dark, the resulting activation of MORs on ipRGCs in dark would greatly inhibit any signal from M1-M3 ipRGCs. We propose that this inhibition helps prevent inappropriate phase shifts of the circadian rhythm and sleep/wake cycle. Additionally, we postulate that endogenous opioid modulation of ipRGCs light response could help define the edges of day/night transitions (dusk/dawn).

5.3. Exogenous opioids

Two converging lines of evidence suggests that systemically applied opioids can cross the tight retina-blood barrier (Hosoya et al., 2011) and might act on MORs expressed by ipRGCs in the retina: (1) After heroin exposure heroin metabolite opiates (including morphine and 6-monoacetylmorphine) accumulate and persist in the vitreous humor of the eye in higher concentrations and longer than in the blood, thus vitreous humor is used in the post-mortem toxicological characterization of suspected heroin deaths (Wyman and Bultman, 2004); (2) Intravitreal injection is the most direct and effective way of ocular drug administration in treating

retinal diseases (Hosoya et al., 2011). Note, that within the retina, ipRGCs are located in the cellular layer closest to the vitreous. Our work has identified a novel retinal μ -opioid system, which we suggest can be influenced by exogenous opioids. Two possible examples are briefly discussed below.

Migraine headaches and photophobia

The World Health Organization estimates that over 10% of adults worldwide suffer from migraine headaches (www.who.int/mediacentre/factsheets/fs277/en/). In the United States, greater than 16% of adults suffer from migraines, accounting for over 1% of all emergency department visits (Smitherman et al., 2013). Studies to understand light-mediated exacerbation of migraine headaches found that ipRGCs play a central role in evoking these symptoms (Noseda et al., 2010; Noseda & Burstein, 2011). Interestingly, opioids in combination with other drugs have demonstrated efficacy in the treatment of acute migraine symptoms including photophobia (Blumenfeld et al., 2012). We suggest that exogenous opioids directly inhibiting ipRGCs could, in part, account for the therapeutic effect of opioid treatment of migraineurs.

Sleep disorders and circadian disruption

According to the 2010 National Survey on Drug Use and Health (NSDUH), approximately 9% of Americans ages 12 or older had used illicit drug in the month prior to the survey (www.samhsa.gov/data/NSDUH/2k10ResultsRev/NSDUHresultsRev2010.htm). The amount of opioid use and abuse in the United States has been characterized by some as reaching epidemic levels (Manchikanti et al., 2013). Animal models of chronic opioid abuse, as well as withdrawal, show behavioral changes associated with disruption of circadian rhythms (Mistlberger & Holmes, 1999; Meijer et al., 2000; Vansteensel et al., 2005; Glaser et al., 2012). Human studies have also shown a loss or change in rhythmicity associated with opioid abuse and withdrawal (reviewed in

Hasler et al., 2012). It has further been suggested that sleep disorders and disruption of circadian rhythm are risk factors for relapse (Hasler et al., 2012).

Activation of MORs can cause receptor desensitization and/or internalization. This effect is highly ligand dependent, a concept referred to as ligand bias (Kelly, 2013). Although we were unable to account for possible desensitization of MORs in our MEA data, it is our hope that future single cell recording experiments could evaluate desensitization of MORs on ipRGCs and/or DACs by different ligands. Importantly, if desensitization did occur, our DAMGO data would underestimate the MOR mediated modulation of ipRGCs light responses.

We postulate that disruption of the endogenous μ -opioid system in the mammalian retina by exogenous opioid use or abuse causes a direct effect on retinal signals responsible for setting the sleep/wake cycle and entraining the circadian rhythm. Acute opioid use could modulate ipRGCs output through inhibition during normal light conditions. Chronic opioid use could lead to desensitization of MORs causing increased ipRGCs activity in dark conditions. Although speculative, these changes in ipRGCs activity could explain some of the human and animal studies linking opioid use or abuse to abnormal sleep/wake cycle and circadian dysfunction.

In identifying a novel μ -opioid system within the mammalian retina and providing a mechanism by which exogenous opioids influence behavior directly through this system, we present a new target for directed therapies in the management of light-mediated disorders. This work further provides new evidence towards understanding the affects of opioid abuse on circadian dysfunction, which could facilitate a shift in treatment paradigms for those recovering from opioid addiction.

References

- 1892 CS 1972 *The Structure of the Retina*. Springfield: Thomas.
- Abdelalim EM & Tooyama I. 2010. NPR-C is expressed in the cholinergic and dopaminergic amacrine cells in the rat retina. *Peptides* 31, 180-183.
- Abdul Y, Akhter N, Husain S 2013 Delta-Opioid Agonist SNC-121 Protects Retinal Ganglion Cell Function in a Chronic Ocular Hypertensive Rat Model. *Investigative Ophthalmology & Visual Science* 54:1816-1828.
- Akil H, Watson SJ, Young E, Lewis ME, Khachaturian H & Walker JM. 1984. Endogenous opioids—biology and function. *Annual Review of Neuroscience* 7, 223-255.
- Altschuler RA, Mosinger JL, Hoffman DW & Parakkal MH. 1982. Immunocytochemical localization of enkephalin-like immunoreactivity in the retina of the guinea-pig. *Proceedings of the National Academy of Sciences of the United States of America-Biological Sciences* 79, 2398-2400.
- Andrade da Costa BL, Hokoc JN. 2003. Coexistence of GAD-65 and GAD-67 with tyrosine hydroxylase and nitric oxide synthase in amacrine and interplexiform cells of the primate, *Cebus apella*. *Vis Neurosci* 20(2):153-63.
- Badea TC, Nathans J 2004. Quantitative analysis of neuronal morphologies in the mouse retina visualized by using a genetically directed reporter. *Journal of Comparative Neurology* 480:331-351.
- Baver SB, Pickard GE, Sollars PJ 2008 Two types of melanopsin retinal ganglion cell differentially innervate the hypothalamic suprachiasmatic nucleus and the olivary pretectal nucleus. *European Journal of Neuroscience* 27:1763-1770.
- Berson DM, Castrucci AM, Provencio I 2010. Morphology and Mosaics of Melanopsin-Expressing Retinal Ganglion Cell Types in Mice. *Journal of Comparative Neurology* 518:2405-2422.
- Berson DM, Dunn FA, Takao M 2002. Phototransduction by retinal ganglion cells that set the circadian clock. *Science* 295:1070-1073.
- Bicknell AB. 2008. The tissue-specific processing of pro-opiomelanocortin. *J Neuroendocrinol* 20(6):692-9.

- Blumenfeld A, Gennings C, Cady R. 2012. Pharmacological Synergy: The Next Frontier on Therapeutic Advancement for Migraine. *Headache* 52:636-647.
- Bolte S & Cordelieres FP. 2006. A guided tour into subcellular colocalization analysis in light microscopy. *Journal of Microscopy-Oxford* 224, 213-232.
- Borbe HO, Wollert U, Muller WE. 1982. Stereospecific [3H]naloxone binding associated with opiate receptors in bovine retina. *Exp Eye Res* 34(4):539-44.
- Boycott BB, Wassle H. 1974. Morphological types of ganglion-cells of domestic cats retina. *Journal of Physiology-London* 240:397-&.
- Brecha N, Johnson J, Kui B, Anton B, Keith D, Evans C, Sternini C. 1995. Mu opioid receptor immunoreactivity is expressed in the retina and retina recipient nuclei. *Analgesia* 1:331-334.
- Brecha NC, Sternini C, Anderson K, Krause JE. 1989. Expression and cellular-localization of substance-P neurokinin-A and neurokinin-B messenger-RNAs in the rat retina. *Visual Neuroscience* 3, 527-535.
- Brecha NC. 2003. Peptide and peptide receptor expression and function in the vertebrate retina. In: Chalupa, Werner, editors. *The visual neurosciences* Cambridge, Massachusetts: The MIT Press. p 334-354.
- Brunelli G, Spano P, Barlati S, Guarneri B, Barbon A, Bresciani R, Pizzi M. 2005. Glutamatergic reinnervation through peripheral nerve graft dictates assembly of glutamatergic synapses at rat skeletal muscle. *Proc Natl Acad Sci U S A* 102(24):8752-7.
- Buhl EH, Dann JF. 1988. Morphological diversity of displaced retinal ganglion-cells in rat—a lucifer yellow study. *Journal of Comparative Neurology* 269:210-218.
- Busch-Dienstfertig M, Stein C. 2010. Opioid receptors and opioid peptide-producing leukocytes in inflammatory pain - Basic and therapeutic aspects. *Brain Behavior and Immunity* 24:683-694.
- Campbell RE, Tour O, Palmer AE, Steinbach PA, Baird GS, Zacharias DA, Tsien RY. 2002. A monomeric red fluorescent protein. *Proc Natl Acad Sci U S A* 99(12):7877-82.
- Caputi A, Rozov A, Blatow M, Monyer H. 2009. Two calretinin-positive GABAergic cell types in layer 2/3 of the mouse neocortex provide different forms of inhibition. *Cereb Cortex* 19(6):1345-59.

- Casini G, Brecha NC. 1992. Colocalization of vasoactive intestinal polypeptide and GABA immunoreactivities in a population of wide-field amacrine cells in the rabbit retina. *Vis Neurosci* 8(4):373-8.
- Chang YC, Gottlieb DI. 1988. Characterization of the proteins purified with monoclonal antibodies to glutamic acid decarboxylase. *J Neurosci* 8(6):2123-30.
- Chen P, Williams SM, Grove KL, Smith MS. 2004. Melanocortin 4 receptor-mediated hyperphagia and activation of neuropeptide Y expression in the dorsomedial hypothalamus during lactation. *J Neurosci* 24(22):5091-100.
- Chen SK, Badea TC, Hattar S 2011. Photoentrainment and pupillary light reflex are mediated by distinct populations of ipRGCs. *Nature* 476:92-+.
- Chieng B, Williams JT 1998. Increased opioid inhibition of GABA release in nucleus accumbens during morphine withdrawal. *Journal of Neuroscience* 18:7033-7039.
- Choi JH, Lee CH, Yoo KY, Hwang IK, Lee IS, Lee YL, Shin HC, Won MH. 2009. Age-related Changes in Calbindin-D28k, Parvalbumin, and Calretinin Immunoreactivity in the Dog Main Olfactory Bulb. *Cell Mol Neurobiol*. Jun 16. [Epub ahead of print]
- Contini M, Raviola E 2003. GABAergic synapses made by a retinal dopaminergic neuron. *Proceedings of the National Academy of Sciences of the United States of America* 100:1358-1363.
- Coombs J, van der List D, Wang GY, Chalupa LM 2006. Morphological properties of mouse retinal ganglion cells. *Neuroscience* 140:123-136.
- Corbett AD, Henderson G, McKnight AT, Paterson SJ 2006. 75 years of opioid research: the exciting but vain quest for the Holy Grail. *British Journal of Pharmacology* 147:S153-S162.
- Costes SV, Daelemans D, Cho EH, Dobbin Z, Pavlakis G & Lockett S. 2004. Automatic and quantitative measurement of protein-protein colocalization in live cells. *Biophysical Journal* 86, 3993-4003.
- Cuenca N, Kolb H 1998. Circuitry and role of substance P-immunoreactive neurons in the primate retina. *Journal of Comparative Neurology* 393:439-456.

- Cuenca N, Kolb H. 1998. Circuitry and role of substance P-immunoreactive neurons in the primate retina. *J Comp Neurol* 393(4):439-56.
- de Melo J, Du GY, Fonseca M, Gillespie LA, Turk WJ, Rubenstein JLR, Eisenstat DD. 2005. Dlx1 and Dlx2 function is necessary for terminal differentiation and survival of late-born retinal ganglion cells in the developing mouse retina. *Development* 132:311-322.
- de Melo J, Qiu XG, Du GY, Cristante L, Eisenstat DD. 2003. Dlx1, Dlx2, Pax6, Brn3b, and Chx10 homeobox gene expression defines the retinal ganglion and inner nuclear layers of the developing and adult mouse retina. *Journal of Comparative Neurology* 461:187-204.
- de Souza FS, Santangelo AM, Bumashny V, Avale ME, Smart JL, Low MJ, Rubinstein M. 2005. Identification of neuronal enhancers of the proopiomelanocortin gene by transgenic mouse analysis and phylogenetic footprinting. *Mol Cell Biol* 25(8):3076-86.
- de Souza FSJ, Santangelo AM, Bumashny V, Avale ME, Smart JL, Low MJ, Rubinstein M. 2005. Identification of neuronal enhancers of the proopiomelanocortin gene by transgenic mouse analysis and phylogenetic footprinting. *Molecular and Cellular Biology* 25:3076-3086.
- Djamgoz MB, Stell WK, Chin CA, Lam DM. 1981. An opiate system in the goldfish retina. *Nature* 292(5824):620-3.
- Dkhissi O, Julien JF, Wasowicz M, il-Thiney N, Nguyen-Legros J, Versaux-Botteri C. 2001. Differential expression of GAD(65) and GAD(67) during the development of the rat retina. *Brain Res* 919(2):242-9.
- Doi M, Uji Y, Yamamura H. 1995. Morphological classification of retinal ganglion-cells in mice. *Journal of Comparative Neurology* 356:368-386.
- Dowling JE, Boycott BB. 1966. Organization of primate retina—electron microscopy. *Proceedings of the Royal Society Series B-Biological Sciences* 166:80-&.
- Dubocovich ML & Weiner N. 1983. Enkephalins modulate H-3 dopamine release from rabbit retina in vitro. *Journal of Pharmacology and Experimental Therapeutics* 224, 634-639.
- Ecker JL, Dumitrescu ON, Wong KY, Alam NM, Chen SK, LeGates T, Renna JM, Prusky GT, Berson

- DM, Hattar S 2010. Melanopsin-Expressing Retinal Ganglion-Cell Photoreceptors: Cellular Diversity and Role in Pattern Vision. *Neuron* 67:49-60.
- Eglen SJ, Raven MA, Tamrazian E, Reese BE. 2003. Dopaminergic amacrine cells in the inner nuclear layer and ganglion cell layer comprise a single functional retinal mosaic. *J Comp Neurol* 466(3):343-55.
- Ehinger B. 1982. Neurotransmitter systems in the retina. *Retina* 2(4):305-21.
- Elias CF, Saper CB, Maratos-Flier E, Tritos NA, Lee C, Kelly J, Tatro JB, Hoffman GE, Ollmann MM, Barsh GS, Sakurai T, Yanagisawa M, Elmquist JK. 1998. Chemically defined projections linking the mediobasal hypothalamus and the lateral hypothalamic area. *J Comp Neurol* 402(4):442-59.
- Esposti D, Esposti G, Lissoni P, Parravicini L, Fraschini F 1988. Action of morphine on melatonin release in the rat. *Journal of Pineal Research* 5:35-39.
- Estevez ME, Fogerson PM, Ilardi MC, Borghuis BG, Chan E, Weng SJ, Auferkorte ON, Demb JB, Berson DM. 2012. Form and Function of the M4 Cell, an Intrinsically Photosensitive Retinal Ganglion Cell Type Contributing to Geniculocortical Vision. *Journal of Neuroscience* 32:13608-13620.
- Euler T, Detwiler PB, Denk W. 2002. Directionally selective calcium signals in dendrites of starburst amacrine cells. *Nature* 418:845-852.
- Famiglietti EV (1983) Starburst amacrine cells and cholinergic neurons—mirror-symmetric ON and OFF amacrine cells of the rabbit retina. *Brain Research* 261:138-144.
- Feng Y, He X, Yang Y, Chao D, Lazarus LH, Xia Y. 2012. Current research in opioid receptor function. *Current Drug Targets* 13:230-246.
- Farajian R, Raven MA, Cusato K, Reese BE. 2004. Cellular positioning and dendritic field size of cholinergic amacrine cells are impervious to early ablation of neighboring cells in the mouse retina. *Vis Neurosci* 21(1):13-22.
- Fischer AJ, Seltner RLP, Stell WK. 1998. Opiate and N-methyl-D-aspartate receptors in form-deprivation myopia. *Visual Neuroscience* 15:1089-1096.

- Ford KJ, Feller MB. 2012. Assembly and disassembly of a retinal cholinergic network. *Visual Neuroscience* 29:61-71.
- Fox MA, Guido W. 2011. Shedding Light on Class-Specific Wiring: Development of Intrinsically Photosensitive Retinal Ganglion Cell Circuitry. *Molecular Neurobiology* 44:321-329.
- Fraschini F, Esposti D, Esposti G, Lucini V, Mariani M, Scaglione F, Vignati G, Della Bella D. 1989. On a possible role of endogenous peptides on melatonin secretion. *Adv. Pineal Res.* 127-132.
- Gábel R, Volgyi B, Pollak E. 1998. Calretinin-immunoreactive elements in the retina and optic tectum of the frog, *Rana esculenta*. *Brain Res* 782(1-2):53-62.
- Gaillard F, Sauve Y. 2007. Cell-based therapy for retina degeneration: The promise of a cure. *Vision Research* 47:2815-2824.
- Galindo-Romero C, Aviles-Trigueros M, Jimenez-Lopez M, Valiente-Soriano FJ, Salinas-Navarro M, Nadal-Nicolas F, Villegas-Perez MP, Vidal-Sanz M & Agudo-Barriuso M. 2011. Axotomy-induced retinal ganglion cell death in adult mice: Quantitative and topographic time course analyses. *Experimental Eye Research* 92, 377-387.
- Gallagher SK, Anglen JN, Mower JM, Vigh J. 2012. Dopaminergic amacrine cells express opioid receptors in the mouse retina. *Visual Neuroscience* 29:203-209.
- Gallagher SK, Witkovsky P, Roux MJ, Low MJ, Otero-Corchon V, Hentges ST & Vigh J. 2010. beta-Endorphin Expression in the Mouse Retina. *Journal of Comparative Neurology* 518, 3130-3148.
- Gerrero MR, McEvelly RJ, Turner E, Lin CR, Oconnell S, Jenne KJ, Hobbs MV, Rosenfeld MG. 1993. Brn-3.0 –A POU-domain protein expressed in the sensory, immune, and endocrine systems that functions on elements distinct from known octamer motifs. *Proceedings of the National Academy of Sciences of the United States of America* 90:10841-10845.
- Ghosh KK, Bujan S, Haverkamp S, Feigenspan A, Wässle H. 2004. Types of bipolar cells in the mouse retina. *J Comp Neurol* 469(1):70-82.
- Glaser AM, Reyes-Vazquez C, Prieto-Gomez B, Burau K, Dafny N. 2012. Morphine administration and abrupt cessation alter the behavioral diurnal activity pattern. *Pharmacology Biochemistry and*

- Behavior 101:544-552.
- Gomes I, Gupta A, Filipovska J, Szeto HH, Pintar JE & Devi LA. 2004. A role for heterodimerization of mu and delta opiate receptors in enhancing morphine analgesia. *Proceedings of the National Academy of Sciences of the United States of America* 101, 5135-5139.
- Gonzalez RC & Wintz P. 1987. *Digital Image Processing*. Addison-Wesley Publishing Company, Reading, MA.
- Graham DM, Wong KY, Shapiro P, Frederick C, Pattabiraman K, Berson DM. 2008. Melanopsin ganglion cells use a membrane-associated rhabdomic phototransduction cascade. *Journal of Neurophysiology* 99:2522-2532.
- Hamano K, Kiyama H, Emson PC, Manabe R, Nakauchi M, Tohyama M. 1990. Localization of two calcium binding proteins, calbindin (28 kD) and parvalbumin (12 kD), in the vertebrate retina. *J Comp Neurol* 302(2):417-24.
- Hannibal J, Fahrenkrug J. 2004. Melanopsin containing retinal ganglion cells are light responsive from birth. *Neuroreport* 15:2317-2320.
- Hannibal J, Moller M, Ottersen OP, Fahrenkrug J. 2000. PACAP and glutamate are co-stored in the retinohypothalamic tract. *J Comp Neurol* 418(2):147-55.
- Harrington ME. 1997. The ventral lateral geniculate nucleus and the intergeniculate leaflet: Interrelated structures in the visual and circadian systems. *Neuroscience and Biobehavioral Reviews* 21:705-727.
- Hasler BP, Smith LJ, Cousins JC, Bootzin RR. 2012. Circadian rhythms, sleep, and substance abuse. *Sleep Medicine Reviews* 16:67-81.
- Hatori M, Le H, Vollmers C, Keding SR, Tanaka N, Schmedt C, Jegla T, Panda S. 2008. Inducible Ablation of Melanopsin-Expressing Retinal Ganglion Cells Reveals Their Central Role in Non-Image Forming Visual Responses. *Plos One* 3.
- Hattar S, Kumar M, Park A, Tong P, Tung J, Yau KW, Berson DM. 2006. Central projections of melanopsin-expressing retinal ganglion cells in the mouse. *Journal of Comparative Neurology*

497:326-349.

Hattar S, Liao HW, Takao M, Berson DM, Yau KW. 2002. Melanopsin-containing retinal ganglion cells: Architecture, projections, and intrinsic photosensitivity. *Science* 295:1065-1070.

Haverkamp S, Inta D, Monyer H, Wässle H. 2009. Expression analysis of green fluorescent protein in retinal neurons of four transgenic mouse lines. *Neuroscience* 160(1):126-39.

Haverkamp S, Wässle H. 2000. Immunocytochemical analysis of the mouse retina. *Journal of Comparative Neurology* 424:1-23.

Haverkamp S, Wässle H. 2000. Immunocytochemical analysis of the mouse retina. *J Comp Neurol* 424(1):1-23.

Hentges ST, Otero-Corchon V, Pennock RL, King CM, Low MJ. 2009. Proopiomelanocortin expression in both GABA and glutamate neurons. *J Neurosci* 29(43):13684-13690.

Herlitze S, Garcia DE, Mackie K, Hille B, Scheuer T, Catterall WA. 1996. Modulation of Ca²⁺ channels by G-protein beta gamma subunits. *Nature* 380:258-262.

Hokfelt T, Broberger C, Xu ZQD, Sergeev V, Ubink R, Diez M. 2000. Neuropeptides - an overview. *Neuropharmacology* 39:1337-1356.

Hosoya K, Tomi M, Tachikawa M. 2011. Strategies for therapy of retinal diseases using systemic drug delivery: relevance of transporters at the blood-retinal barrier. *Expert Opinion on Drug Delivery* 8:1571-1587.

Howells RD, Groth J, Hiller JM, Simon EJ. 1980. Opiate binding sites in the retina: properties and distribution. *J Pharmacol Exp Ther* 215(1):60-4.

Huang H, Wang ZF, Weng SJ, Sun XH, Yang XL. 2013. Neuromodulatory role of melatonin in retinal information processing. *Progress in Retinal and Eye Research* 32:64-87.

Husain S, Abdul Y, Potter DE. 2012. Non-Analgesic Effects of Opioids: Neuroprotection in the Retina. *Current Pharmaceutical Design* 18:6101-6108.

Husain S, Potter DE, Crosson CE. 2009. Opioid Receptor-Activation: Retina Protected from Ischemic Injury. *Investigative Ophthalmology & Visual Science* 50:3853-3859.

- Ingram SL, Williams JT (1994) Opioid inhibition of I_h via adenylyl-cyclase. *Neuron* 13:179-186.
- Isayama T & Zagon IS. 1991. Localization of preproenkephalin-A messenger-RNA in the neonatal rat retina. *Brain Research Bulletin* 27, 805-808.
- Jackson IM, Bolaffi JL, Guillemin R. 1980. Presence of immunoreactive beta-endorphin and enkephalin-like material in the retina and other tissues of the frog, *Rana pipiens*. *Gen Comp Endocrinol* 42(4):505-8.
- Jain V, Ravindran E, Dhingra NK. 2012. Differential expression of Brn3 transcription factors in intrinsically photosensitive retinal ganglion cells in mouse. *Journal of Comparative Neurology* 520:742-755.
- Jan LY, Jan YN. 1997. Receptor-regulated ion channels. *Current Opinion in Cell Biology* 9:155-160.
- Jeon CJ, Strettoi E, Masland RH. 1998. The major cell populations of the mouse retina. *Journal of Neuroscience* 18:8936-8946.
- Kabli N & Cahill CM. 2007. Anti-allodynic effects of peripheral delta opioid receptors in neuropathic pain. *Pain* 127, 84-93.
- Kang TH, Ryu YH, Kim IB, Oh GT, Chun MH. 2004. Comparative study of cholinergic cells in retinas of various mouse strains. *Cell Tissue Res* 317(2):109-15.
- Karnas D, Mordel J, Bonnet D, Pevet P, Hicks D, Meissl H. 2013. Heterogeneity of intrinsically photosensitive retinal ganglion cells in the mouse revealed by molecular phenotyping. *Journal of Comparative Neurology* 521:912-932.
- Kelly E. 2013. Ligand bias at the mu-opioid receptor. *Biochemical Society Transactions* 41:218-224.
- Khalap A, Bagrosky B, LeCaude S, Youson J, Danielson P, Dores RM (2005) Trends in the evolution of the proenkephalin and prodynorphin genes in gnathostomes. *Trends in Comparative Endocrinology and Neurobiology* 1040:22-37.
- Kieffer BL. 1995. Recent advances in molecular recognition and signal transduction of active peptides: Receptors for opioid peptides. *Cellular and Molecular Neurobiology* 15:615-635.

- Kielczewski JL, Pease ME, Quigley HA. 2005. The effect of experimental glaucoma and optic nerve transection on amacrine cells in the rat retina. *Invest Ophthalmol Vis Sci* 46(9):3188-96.
- Kolb H. 1997. Amacrine cells of the mammalian retina: Neurocircuitry and functional roles. *Eye* 11:904-923.
- Kolbinger W & Weiler R. 1993. Modulation of endogenous dopamine release in the turtle retina—effects of light, calcium, and neurotransmitters. *Visual Neuroscience* 10, 1035-1041.
- Kong JH, Fish DR, Rockhill RL, Masland RH. 2005. Diversity of ganglion cells in the mouse retina: unsupervised morphological classification and its limits. *J Comp Neurol* 489(3):293-310.
- Kosterlitz HW, Lord JAH, Paterson SJ & Waterfield AA. 1980. Effects of changes in the structure of enkephalins and of narcotic analgesic drugs on their interactions with mu-receptors and delta-receptors. *British Journal of Pharmacology* 68, 333-342.
- Kwon MS, Seo YJ, Choi SM, Lee JK, Jung JS, Park SH & Suh HW. 2008. The effect of formalin pretreatment on nicotine-induced antinociceptive effect: The role of mu-opioid receptor in the hippocampus. *Neuroscience* 154, 415-423.
- Lall GS, Revell VL, Momiji H, Al Enezi J, Altimus CM, Guler AD, Aguilar C, Cameron MA, Allender S, Hankins MW, Lucas RJ. 2010. Distinct Contributions of Rod, Cone, and Melanopsin Photoreceptors to Encoding Irradiance. *Neuron* 66:417-428.
- Lam TT, Takahashi K, Tso MO. 1994. The effects of naloxone on retinal ischemia in rats. *J Ocul Pharmacol* 10(2):481-92.
- Lamba D, Karl M, Rehl T. 2008. Neural regeneration and cell replacement: A view from the eye. *Cell Stem Cell* 2:538-549.
- Loh HH, Brase DA, Sampathkhanna S, Mar JB, Way EL & Li CH. 1976. Beta-endorphin invitro inhibition of striatal dopamine release. *Nature* 264, 567-568.
- Lucas RJ, Lall GS, Allen AE, Brown TM. 2012. How rod, cone, and melanopsin photoreceptors come together to enlighten the mammalian circadian clock. *Prog Brain Res.*199:1-18
- Lupp A, Richter N, Doll C, Nagel F & Schulz S. 2011. UMB-3, a novel rabbit monoclonal antibody, for assessing

- mu-opioid receptor expression in mouse, rat and human formalin-fixed and paraffin-embedded tissues. *Regulatory Peptides* 167, 9-13.
- Ma MC, Qian H, Ghassemi F, Zhao P, Xia Y. 2005. Oxygen-sensitive delta-opioid receptor-regulated survival and death signals - Novel insights into neuronal preconditioning and protection. *Journal of Biological Chemistry* 280:16208-16218.
- MacNeil MA, Masland RH. 1998. Extreme diversity among amacrine cells: implications for function. *Neuron* 20(5):971-82.
- Manchikanti L, Helm S, Fellows B, Janata JW, Pampati V, Grider JS, Boswell MV. 2012. Opioid Epidemic in the United States. *Pain Physician* 15:ES9-ES38.
- Marc RE. 1986. Neurochemical stratification in the inner plexiform layer of the vertebrate retina. *Vision Research* 26:223-238.
- Marc RE, Murry RF, Fisher SK, Linberg KA, Lewis GP, Kalloniatis M. 1998. Amino acid signatures in the normal cat retina. *Invest Ophthalmol Vis Sci* 39(9):1685-93.
- Masland RH. 2001. Neuronal diversity in the retina. *Current Opinion in Neurobiology* 11:431-436.
- Masland RH. 2005. The many roles of starburst amacrine cells. *Trends in Neurosciences* 28:395-396.
- Masland RH. 2012. The tasks of amacrine cells. *Visual Neuroscience* 29:3-9.
- Masland RH, Mills JW. 1979. Autoradiographic identification of acetylcholine in the rabbit retina. *J Cell Biol* 83(1):159-78.
- Matilla A, Gorbea C, Einum DD, Townsend J, Michalik A, van BC, Jensen CC, Murphy KJ, Ptacek LJ, Fu YH. 2001. Association of ataxin-7 with the proteasome subunit S4 of the 19S regulatory complex. *Hum Mol Genet* 10(24):2821-31.
- Matilla A, Gorbea C, Einum DD, Townsend J, Michalik A, van Broeckhoven C, Jensen CC, Murphy KJ, Ptacek LJ, Fu YH. 2001. Association of ataxin-7 with the proteasome subunit S4 of the 19S regulatory complex. *Human Molecular Genetics* 10:2821-2831.
- May CA, Nakamura K, Fujiyama F & Yanagawa Y. 2008. Quantification and characterization of GABA-ergic amacrine cells in the retina of GAD67-GFP knock-in mice. *Acta Ophthalmologica* 86, 395-

400.

May CA, Nakamura K, Fujiyama F, Yanagawa Y. 2008. Quantification and characterization of GABA-ergic amacrine cells in the retina of GAD67-GFP knock-in mice. *Acta Ophthalmologica* 86:395-400.

Medzihradsky F. 1976. Stereospecific binding of etorphine in isolated neural cells and in retina, determined by a sensitive microassay. *Brain Res* 108(1):212-9.

Meijer JH, Ruijs ACJ, Albus H, van de Geest B, Duindam H, Zwinderman AH, Dahan A. 2000. Fentanyl, a mu-opioid receptor agonist, phase shifts the hamster circadian pacemaker. *Brain Research* 868:135-140.

Millington GW. 2007. The role of proopiomelanocortin (POMC) neurones in feeding behaviour. *Nutr Metab (Lond)* 4:18.

Mistlberger RE, Holmes MM. 1999. Morphine-induced activity attenuates phase shifts to light in C57BL/6J mice. *Brain Research* 829:113-119.

Moon JI, Kim IB, Gwon JS, Park MH, Kang TH, Lim EJ, Choi KR, Chun MH. 2005. Changes in retinal neuronal populations in the DBA/2J mouse. *Cell Tissue Res* 320(1):51-9.

Morgan IG & Boelen MK. 1996. A retinal dark-light switch: A review of the evidence. *Visual Neuroscience* 13, 399-409.

Morgan MM, Christie MJ. 2011. Analysis of opioid efficacy, tolerance, addiction and dependence from cell culture to human. *British Journal of Pharmacology* 164:1322-1334.

Muller LPD, Shelley J, Weiler R. 2007. Displaced amacrine cells of the mouse retina. *Journal of Comparative Neurology* 505:177-189.

Nadal-Nicolas FM, Jimenez-Lopez M, Sobrado-Calvo P, Nieto-Lopez L, Canovas-Martinez I, Salinas-Navarro M, Vidal-Sanz M & Agudo M. 2009. Brn3a as a Marker of Retinal Ganglion Cells: Qualitative and Quantitative Time Course Studies in Naive and Optic Nerve-Injured Retinas. *Investigative Ophthalmology & Visual Science* 50, 3860-3868.

Nathans J, Thomas D, Hogness DS. 1986. Molecular-genetics of human color-vision—the genes

- encoding blue, green, and red pigments. *Science* 232:193-202.
- NC B. 2003. Peptide and peptide receptor expression and function in the vertebrate retina. In: *The visual neurosciences* (Chalupa LM WJ, ed), pp 334-354. Cambridge: The MIT Press.
- Neal MJ, Paterson SJ, Cunningham JR. 1994. Enhancement of retinal acetylcholine release by DAMGO: possibly a direct opioid receptor-mediated excitatory effect. *Br J Pharmacol* 113(3):789-94.
- Newkirk GS, Hoon M, Wong RO, Detwiler PB. 2013. Inhibitory inputs tune the light response properties of dopaminergic amacrine cells in mouse retina. *J. Neurophysiol.* Epub ahead of print
- Nosedá R, Burstein R. 2011. Advances in understanding the mechanisms of migraine-type photophobia. *Current Opinion in Neurology* 24:197-202.
- Nosedá R, Kainz V, Jakubowski M, Gooley JJ, Saper CB, Digre K, Burstein R. 2010. A neural mechanism for exacerbation of headache by light. *Nature Neuroscience* 13:239-U128.
- Oliva AA, Jr., Jiang M, Lam T, Smith KL, Swann JW. 2000. Novel hippocampal interneuronal subtypes identified using transgenic mice that express green fluorescent protein in GABAergic interneurons. *J Neurosci* 20(9):3354-68.
- Omally DM, Masland RH. 1989. Co-release of acetylcholine and gamma-aminobutyric acid by a retinal neuron. *Proceedings of the National Academy of Sciences of the United States of America* 86:3414-3418.
- Overstreet LS, Hentges ST, Bumashny VF, de Souza FS, Smart JL, Santangelo AM, Low MJ, Westbrook GL, Rubinstein M. 2004. A transgenic marker for newly born granule cells in dentate gyrus. *J Neurosci* 24(13):3251-9.
- Pan HL, Wu ZZ, Zhou HY, Chen SR, Zhang HM & Li DP. 2008. Modulation of pain transmission by G-protein-coupled receptors. *Pharmacology & Therapeutics* 117, 141-161.
- Panda S, Sato TK, Castrucci AM, Rollag MD, DeGrip WJ, Hogenesch JB, Provencio I, Kay SA. 2002. Melanopsin (Opn4) requirement for normal light-induced circadian phase shifting. *Science* 298:2213-2216.
- Peng PH, Huang HS, Lee YJ, Chen YS, Ma MC. 2009. Novel role for the delta-opioid receptor in

- hypoxic preconditioning in rat retinas. *Journal of Neurochemistry* 108:741-754.
- Perez-Leighton CE, Schmidt TM, Abramowitz J, Birnbaumer L, Kofuji P. 2011. Intrinsic phototransduction persists in melanopsin-expressing ganglion cells lacking diacylglycerol-sensitive TRPC subunits. *European Journal of Neuroscience* 33:856-867.
- Persson AI, Thorlin T & Eriksson PS. 2005. Comparison of immunoblotted delta opioid receptor proteins expressed in the adult rat brain and their regulation by growth hormone. *Neuroscience Research* 52, 1-9.
- Pierce KL, Premont RT, Lefkowitz RJ. 2002. Seven-transmembrane receptors. *Nature Reviews Molecular Cell Biology* 3:639-650.
- Polyak S. 1941. *The Retina*. Chicago: University of Chicago.
- Pow DV. 1998. Transport is the primary determinant of glycine content in retinal neurons. *J Neurochem* 70(6):2628-36.
- Pragst F, Spiegel K, Leuschner U, Hager A. 1999. Detection of 6-acetylmorphine in vitreous humor and cerebrospinal fluid - Comparison with urinary analysis for proving heroin administration in opiate fatalities. *Journal of Analytical Toxicology* 23:168-172.
- Quina LA, Pak W, Lanier J, Banwait P, Gratwick K, Liu Y, Velasquez T, O'Leary DDM, Goulding M, Turner EE. 2005. Brn3a-expressing retinal ganglion cells project specifically to thalamocortical and collicular visual pathways. *Journal of Neuroscience* 25:11595-11604.
- Raymond ID, Vila A, Huynh UC, Brecha NC. 2008. Cyan fluorescent protein expression in ganglion and amacrine cells in a thy1-CFP transgenic mouse retina. *Mol Vis* 14:1559-74.
- Riazi-Esfahani M, Kiumehr S, Asadi-Amoli F & Dehpour AR. 2009. Effects of intravitreal morphine administered at different time points after reperfusion in a rabbit model of ischemic retinopathy. *Retina-the Journal of Retinal and Vitreous Diseases* 29, 262-268.
- Roux MJ, Robe A, Kiffer BL. Localization of the delta opioid receptor (DOR) and identification of enkephalin-expressing cells in the mouse retina. ARVO Meeting, Fort Lauderdale FL, Invest Ophthalmol Vis Sci 2011;454: E-Abstract 4557

- Rozenfeld R & Devi LA. 2011. Exploring a role for heteromerization in GPCR signalling specificity. *Biochemical Journal* 433, 11-18.
- Sand A, Schmidt TM, Kofuji P. 2012. Diverse types of ganglion cell photoreceptors in the mammalian retina. *Progress in Retinal and Eye Research* 31:287-302.
- Sarthy V, Hoshi H, Mills S, Dudley VJ. 2007. Characterization of green fluorescent protein-expressing retinal cells in CD 44-transgenic mice. *Neuroscience* 144(3):1087-93.
- Sassone-Corsi P. 2012. The Cyclic AMP Pathway. *Cold Spring Harbor Perspectives in Biology* 4.
- Sauriyal DS, Jaggi AS, Singh N. 2011. Extending pharmacological spectrum of opioids beyond analgesia: Multifunctional aspects in different pathophysiological states. *Neuropeptides* 45:175-188.
- Scherrer G, Imamachi N, Cao YQ, Contet C, Mennicken F, O'Donnell D, Kieffer BL, Basbaum AI. 2009. Dissociation of the Opioid Receptor Mechanisms that Control Mechanical and Heat Pain. *Cell* 137:1148-1159.
- Schmidt TM, Kofuji P. 2009. Functional and Morphological Differences among Intrinsically Photosensitive Retinal Ganglion Cells. *Journal of Neuroscience* 29:476-482.
- Schmidt TM, Kofuji P. 2011. Structure and Function of Bistratified Intrinsically Photosensitive Retinal Ganglion Cells in the Mouse. *Journal of Comparative Neurology* 519:1492-1504.
- Schmidt TM, Taniguchi K, Kofuji P. 2008. Intrinsic and extrinsic light responses in melanopsin-expressing ganglion cells during mouse development. *Journal of Neurophysiology* 100:371-384.
- Schwarzer C. 2009. 30 years of dynorphins - New insights on their functions in neuropsychiatric diseases. *Pharmacology & Therapeutics* 123:353-370.
- Sekaran S, Lupi D, Jones SL, Sheely CJ, Hattar S, Yau KW, Lucas RJ, Foster RG, Hankins MW. 2005. Melanopsin-dependent photoreception provides earliest light detection in the mammalian retina. *Current Biology* 15:1099-1107.
- Seltner RLP, Rohrer B, Grant V, Stell WK. 1997. Endogenous opiates in the chick retina and their role in form-deprivation myopia. *Visual Neuroscience* 14:801-809.
- Sernagor E, Eglén SJ, Wong ROL. 2001. Development of retinal ganglion cell structure and function.

- Progress in Retinal and Eye Research 20:139-174.
- Shavali S, Ho B, Govitrapong P, Sawlom S, Ajjimaporn A, Klongpanichapak S, Ebadi M. 2005. Melatonin exerts its analgesic actions not by binding to opioid receptor subtypes but by increasing the release of beta-endorphin an endogenous opioid. *Brain Research Bulletin* 64:471-479.
- Shoji Y, Delfs J, Williams JT. 1999. Presynaptic inhibition of GABA(B)-mediated synaptic potentials in the ventral tegmental area during morphine withdrawal. *Journal of Neuroscience* 19:2347-2355.
- Slaughter MM, Mattler JA, Gottlieb DI. 1985. Opiate binding sites in the chick, rabbit and goldfish retina. *Brain Res* 339(1):39-47.
- Smart JL, Tolle V, Low MJ. 2006. Glucocorticoids exacerbate obesity and insulin resistance in neuron-specific proopiomelanocortin-deficient mice. *J Clin Invest* 116(2):495-505.
- Smitherman TA, Burch R, Sheikh H, Loder E. 2013. The Prevalence, Impact, and Treatment of Migraine and Severe Headaches in the United States: A Review of Statistics From National Surveillance Studies. *Headache* 53:427-436.
- Sternini C, Spann M, Anton B, Keith DE, Bunnett NW, vonZastrow M, Evans C, Brecha NC. 1996. Agonist-selective endocytosis of mu opioid receptor by neurons in vivo. *Proceedings of the National Academy of Sciences of the United States of America* 93:9241-9246.
- Storch KF, Paz C, Signorovitch J, Raviola E, Pawlyk B, Li T, Weitz CJ. 2007. Intrinsic circadian clock of the mammalian retina: importance for retinal processing of visual information. *Cell* 130(4):730-41.
- Su YY, Watt CB, Lam DM. 1985. Opioid pathways in an avian retina. I. The content, biosynthesis, and release of Met5-enkephalin. *J Neurosci* 5(4):851-6.
- Su YYT & Watt CB. 1987. Interaction between enkephalin and dopamine in the avian retina. *Brain Research* 423, 63-70.
- Sun WZ, Li N, He SG. 2002. Large-scale morphological survey of mouse retinal ganglion cells. *Journal of Comparative Neurology* 451:115-126.

- Sung CH, Chuang JZ. 2010. The cell biology of vision. *Journal of Cell Biology* 190:953-963.
- Svoboda KR, Lupica CR. 1998. Opioid inhibition of hippocampal interneurons via modulation of potassium and hyperpolarization-activated cation (I-h) currents. *Journal of Neuroscience* 18:7084-7098.
- Tamamaki N, Yanagawa Y, Tomioka R, Miyazaki J, Obata K, Kaneko T. 2003. Green fluorescent protein expression and colocalization with calretinin, parvalbumin, and somatostatin in the GAD67-GFP knock-in mouse. *J Comp Neurol* 467(1):60-79.
- Tamamaki N, Yanagawa Y, Tomioka R, Miyazaki JI, Obata K, Kaneko T. 2003. Green fluorescent protein expression and colocalization with calretinin, parvalbumin, and somatostatin in the GAD67-GFP knock-in mouse. *Journal of Comparative Neurology* 467:60-79.
- Tauchi M, Masland RH. 1984. The shape and arrangement of the cholinergic neurons in the rabbit retina. *Proceedings of the Royal Society B-Biological Sciences* 223:101-+.
- Taylor WR, Smith RG. 2012. The role of starburst amacrine cells in visual signal processing. *Visual Neuroscience* 29:73-81.
- Tosini G, Baba K, Hwang CK, Iuvone PM. 2012. Melatonin: An underappreciated player in retinal physiology and pathophysiology. *Experimental Eye Research* 103:82-89.
- Tu DC, Zhang D, Demas J, Van Gelder RN. 2005. Functional development of intrinsically photosensitive retinal ganglion cells. *Investigative Ophthalmology & Visual Science* 46.
- Van Hook MJ, Wong KY, Berson DM. 2012. Dopaminergic modulation of ganglion-cell photoreceptors in rat. *European Journal of Neuroscience* 35:507-518.
- Vaney DI, Nelson JC, Pow DV. 1998. Neurotransmitter coupling through gap junctions in the retina. *J Neurosci* 18(24):10594-602.
- Vansteensel MJ, Magnone MC, van Oosterhout F, Baeriswyl S, Albrecht U, Albus H, Dahan A, Meijer JH. 2005. The opioid fentanyl affects light input, electrical activity and Per gene expression in the hamster suprachiasmatic nuclei. *European Journal of Neuroscience* 21:2958-2966.
- Vardi N, Auerbach P. 1995. Specific cell types in cat retina express different forms of glutamic acid

- decarboxylase. *J Comp Neurol* 351(3):374-84.
- Vitanova L, Popova E, Kuppenova P, Kosteljanetz N, Belcheva S. 1990. Comparative studies on the effects of some enkephalin agonists on the ERG of frog and turtle. *Comp Biochem Physiol C* 97(1):93-8.
- Voigt T. 1986. Cholinergic amacrine cells in the rat retina. *J Comp Neurol* 248(1):19-35.
- Volgyi B, Chheda S, Bloomfield SA. 2009. Tracer Coupling Patterns of the Ganglion Cell Subtypes in the Mouse Retina. *Journal of Comparative Neurology* 512:664-687.
- von Engelhardt J, Eliava M, Meyer AH, Rozov A, Monyer H. 2007. Functional characterization of intrinsic cholinergic interneurons in the cortex. *J Neurosci* 27(21):5633-42.
- Wamsley JK, Palacios JM & Kuhar MJ. 1981. Autoradiographic localization of opioid receptors in the mammalian retina. *Neuroscience Letters* 27, 19-24.
- Wamsley JK, Palacios JM, Kuhar MJ. 1981. Autoradiographic localization of opioid receptors in the mammalian retina. *Neurosci Lett* 27(1):19-24.
- Wang HB, Zhao B, Zhong YQ, Li KC, Li ZY, Wang QO, Lu YJ, Zhang ZN, He SQ, Zheng HC, Wu SX, Hokfelt TGM, Bao L & Zhang X. 2010. Coexpression of delta- and mu-opioid receptors in nociceptive sensory neurons. *Proceedings of the National Academy of Sciences of the United States of America* 107, 13117-13122.
- Wässle H. 2004. Parallel processing in the mammalian retina. *Nature Reviews Neuroscience* 5:747-757.
- Wässle H, Riemann HJ. 1978. The mosaic of nerve cells in the mammalian retina. *Proc R Soc Lond B Biol Sci* 200(1141):441-61.
- Watt CB, Li T, Lam DM, Wu SM. 1988. Quantitative studies of enkephalin's coexistence with gamma-aminobutyric acid, glycine and neurotensin in amacrine cells of the chicken retina. *Brain Res* 444(2):366-70.
- Watt CB, Su YY, Lam DM. 1984. Interactions between enkephalin and GABA in avian retina. *Nature* 311(5988):761-3.
- Weng SJ, Wong KY, Berson DM. 2009. Circadian Modulation of Melanopsin-Driven Light Response in

- Rat Ganglion-Cell Photoreceptors. *Journal of Biological Rhythms* 24:391-402.
- Werblin FS, Dowling JE. 1969. Organization of retina of mudpuppy necturus maculosus. 2. Intracellular recording. *Journal of Neurophysiology* 32:339-&.
- Whitney IE, Keeley PW, Raven MA, Reese BE. 2008. Spatial patterning of cholinergic amacrine cells in the mouse retina. *Journal of Comparative Neurology* 508:1-12.
- Wiechmann AF, Sherry DM. 2013. Role of Melatonin and Its Receptors in the Vertebrate Retina. *International Review of Cell and Molecular Biology*, Vol 300 300:211-242.
- Williams JT, Christie MJ, Manzoni O. 2001. Cellular and synaptic adaptations mediating opioid dependence. *Physiological Reviews* 81:299-343.
- Witkovsky P. 2004. Dopamine and retinal function. *Documenta Ophthalmologica* 108:17-40.
- Witkovsky P, Arango-Gonzalez B, Haycock JW & Kohler K. 2005. Rat retinal dopaminergic neurons: Differential maturation of somatodendritic and axonal compartments. *Journal of Comparative Neurology* 481, 352-362.
- Witkovsky P, Gabriel R & Krizaj D. 2008. Anatomical and neurochemical characterization of dopaminergic interplexiform processes in mouse and rat retinas. *Journal of Comparative Neurology* 510, 158-174.
- Wulle I, Wagner HJ. 1990. GABA and tyrosine-hydroxylase immunocytochemistry reveal different patterns of colocalization in retinal neurons of various vertebrates. *Journal of Comparative Neurology* 296:173-178.
- Wyman J, Bultman S. 2004. Postmortem distribution of heroin metabolites in femoral blood, liver, cerebrospinal fluid, and vitreous humor. *Journal of Analytical Toxicology* 28:260-263.
- Xi H, Treacy MN, Simmons DM, Ingraham HA, Swanson LW, Rosenfeld MG. 1989. Expression of a large family of POU-domain regulatory genes in mammalian brain-development. *Nature* 340:35-42.
- Xiang MQ, Gan L, Zhou LJ, Klein WH, Nathans J. 1996. Targeted deletion of the mouse POU domain gene *Brn-3a* causes a selective loss of neurons in the brainstem and trigeminal ganglion,

- uncoordinated limb movement, and impaired suckling. *Proceedings of the National Academy of Sciences of the United States of America* 93:11950-11955.
- Xiang MQ, Zhou LJ, Macke JP, Yoshioka T, Hendry SHC, Eddy RL, Shows TB & Nathans J. 1995. The Brn-3 family of POU-domain factors—primary structure, binding-specificity, and expression in subsets of retinal ganglion-cells and somatosensory neurons. *Journal of Neuroscience* 15, 4762-4785.
- Xiang MQ, Zhou LJ, Peng YW, Eddy RL, Shows TB, Nathans J. 1993. BRN-3B - A POU domain gene expressed in a subset of retinal ganglion-cells. *Neuron* 11:689-701.
- Yamamoto T, Yamato E, Tashiro F, Sato T, Noso S, Ikegami H, Tamura S, Yanagawa Y, Miyazaki JI. 2004. Development of autoimmune diabetes in glutamic acid decarboxylase 65 (GAD65) knockout NOD mice. *Diabetologia* 47(2):221-4.
- Yamasaki EN, Barbosa VD, De Mello FG, Hokoc JN. 1999. GABAergic system in the developing mammalian retina: dual sources of GABA at early stages of postnatal development. *Int J Dev Neurosci* 17(3):201-13.
- Yang DS, Boelen MK, Morgan IG. 1997. Development of the enkephalin-, neurotensin- and somatostatin-like (ENSLI) amacrine cells in the chicken retina. *Brain Res Dev Brain Res* 101(1-2):57-65.
- Yoshida K, Watanabe D, Ishikane H, Tachibana M, Pastan I, Nakanishi S. 2001. A key role of starburst amacrine cells in originating retinal directional selectivity and optokinetic eye movement. *Neuron* 30:771-780.
- Zafra F, Aragon C, Olivares L, Danbolt NC, Gimenez C, Storm-Mathisen J. 1995. Glycine transporters are differentially expressed among CNS cells. *J Neurosci* 15(5 Pt 2):3952-69.
- Zalutsky RA, Miller RF. 1990a. The physiology of somatostatin in the rabbit retina. *J Neurosci* 10(2):383-93.
- Zalutsky RA, Miller RF. 1990b. The physiology of substance P in the rabbit retina. *J Neurosci* 10(2):394-402.

Zheng JJ, Lee S, Zhou ZJ. 2004. A developmental switch in the excitability and function of the starburst network in the mammalian retina. *Neuron* 44:851-864.

Zhou ZJ, Lee S. 2008. Synaptic physiology of direction selectivity in the retina. *J Physiol* 586(Pt 18):4371-6.

Appendices

Appendix I:

Copyright Clearance: Springer

License Agreement for the use of figures

SPRINGER LICENSE TERMS AND CONDITIONS

Jul 15, 2013

This is a License Agreement between Shannon K Gallagher ("You") and Springer ("Springer") provided by Copyright Clearance Center ("CCC"). The license consists of your order details, the terms and conditions provided by Springer, and the payment terms and conditions.

All payments must be made in full to CCC. For payment instructions, please see information listed at the bottom of this form.

License Number	3158931225541
License date	May 30, 2013
Licensed content publisher	Springer
Licensed content publication	Molecular Neurobiology
Licensed content title	Shedding Light on Class-Specific Wiring: Development of Intrinsically Photosensitive Retinal Ganglion Cell Circuitry
Licensed content author	Michael A. Fox
Licensed content date	Jan 1, 2011
Volume number	44
Issue number	3
Type of Use	Thesis/Dissertation
Portion	Figures
Author of this Springer article	No
Order reference number	
Title of your thesis / dissertation	mu-opioid system in the mammalian retina
Expected completion date	Aug 2013
Estimated size(pages)	90
Total	0.00 USD
Terms and Conditions	

Introduction

The publisher for this copyrighted material is Springer Science + Business Media. By

clicking "accept" in connection with completing this licensing transaction, you agree that the following terms and conditions apply to this transaction (along with the Billing and Payment terms and conditions established by Copyright Clearance Center, Inc. ("CCC"), at the time that you opened your Rightslink account and that are available at any time at <http://myaccount.copyright.com>).

Limited License

With reference to your request to reprint in your thesis material on which Springer Science and Business Media control the copyright, permission is granted, free of charge, for the use indicated in your enquiry.

Licenses are for one-time use only with a maximum distribution equal to the number that you identified in the licensing process.

This License includes use in an electronic form, provided its password protected or on the university's intranet or repository, including UMI (according to the definition at the Sherpa website: <http://www.sherpa.ac.uk/romeo/>). For any other electronic use, please contact Springer at (permissions.dordrecht@springer.com or permissions.heidelberg@springer.com).

The material can only be used for the purpose of defending your thesis, and with a maximum of 100 extra copies in paper.

Although Springer holds copyright to the material and is entitled to negotiate on rights, this license is only valid, subject to a courtesy information to the author (address is given with the article/chapter) and provided it concerns original material which does not carry references to other sources (if material in question appears with credit to another source, authorization from that source is required as well).

Permission free of charge on this occasion does not prejudice any rights we might have to charge for reproduction of our copyrighted material in the future.

Altering/Modifying Material: Not Permitted

You may not alter or modify the material in any manner. Abbreviations, additions, deletions and/or any other alterations shall be made only with prior written authorization of the author(s) and/or Springer Science + Business Media. (Please contact Springer at (permissions.dordrecht@springer.com or permissions.heidelberg@springer.com))

Reservation of Rights

Springer Science + Business Media reserves all rights not specifically granted in the combination of (i) the license details provided by you and accepted in the course of this licensing transaction, (ii) these terms and conditions and (iii) CCC's Billing and Payment terms and conditions.

Copyright Notice:Disclaimer

You must include the following copyright and permission notice in connection with any

reproduction of the licensed material: "Springer and the original publisher /journal title, volume, year of publication, page, chapter/article title, name(s) of author(s), figure number(s), original copyright notice) is given to the publication in which the material was originally published, by adding; with kind permission from Springer Science and Business Media"

Warranties: None

Example 1: Springer Science + Business Media makes no representations or warranties with respect to the licensed material.

Example 2: Springer Science + Business Media makes no representations or warranties with respect to the licensed material and adopts on its own behalf the limitations and disclaimers established by CCC on its behalf in its Billing and Payment terms and conditions for this licensing transaction.

Indemnity

You hereby indemnify and agree to hold harmless Springer Science + Business Media and CCC, and their respective officers, directors, employees and agents, from and against any and all claims arising out of your use of the licensed material other than as specifically authorized pursuant to this license.

No Transfer of License

This license is personal to you and may not be sublicensed, assigned, or transferred by you to any other person without Springer Science + Business Media's written permission.

No Amendment Except in Writing

This license may not be amended except in a writing signed by both parties (or, in the case of Springer Science + Business Media, by CCC on Springer Science + Business Media's behalf).

Objection to Contrary Terms

Springer Science + Business Media hereby objects to any terms contained in any purchase order, acknowledgment, check endorsement or other writing prepared by you, which terms are inconsistent with these terms and conditions or CCC's Billing and Payment terms and conditions. These terms and conditions, together with CCC's Billing and Payment terms and conditions (which are incorporated herein), comprise the entire agreement between you and Springer Science + Business Media (and CCC) concerning this licensing transaction. In the event of any conflict between your obligations established by these terms and conditions and those established by CCC's Billing and Payment terms and conditions, these terms and conditions shall control.

Jurisdiction

All disputes that may arise in connection with this present License, or the breach thereof, shall be settled exclusively by arbitration, to be held in The Netherlands, in accordance with Dutch law, and to be conducted under the Rules of the 'Netherlands Arbitrage Instituut'

(Netherlands Institute of Arbitration).*OR:*

All disputes that may arise in connection with this present License, or the breach thereof, shall be settled exclusively by arbitration, to be held in the Federal Republic of Germany, in accordance with German law.

Permission to modify figures from publisher and corresponding author

Dear Shannon,

Thanks for your request. Permission to make these modifications is granted, provided permission is obtained from the authors as well and a proper reference is included. “

Best wishes,

Maaïke

Maaïke Duine

Springer

Rights and Permissions

Van Godewijckstraat 30 | 3311 GX

P.O. Box 17 | 3300 AADordrecht |

The Netherlandstel

+31 (0) 78 657 6537

fax+31 (0) 78 657 6377

maaïke.duine@springer.com

Hi Shannon

Yes, of course. No problem.

And kudos for tracking me down since I moved my lab a few months ago and have only just gotten papers out with the new address.

Best of luck with your thesis, defense, and whatever you have lined up afterwards

Mike

Michael A. Fox, Ph.D.

Associate Professor, Virginia Tech Carilion Research Institute

Associate Professor, Department of Biological Sciences, Virginia Tech

Virginia Tech Carilion Research Institute

2 Riverside Circle,

Roanoke, VA 24016

Copyright Clearance: John Wiley and Sons

License Agreement for the use of full article

JOHN WILEY AND SONS LICENSE TERMS AND CONDITIONS

Jul 15, 2013

This is a License Agreement between Shannon K Gallagher ("You") and John Wiley and Sons ("John Wiley and Sons") provided by Copyright Clearance Center ("CCC"). The license consists of your order details, the terms and conditions provided by John Wiley and Sons, and the payment terms and conditions.

All payments must be made in full to CCC. For payment instructions, please see information listed at the bottom of this form.

License Number	3166601407281
License date	Jun 12, 2013
Licensed content publisher	John Wiley and Sons
Licensed content publication	Journal of Comparative Neurology
Licensed content title	β -Endorphin expression in the mouse retina
Licensed copyright line	Copyright © 2010 Wiley-Liss, Inc.
Licensed content author	Shannon K. Gallagher, Paul Witkovsky, Michel J. Roux, Malcolm J. Low, Veronica Otero-Corchon, Shane T. Hentges, Jozsef Vigh
Licensed content date	Mar 23, 2010
Start page	3130

End page	3148
Type of use	Dissertation/Thesis
Requestor type	Author of this Wiley article
Format	Print and electronic
Portion	Full article
Will you be translating?	No
Total	0.00 USD
Terms and Conditions	

TERMS AND CONDITIONS

This copyrighted material is owned by or exclusively licensed to John Wiley & Sons, Inc. or one of its group companies (each a "Wiley Company") or a society for whom a Wiley Company has exclusive publishing rights in relation to a particular journal (collectively "WILEY"). By clicking "accept" in connection with completing this licensing transaction, you agree that the following terms and conditions apply to this transaction (along with the billing and payment terms and conditions established by the Copyright Clearance Center Inc., ("CCC's Billing and Payment terms and conditions"), at the time that you opened your RightsLink account (these are available at any time at <http://myaccount.copyright.com>).

Terms and Conditions

1. The materials you have requested permission to reproduce (the "Materials") are protected by copyright.

2. You are hereby granted a personal, non-exclusive, non-sublicensable, non-transferable, worldwide, limited license to reproduce the Materials for the purpose specified in the licensing process. This license is for a one-time use only with a maximum distribution equal to the number that you identified in the licensing process. Any form of republication granted by this license must be completed within two years of the date of the grant of this license (although copies prepared before may be distributed thereafter). The Materials shall not be used in any other manner or for any other purpose. Permission is granted subject to an appropriate acknowledgement given to the author, title of the material/book/journal and the publisher. You shall also duplicate the copyright notice that appears in the Wiley publication in your use of the Material. Permission is also granted on the understanding that nowhere in the text is a previously published source acknowledged for all or part of this Material. Any third party material is expressly excluded from this permission.

3. With respect to the Materials, all rights are reserved. Except as expressly granted by the terms of the license, no part of the Materials may be copied, modified, adapted (except for minor reformatting required by the new Publication), translated, reproduced, transferred or distributed, in any form or by any means, and no derivative works may be made based on the Materials without the prior permission of the respective copyright owner. You may not alter, remove or suppress in any manner any copyright, trademark or other notices displayed

by the Materials. You may not license, rent, sell, loan, lease, pledge, offer as security, transfer or assign the Materials, or any of the rights granted to you hereunder to any other person.

4. The Materials and all of the intellectual property rights therein shall at all times remain the exclusive property of John Wiley & Sons Inc or one of its related companies (WILEY) or their respective licensors, and your interest therein is only that of having possession of and the right to reproduce the Materials pursuant to Section 2 herein during the continuance of this Agreement. You agree that you own no right, title or interest in or to the Materials or any of the intellectual property rights therein. You shall have no rights hereunder other than the license as provided for above in Section 2. No right, license or interest to any trademark, trade name, service mark or other branding ("Marks") of WILEY or its licensors is granted hereunder, and you agree that you shall not assert any such right, license or interest with respect thereto.

5. NEITHER WILEY NOR ITS LICENSORS MAKES ANY WARRANTY OR REPRESENTATION OF ANY KIND TO YOU OR ANY THIRD PARTY, EXPRESS, IMPLIED OR STATUTORY, WITH RESPECT TO THE MATERIALS OR THE ACCURACY OF ANY INFORMATION CONTAINED IN THE MATERIALS, INCLUDING, WITHOUT LIMITATION, ANY IMPLIED WARRANTY OF MERCHANTABILITY, ACCURACY, SATISFACTORY QUALITY, FITNESS FOR A PARTICULAR PURPOSE, USABILITY, INTEGRATION OR NON-INFRINGEMENT AND ALL SUCH WARRANTIES ARE HEREBY EXCLUDED BY WILEY AND ITS LICENSORS AND WAIVED BY YOU.

6. WILEY shall have the right to terminate this Agreement immediately upon breach of this Agreement by you.

7. You shall indemnify, defend and hold harmless WILEY, its Licensors and their respective directors, officers, agents and employees, from and against any actual or threatened claims, demands, causes of action or proceedings arising from any breach of this Agreement by you.

8. IN NO EVENT SHALL WILEY OR ITS LICENSORS BE LIABLE TO YOU OR ANY OTHER PARTY OR ANY OTHER PERSON OR ENTITY FOR ANY SPECIAL, CONSEQUENTIAL, INCIDENTAL, INDIRECT, EXEMPLARY OR PUNITIVE DAMAGES, HOWEVER CAUSED, ARISING OUT OF OR IN CONNECTION WITH THE DOWNLOADING, PROVISIONING, VIEWING OR USE OF THE MATERIALS REGARDLESS OF THE FORM OF ACTION, WHETHER FOR BREACH OF CONTRACT, BREACH OF WARRANTY, TORT, NEGLIGENCE, INFRINGEMENT OR OTHERWISE (INCLUDING, WITHOUT LIMITATION, DAMAGES BASED ON LOSS OF PROFITS, DATA, FILES, USE, BUSINESS OPPORTUNITY OR CLAIMS OF THIRD PARTIES), AND WHETHER OR NOT THE PARTY HAS BEEN ADVISED OF THE POSSIBILITY OF SUCH DAMAGES. THIS LIMITATION SHALL APPLY NOTWITHSTANDING ANY FAILURE OF ESSENTIAL PURPOSE OF ANY LIMITED

REMEDY PROVIDED HEREIN.

9. Should any provision of this Agreement be held by a court of competent jurisdiction to be illegal, invalid, or unenforceable, that provision shall be deemed amended to achieve as nearly as possible the same economic effect as the original provision, and the legality, validity and enforceability of the remaining provisions of this Agreement shall not be affected or impaired thereby.

10. The failure of either party to enforce any term or condition of this Agreement shall not constitute a waiver of either party's right to enforce each and every term and condition of this Agreement. No breach under this agreement shall be deemed waived or excused by either party unless such waiver or consent is in writing signed by the party granting such waiver or consent. The waiver by or consent of a party to a breach of any provision of this Agreement shall not operate or be construed as a waiver of or consent to any other or subsequent breach by such other party.

11. This Agreement may not be assigned (including by operation of law or otherwise) by you without WILEY's prior written consent.

12. Any fee required for this permission shall be non-refundable after thirty (30) days from receipt

13. These terms and conditions together with CCC's Billing and Payment terms and conditions (which are incorporated herein) form the entire agreement between you and WILEY concerning this licensing transaction and (in the absence of fraud) supersedes all prior agreements and representations of the parties, oral or written. This Agreement may not be amended except in writing signed by both parties. This Agreement shall be binding upon and inure to the benefit of the parties' successors, legal representatives, and authorized assigns.

14. In the event of any conflict between your obligations established by these terms and conditions and those established by CCC's Billing and Payment terms and conditions, these terms and conditions shall prevail.

15. WILEY expressly reserves all rights not specifically granted in the combination of (i) the license details provided by you and accepted in the course of this licensing transaction, (ii) these terms and conditions and (iii) CCC's Billing and Payment terms and conditions.

16. This Agreement will be void if the Type of Use, Format, Circulation, or Requestor Type was misrepresented during the licensing process.

17. This Agreement shall be governed by and construed in accordance with the laws of the State of New York, USA, without regards to such state's conflict of law rules. Any legal action, suit or proceeding arising out of or relating to these Terms and Conditions or the breach thereof shall be instituted in a court of competent jurisdiction in New York County in the State of New York in the United States of America and each party hereby consents

and submits to the personal jurisdiction of such court, waives any objection to venue in such court and consents to service of process by registered or certified mail, return receipt requested, at the last known address of such party.

Wiley Open Access Terms and Conditions

Wiley publishes Open Access articles in both its Wiley Open Access Journals program [<http://www.wileyopenaccess.com/view/index.html>] and as Online Open articles in its subscription journals. The majority of Wiley Open Access Journals have adopted the [Creative Commons Attribution License](#) (CC BY) which permits the unrestricted use, distribution, reproduction, adaptation and commercial exploitation of the article in any medium. No permission is required to use the article in this way provided that the article is properly cited and other license terms are observed. A small number of Wiley Open Access journals have retained the [Creative Commons Attribution Non Commercial License](#) (CC BY-NC), which permits use, distribution and reproduction in any medium, provided the original work is properly cited and is not used for commercial purposes.

Online Open articles - Authors selecting Online Open are, unless particular exceptions apply, offered a choice of Creative Commons licenses. They may therefore select from the CC BY, the CC BY-NC and the [Attribution-NoDerivatives](#) (CC BY-NC-ND). The CC BY-NC-ND is more restrictive than the CC BY-NC as it does not permit adaptations or modifications without rights holder consent.

Wiley Open Access articles are protected by copyright and are posted to repositories and websites in accordance with the terms of the applicable Creative Commons license referenced on the article. At the time of deposit, Wiley Open Access articles include all changes made during peer review, copyediting, and publishing. Repositories and websites that host the article are responsible for incorporating any publisher-supplied amendments or retractions issued subsequently.

Wiley Open Access articles are also available without charge on Wiley's publishing platform, **Wiley Online Library** or any successor sites.

Conditions applicable to all Wiley Open Access articles:

- The authors' moral rights must not be compromised. These rights include the right of "paternity" (also known as "attribution" - the right for the author to be identified as such) and "integrity" (the right for the author not to have the work altered in such a way that the author's reputation or integrity may be damaged).
- Where content in the article is identified as belonging to a third party, it is the obligation of the user to ensure that any reuse complies with the copyright policies of the owner of that content.
- If article content is copied, downloaded or otherwise reused for research and other purposes as permitted, a link to the appropriate bibliographic citation (authors, journal, article title, volume, issue, page numbers, DOI and the link to the definitive

published version on Wiley Online Library) should be maintained. Copyright notices and disclaimers must not be deleted.

- Creative Commons licenses are copyright licenses and do not confer any other rights, including but not limited to trademark or patent rights.

- Any translations, for which a prior translation agreement with Wiley has not been agreed, must prominently display the statement: "This is an unofficial translation of an article that appeared in a Wiley publication. The publisher has not endorsed this translation."

Conditions applicable to non-commercial licenses (CC BY-NC and CC BY-NC-ND)

For non-commercial and non-promotional purposes individual non-commercial users may access, download, copy, display and redistribute to colleagues Wiley Open Access articles. In addition, articles adopting the CC BY-NC may be adapted, translated, and text- and data-mined subject to the conditions above.

Use by commercial "for-profit" organizations

Use of non-commercial Wiley Open Access articles for commercial, promotional, or marketing purposes requires further explicit permission from Wiley and will be subject to a fee. Commercial purposes include:

- Copying or downloading of articles, or linking to such articles for further redistribution, sale or licensing;
- Copying, downloading or posting by a site or service that incorporates advertising with such content;
- The inclusion or incorporation of article content in other works or services (other than normal quotations with an appropriate citation) that is then available for sale or licensing, for a fee (for example, a compilation produced for marketing purposes, inclusion in a sales pack)
- Use of article content (other than normal quotations with appropriate citation) by for-profit organizations for promotional purposes
- Linking to article content in e-mails redistributed for promotional, marketing or educational purposes;
- Use for the purposes of monetary reward by means of sale, resale, license, loan, transfer or other form of commercial exploitation such as marketing products

- Print reprints of Wiley Open Access articles can be purchased from: corporatesales@wiley.com

The modification or adaptation for any purpose of an article referencing the CC BY-NC-ND License requires consent which can be requested from RightsLink@wiley.com .

Other Terms and Conditions:

BY CLICKING ON THE "I AGREE..." BOX, YOU ACKNOWLEDGE THAT YOU HAVE READ AND FULLY UNDERSTAND EACH OF THE SECTIONS OF AND PROVISIONS SET FORTH IN THIS AGREEMENT AND THAT YOU ARE IN AGREEMENT WITH AND ARE WILLING TO ACCEPT ALL OF YOUR OBLIGATIONS AS SET FORTH IN THIS AGREEMENT.

Copyright Clearance: Cambridge University Press

License Agreement for the use of full article

CAMBRIDGE UNIVERSITY PRESS LICENSE TERMS AND CONDITIONS

Jul 15, 2013

This is a License Agreement between Shannon K Gallagher ("You") and Cambridge University Press ("Cambridge University Press") provided by Copyright Clearance Center ("CCC"). The license consists of your order details, the terms and conditions provided by Cambridge University Press, and the payment terms and conditions.

All payments must be made in full to CCC. For payment instructions, please see information listed at the bottom of this form.

License Number	3166610153041
License date	Jun 12, 2013
Licensed content publisher	Cambridge University Press
Licensed content publication	Visual Neuroscience
Licensed content title	Dopaminergic amacrine cells express opioid receptors in the mouse retina

Licensed content author	SHANNON K. GALLAGHER, JULIA N. ANGLIN, JUSTIN M. MOWER and JOZSEF VIGH
Licensed content date	May 1, 2012
Volume number	29
Issue number	03
Start page	203
End page	209
Type of Use	Dissertation/Thesis
Requestor type	Author
Portion	Full article
Author of this Cambridge University Press article	Yes
Author / editor of the new work	Yes
Order reference number	
Territory for reuse	North America Only
Title of your thesis / dissertation	mu-opioid system in the mammalian retina
Expected completion date	Aug 2013
Estimated size(pages)	90
Billing Type	Invoice
Billing address	Colorado State University 1680 Campus Delivery FORT COLLINS, CO 80523 United States
Total	0.00 USD
Terms and Conditions	
Terms and Conditions are not available at this time.	

Appendix II:

Multielectrode array materials and methods:

Postnatal day 6-11 (P6-P11) rats were anesthetized with isoflurane and euthanized via decapitation. Eyes were enucleated and their anterior chambers removed. Retinas were isolated from eye cups in dissecting solution consisting of bicarbonate buffered Ames' medium (A1372-25; US Biological, Swampscott, MA) with 0.1mM EGTA added and bubbled with 95% O₂ 5% CO₂. A flat portion of the central retina devoid the optic nerve head was transferred to a MEA-1060 multielectrode array (Multi Channel Systems Reutlingen, Germany) recording chamber (60MEA200/30iR-ITO; ALA Scientific Instruments Inc. Farmingdale, NY). The retina was oriented, with the ganglion-cell layer (GCL) down, over the recording electrodes and secured in place with nylon mesh and wire weight.

For all recordings retinas were super-fused with Ames' medium equilibrated with 95% O₂ 5% CO₂ at 37 °C. To evaluate the effect of μ -opioid receptor (MOR) activity on ipRGCs light responses, single doses (1nM-10 μ M) of [D-Ala², MePhe⁴, Gly-ol⁵]-enkephalin (DAMGO, MOR specific agonist) were bath applied with the synaptic blockers.

Full-field light stimuli were generated using a blue (470 \pm 5 nm) LED (00-469-ND, Digi-key, USA). The intensity of light pulses were controlled by the command voltage of a 50 mHz Function generator (Berkley Nucleonics, CA) with mV precision, calibrated to 4 x 10¹⁵ photons x cm⁻² x s⁻¹ by an Optical Meter (model 1918-C). Retinas were dark adapted for at least one hour prior to light stimulation and light responses were recorded from 20 second flashes every 20 minutes. Spiking activity was amplified, band-pass filtered between 500 Hz and 1.5 kHz and digitized at 25 kHz using MCRack software (Multi Channel Systems). Extracellular spikes were isolated from raw data using a -4.5 standard deviation of noise threshold filter (MCRack

software, MCS). Cluster analysis of the spike data was performed using Offline Sorter software (Plexon Inc., Dallas, TX) in two consecutive steps (T distribution Error of Mean followed by K mean sorting) and inspected manually to ensure proper separation of extracellular spike wave forms. Data were further processed using Neuroexplorer software (Plexon Inc., Dallas, TX) temporal relationship between spikes and light stimuli.

Analysis of data was performed using Microsoft Excel (2007). Only channels showing greater than twice the number of spikes during the first 10 seconds of light stimulation then during the 10 seconds prior to that in dark were used for further analysis. These channels were binned to 1 second, normalized to maximum spike frequency, then were pooled and averaged per bin to yield a light response for a given retina.